Universidade do Minho
Escola de Medicina

João Luís Vaz Lima da Silva

**Unraveling the synaptic role of Rab35:
implications for Alzheimer's disease pathology**

Sou

(spine)
João Luís Vaz Lima da Silva
**Unraveling the synaptic role of Rab35:
implications for Alzheimer's disease pathology**

UMinho|2019

p

evere

fevereiro de 2019

Universidade do Minho
Escola de Medicina

João Luís Vaz Lima da Silva

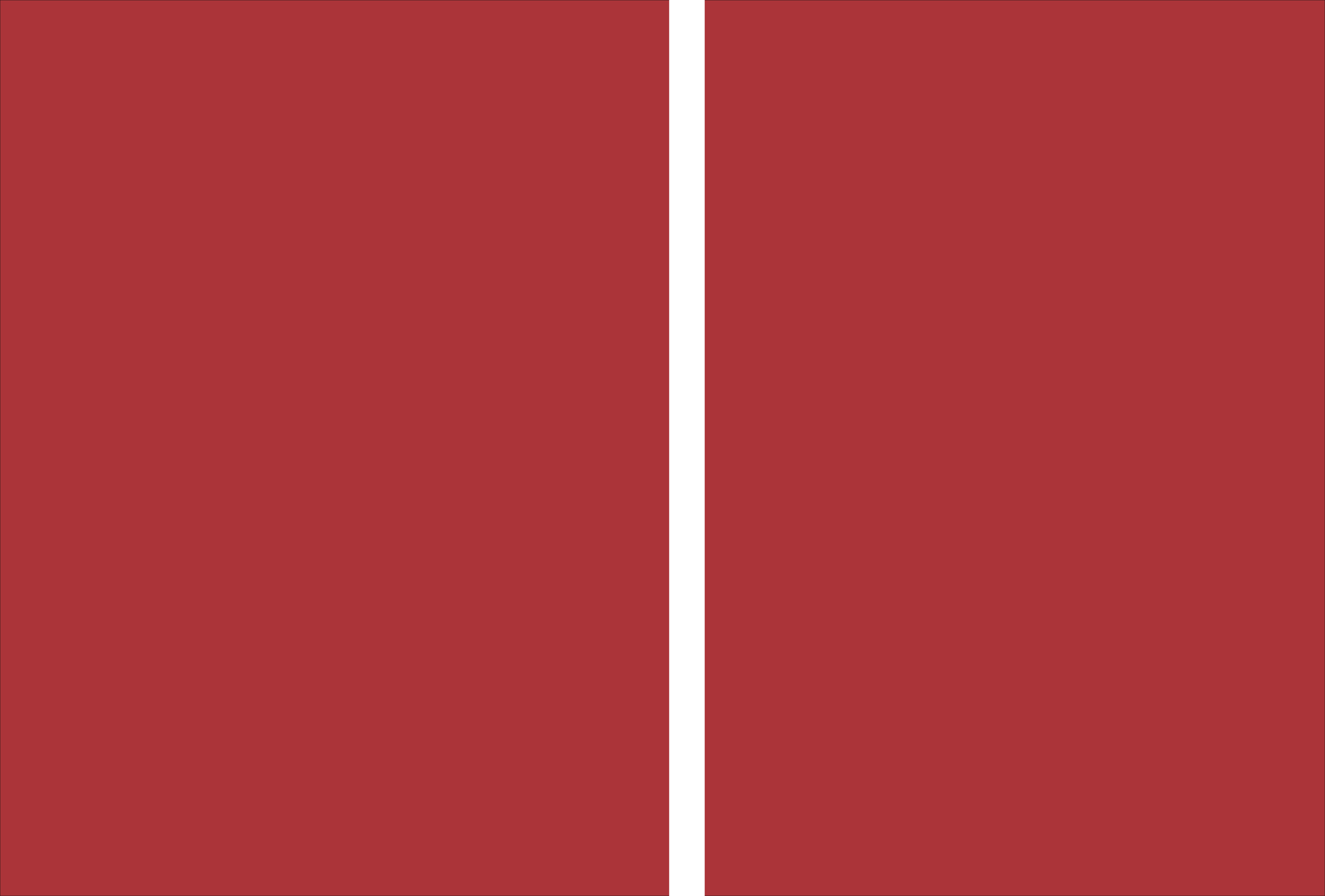# Unraveling the synaptic role of Rab35: implications for Alzheimer's disease pathology

Tese de Doutoramento em Medicina

Trabalho efetuado sob a orientação do
Doutor Ioannis Sotiropoulos
e da
Doutora Clarissa Waites

fevereiro de 2019

ii

"Para compreender, destruí-me."

"To understand, I've destroyed me"

Bernardo Soares

ACKNOWLEDGEMENTS

First of all, I would like to thank both my supervisors, Dr. Ioannis Sotiropoulos and Dr. Clarissa Waites, for their mentorship, patience, motivation and commitment.

To Dr. Ioannis Sotiropoulos, I would like to acknowledge his belief and motivation to keep on moving forward throughout the years, as well as his advice and support to follow new paths and challenge new ideas, even when these are not the easiest to follow. Your passion has been indispensable.

To Dr. Clarissa Waites, I thank the risk taken on an unfamiliar project, idea and person. I thank her mentorship and trust in my ideas, the opportunity to develop this work in an amazing lab and her constant availability over these years. And specially, her confidence and patient with my caution and common everyday pessimism, which taught me to hope for the best.

It has been a pleasure to work with such mentors, which helped me grow as a thinker, a researcher and as a person. I feel truly blessed.

I would like to thank all my friends at the NeRD team in ICVS for their help and support, they were essential in my first steps in the lab, helping me develop confidence in my work, while supporting me in the initial mistakes and misdirections, and celebrating the achievements.

I thank all the members of the Waites lab, past and present, for everything I've learned with them, for their constant help, for all the fun moments that made scientific work easier and all their friendship in the good and bad moments.

I would like to address a special acknowledgment to the MD/PhD program directors and all the academic staff behind it for this amazing opportunity to develop science on such exciting and thriving environments.

Por fim, agradeço aos meus pais, à minha irmã, à Maria e à Gabriela, por tudo.

Obrigado a todos,

ABSTRACT

Despite considerable progress in the understanding of molecular underpinnings of neuronal malfunction and cognitive impairment associated with Alzheimer's disease (AD), the physiopathology of the disorder is complex and poorly understood. Chronic environmental stress and the major stress hormones, glucocorticoids (GC), are suggested precipitating factors for AD, and have been shown to trigger APP misprocessing and Aβ production as well as Tau hyperphosphorylation, accumulation and downstream neuronal atrophy and malfunction. However, the mechanisms that regulate intraneuronal trafficking and homeostasis of Aβ & Tau remain poorly understood. Given the critical role of Rab GTPases as master regulators of endosomal protein trafficking, these PhD studies have explored the role of Rabs in Aβ & Tau proteostasis and their significance in AD pathogenesis. We found that the levels of a specific Rab, Rab35, are significantly decreased aged animals, as well in animals exposed to high GC levels or chronic stress, known triggers of APP misprocessing. Using a gain-of-function screen of Rabs that regulate endocytic protein trafficking, we showed that Rab35 is the most potent suppressor of the interaction of APP and BACE, the first enzyme involved in APP misprocessing towards the generation of Aβ. On the contrary, reduced Rab35 may promote the APP misprocessing suggesting Rab35 as an important regulator of the intraneuronal cascade that generates Aβ. In another set of studies of this PhD thesis, we demonstrated for the first time that Rab35 also controls degradation of Tau protein into the endolysosomal pathway through the Rab35-driven induction of the endosomal sorting complex required for transport (ESCRT) machinery. We also detected a phospho-dependent selectivity of Tau sorting into the Rab35/ESCRT pathway, while high GC levels suppress Rab35 expression and ESCRT machinery leading to Tau accumulation on both *in vitro* and *in vivo* studies. Importantly, AAV-mediated Rab35 expression rescues both GC-induced Tau accumulation and neuronal atrophy in the hippocampus of experimental animals. Altogether, the findings of these PhD studies suggest an essential role for Rab35 in the intraneuronal mechanisms underlying Aβ generation and Tau accumulation in AD as well as their significance to the precipitating role of chronic stress towards brain pathology. As emerging evidence suggest that the involvement of Tau in multiple neuropathological conditions, including Alzheimer's disease, frontotemporal dementia, chronic stress and epilepsy, identifying the cellular pathways responsible for Tau intra- and extra-cellular trafficking, as well as positive and negative regulators of these pathways, has broad therapeutic relevance.

x

Resumo

Apesar do progresso considerável na compreensão das bases moleculares do mau funcionamento neuronal e do comprometimento cognitivo associado à doença de Alzheimer (DA), a fisiopatologia da doença é complexa e pouco compreendida. O stress ambiental crónico e as principais hormonas do stress, os glucocorticóides (GC), são sugeridos como factores desencadeantes da DA, e têm mostrado desencadear o mal processamento da APP e a produção de Aβ, bem como a hiperfosforilação e acumulação da Tau, conduzindo a atrofia neuronal. No entanto, os mecanismos que regulam o tráfego intraneuronal e a homeostase de Aβ e Tau permanecem pouco compreendidos. Dado o papel crítico das Rab GTPases como reguladores do tráfego de proteína endossomais, este trabalho de doutoramento explorara o papel das Rabs na proteostase da Aβ e da Tau, assim como a sua importância na patogénese da DA. Descobrimos que os níveis de uma Rab específica, Rab35, estão significativamente diminuídos em animais envelhecidos, assim como em animais expostos a altos níveis de GC ou stress crónico, desencadeadores do processamento amiloidogénico de APP. Usando um ensaio de ganho de função de Rabs, que regulam o tráfego de proteínas endocíticas, mostramos que a Rab35 é o supressor mais potente, entre estas, da interação entre APP e BACE, a primeira enzima envolvida no processamento de APP em Aβ. Pelo contrário, a redução dos níveis de Rab35 pode promover o processamento amiloidogénico de APP, sugerindo que a Rab35 é um importante regulador da cascata intraneuronal que gera Aβ. Noutro conjunto de estudos desta tese de doutoramento, demonstramos pela primeira vez que a Rab35 também é capaz de controlar a degradação da proteína Tau na via endolisossomal através da indução do complexo Endosomal Sorting Complex Required for Transport (ESCRT) pela Rab35. Detectamos também que a selecção para a via Rab35/ESCRT é dependente do estado de fosforilação da Tau, enquanto que altos níveis de GC suprimem a expressão de Rab35, levando à acumulação de Tau in vitro e in vivo. A expressão de Rab35 mediada por AAV é capaz de resgatar tanto a acumulação de Tau induzida por GC, como a atrofia neuronal no hipocampo destes animais. Em conjunto, os resultados apresentados nesta tese de doutoramento, sugerem um papel essencial para Rab35 nos mecanismos intraneuronais subjacentes à geração de Aβ e ao acúmulo de Tau na DA, bem como a sua importância para o efeito do stress na indução de patologia cerebral. Evidências emergentes sugerem que a Tau está envolvida em múltiplos mecanismos neuropatológicas, incluindo a doença de Alzheimer, demência frontotemporal, stress crónico e epilepsia, assim, identificar as vias celulares responsáveis pelo tráfego intra e extra-celular da Tau, bem como os seus reguladores positivos e negativos, tem uma ampla relevância terapêutica.

Table of Contents

Abbreviations

Aβ – amyloid- β

ACTH – adrenocorticotropic hormone

AD – Alzheimer's disease

APP – amyloid precursor protein

BACE1 – β-secretase enzyme

BioGRID – Biological General Repository for Interaction Datasets

CMA – Chaperone-mediated autophagy

CRH – Corticotropin-releasing hormone

ESCRT - Endosomal sorting complex required for transport

EE - Early Endosome

ER – Endoplasmatic Reticulum

FTD – frontotemporal dementia

GC – Glucocorticoids

GDI – Rab GDP dissociation inhibitor

GR – glucocorticoid receptor

GWAS - Genome-wide association studies

HPA – hypothalamus-pituitary-adrenal

Hrs – hepatocyte growth factor (HGF)-regulated tyrosine kinase substrate

ILV – intraluminal vesicle

LAMP-1 – lysosomal membrane associated protein 1

LE – Late Endosome

LOAD – late onset Alzheimer's disease

LTP – Long-term potentiation

LTD – Long-term depression

MAP – Microtubule associated protein

MB – Microtubule-binding

MR – mineralocorticoid receptor

MVB – multivesicular bodies

MT – Microtubule

NFT – Neurofibrillary tangle

NMDA – N-methyl-d-aspartate receptor

NPC – Niemann-Pick Disease type C

PM – Plasma Membrane

PVN – paraventricular nucleus of the hypothalamus

PTM – Post-translational modifications

SNA – autonomic nervous system

TGN – trans-Golgi Network

TSG101 – Tumor susceptibility gene 101

UPS – Ubiquitin-Proteasome System

WHO – World Health Organization

CHAPTER 1

INTRODUCTION

1. INTRODUCTION

1.1 Alzheimer's Disease – a world health problem

The advances in medicine and biomedical research over the past decades have led to a shift in the world demographics, with an increase in average life expectancy and a progressive ageing of the world's population being registered by the World Health Organization (WHO). As a consequence, the incidence of age-related disorders such as dementia has been increasing, representing a tremendous burden for world health. Accordingly, WHO has declared dementia and Alzheimer's disease (AD), the most common type of dementia, as first priority for the 2017-2026 world health plan. Indeed, WHO reports that 47 million people worldwide suffer from dementia, with approximately 9.9 million new cases every year.

Alzheimer's Disease (AD) is the most common cause of dementia (60-70% of dementia cases), currently afflicting as many as 33 million people worldwide and 180.000 people in Portugal (Alzheimer Europe, 2013), being the European country with the 4th highest prevalence of AD dementia (OECD Indicators, 2017). These numbers are expected to double every 20 years, at least until 2040 (Mayeux and Stern, 2012). AD incidence in the elderly is very high and has been consistently shown to increase with age, from an incidence rate of 0,5% per year in individuals aged between 65 to 70 years to 6-8% in individuals over 85 years (Mayeux and Stern, 2012). AD not only shortens life expectancy, but is also the major cause of disability, decreased quality of life, and institutionalization among the elderly. Indeed, among individuals over 60 years of age, dementia is responsible for a higher percentage of years lived with disability than stroke, musculoskeletal disorders or cardiovascular disease (Qiu and Kivipelto, 2009). Furthermore, AD inflicts a devastating burden on caregivers, severely affecting family health and welfare as well as the healthcare systems of many countries around the world. Thus, there is global concern about the growing AD epidemic, and both research and clinical efforts have been increasingly focused on identifying prophylactic as well as therapeutic strategies against AD.

1.2 Alzheimer's Disease – Clinical presentation and mechanisms of pathology

AD patients suffer from progressive memory loss, with other cognitive functions being gradually affected/damaged as the disease progresses, such as language, executive and visuospatial functions,

and emotional regulation. Additionally, patients can display mood and personality changes as well as increased anxiety and confusion. This variety of symptoms arises from underlying cellular dysfunction in the brain, leading to widespread neuronal atrophy and loss that disturbs complex processes such as memory and cognition. The neuropathological hallmarks of AD are senile plaques, composed of extracellular aggregates of Aβ peptide, and neurofibrillary tangles (NFTs), arising from the intracellular aggregation of hyperphosphorylated Tau protein (Querfurth and Laferla, 2010), which are accompanied by astrogliosis and microglial cell activation (Serrano-pozo et al., 2011). Each lesion has a characteristic pattern of distribution, appearing in specific brain regions and spreading throughout the brain as the disease progresses (Serrano-pozo et al., 2011; Spires-jones and Hyman, 2014). Amyloid plaques appear and mainly accumulate in the neocortex, while the allocortex, basal ganglia, brainstem and cerebellum are affected afterwards and to a lesser extent (Serrano-pozo et al., 2011). NFTs have a more predictable spatiotemporal pattern of distribution compared to amyloid plaques. NFTs start in the allocortex of the medial temporal lobe, which includes the entorhinal cortex and hippocampus, spreading later to the associative neocortex, while somewhat sparing the primary sensory, motor and visual areas (Serrano-pozo et al., 2011). Several studies have established that the amount and distribution of NFTs correlates with both the severity and duration of the disease (Giannakopoulos and Herrmann, 2003; Gomez-isla et al., 1997; Ingelsson et al., 2004). However, the quantity of amyloid lesions exhibits no correlation with the severity or duration of disease (Giannakopoulos and Herrmann, 2003; Ingelsson et al., 2004; Spires-jones and Hyman, 2014). Despite these differences in the clinicopathological correlations of amyloid and Tau lesions, it is known that the accumulation of both neurotoxic products is required for the development of AD. Interestingly, these lesions are also found in the brains of healthy aged individuals, supporting the idea that they can also occur during normal ageing.
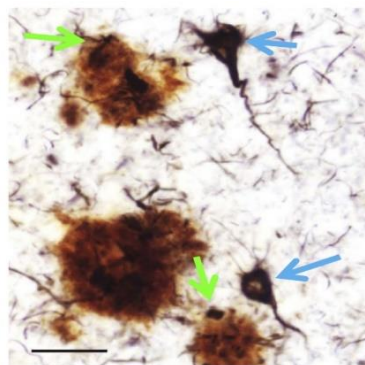
Figure 1. Neuropathologival hallmarks of Alzheimer's Disease. Brain section from neocortex of an AD patient, stained using double label immunohistochemistry for Aβ, showing senile plaques (green arrows), and Tau protein, staining NFTs (blue arrows); adapted from (Nelson et al., 2012)).

1.2.1 Amyloid-β – the initiator of AD neurodegeneration?

The main component of amyloid plaques is Aβ, which is formed from the sequential cleavage of Amyloid Precursor Protein (APP). APP is a type I transmembrane protein, consisting of a single membrane-spanning domain, a large extracellular N-terminus, and a shorter cytoplasmic C-terminus (Haass et al., 2012). The rate limiting step for Aβ production is the proteolytic cleavage of APP by β-secretase (BACE), resulting in a short, membrane-associated C-terminal fragment, C99. This fragment undergoes a second cleavage by γ-secretase within the transmembrane domain, resulting in its membrane release and generating Aβ (Agostinho and Pli, 2015; Haass et al., 2012).
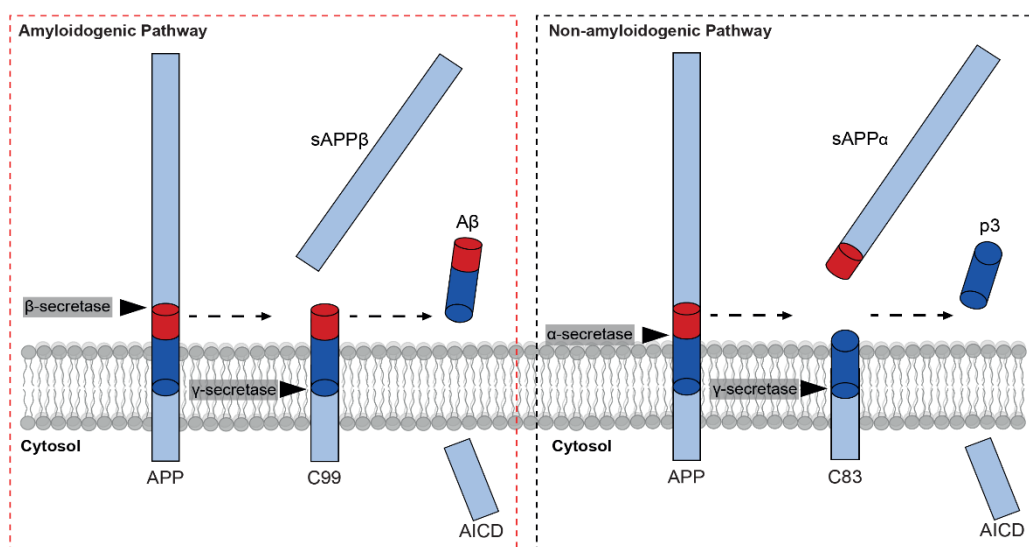
Figure 2. Proteolytic processing of APP through the amyloidogenic and non-amyloidogenic pathways. APP can undergo cleavage through the amyloidogenic or non-amyloidogenic pathways. In the former, APP is cleaved by BACE1, leading to the formation of C99, which is then cleaved by γ-secretase to produce Aβ. In the latter, APP is cleaved within the Aβ sequence, thus preventing its formation, and instead generating C83, which is then cleaved by γ-secretase to produce p3; adapted from Vaz-Silva J's Master thesis.

APP intracellular trafficking and distribution within the cell determines its proteolytic fate. APP is synthetized in the endoplasmatic reticulum (ER), being transported to plasma membrane (PM) trough the secretory pathway, where it undergoes post-translational modifications by N- and O-linked glycosylation. A small fraction of APP is reported to reach the PM, while the majority of APP localizes to the Golgi pathway and trans-Golgi Network (TGN), however most studies were performed under APP overexpressing conditions (Haass et al., 2012). At the PM, surface APP is rapidly endocytosed into early endosomes and recycling endosomes, where it can be recycled back to the PM or to TGN (Ubelmann et al., 2017). Additionally, endosomal APP can also be sorted for degradation in the

lysosome through the endo-lysosomal pathway (Edgar et al., 2015; Haass et al., 1992). Surface APP at the PM is cleaved by α-secretase, which cleaves APP within the Aβ sequence and thus, prevents Aβ generation (Agostinho and Pli, 2015). BACE and γ-secretase cleavage mainly occurs in the endosomal compartments, which presents an acidic environment that is ideal for BACE activity. Endocytosis of both APP and BACE is essential for Aβ production. Indeed, inhibiting endocytosis has been shown to reduce Aβ levels, while synaptic activity, which leads to increased endocytosis, increases Aβ levels (Cirrito et al., 2005). Since neuronal trafficking of APP and BACE is mainly segregated, endocytosis promotes the convergence of both proteins within the endosomal compartment (Ubelmann et al., 2017). Interestingly, several genes identified as being strongly linked to AD, such as BIN1, CD2AP and SORL1, have been implicated in regulation of trafficking pathways into and out of endosomes (Small et al., 2017). Indeed, deregulation of these proteins seems to be involved in endosomal traffic jams that destabilizes membrane trafficking and promotes increased residence time of APP and/or BACE within the endosomal pathway, thus affecting Aβ levels (Small et al., 2017). Once produced, Aβ is either secreted to the extracellular environment or it can be accumulated in endosomes.
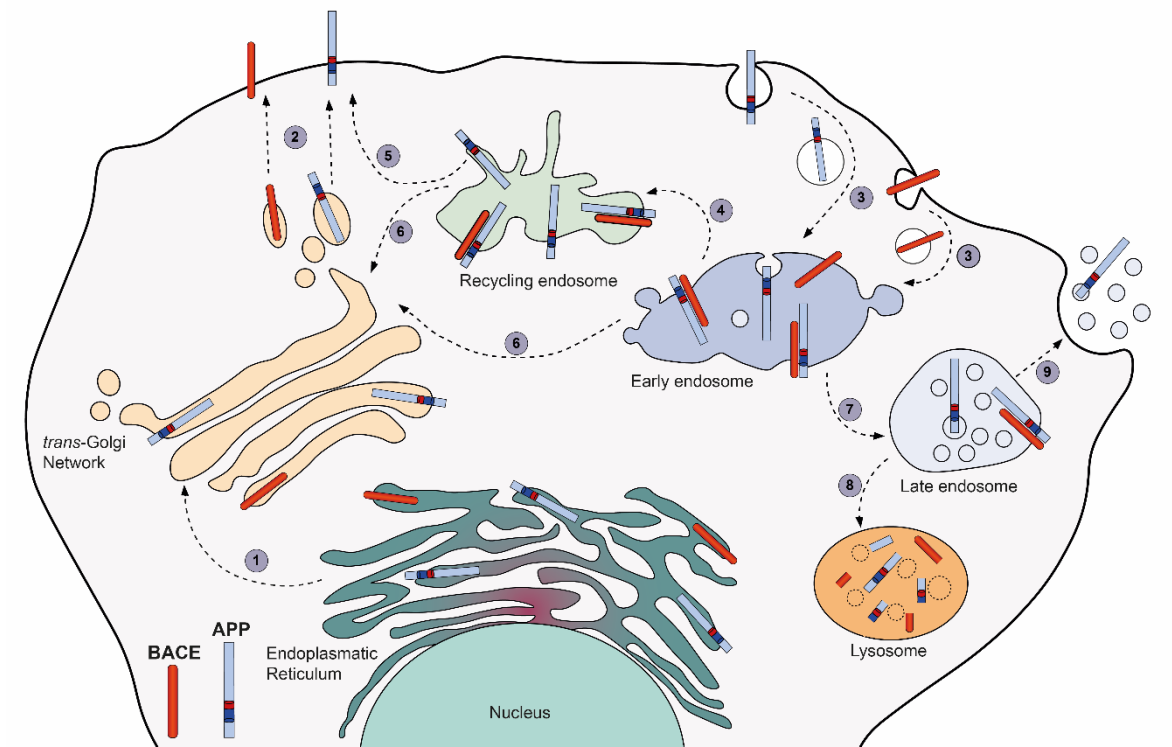
Figure 3. APP and BACE membrane trafficking dynamics. Recently synthetized proteins travel and mature through the secretory pathway (1) until the plasma membrane (PM) (2). APP and BACE are internalized from the PM and meet within the endocytic pathway (3), which provide the necessary acidic environment for BACE activity. At the early endosome, APP and/or BACE can be recycled through recycling endosomes (4) to the PM (5) or back to the trans-Golgi Network (6). They can be sorted through the endosomal system into late

endosomes (7), which can either fuse with lysosomes for protein degradation (8) or fuse with the PM and release their contents in the form of exosomes (9).; adapted from Vaz-Silva J's Master thesis.

The majority of Aβ peptide produced has a length of 40 residues (Aβ40), while a 42 residue peptide variant (Aβ42) is produced to a lesser extent. Aβ42 is more hydrophobic, and thus more prone to fibril formation and aggregation, and represents the predominant isoform found in senile plaques (Masters and Selkoe, 2012). Aβ isolation and sequencing represented a turning point in AD research, and decades of research has presented strong evidence about its role in AD development, being associated with profound neuronal and synaptic changes in the brain.

Initially, Aβ plaques were considered the main accountable for neurotoxicity, however further studies proposed Aβ oligomers as the primary source of Aβ-induced toxicity. Indeed, APP transgenic mice, which overproduce Aβ, present synaptic changes and cognitive impairments before developing amyloid plaques, which suggests a neurotoxic influence of soluble Aβ (Mucke and Selkoe, 2012). Aβ oligomers have been shown to regulate both pre- and post-synaptic functions. At physiological low levels, Aβ was shown to facilitate presynaptic function, improving the release probability of synaptic vesicles and enhancing synaptic activity (Mucke and Selkoe, 2012). At high levels, Aβ is known to alter excitatory glutamatergic signaling and lead to synaptic loss (Palop and Mucke, 2010). Indeed, Aβ was suggested to function has a feedback loop controlling neuronal excitability at the post-synaptic level, since its extracellular release increases with neuronal activity (Cirrito et al., 2005). Additionally, pathological levels of Aβ oligomers are known to impair long-term potentiation (LTP) and induce long-term depression (LTD) and spine loss (Palop and Mucke, 2010), while also altering dendritic architecture through cytoskeleton remodeling through activation of through its activation of extracellular-signal regulated kinase/mitogen activated protein kinase (ERK/MAP kinase) (Small et al., 2001).

Additionally, Aβ has been shown to stimulate Tau hyperphosphorylation through GSK3β activation (Lloret et al., 2015), as well as to impair protein homeostasis by destabilization of the proteasome system (Tseng et al., 2008). Indeed, not only Aβ, but also APP amyloidogenic processing into β-CTF, has been shown to destabilize Tau proteostasis (Moore et al., 2015), inducing Tau accumulation and hyperphosphorylation, thus suggesting an interplay between the Aβ overproduction and Tau pathology.

1.2.2 Tau protein – the final executor of neurodegeneration?

As NFTs are mainly composed of hyperphosphorylated Tau protein, and emerging evidence suggests that the major detrimental effects of Aβ require Tau (Roberson et al., 2007), recent research efforts have focused on Tau's role in neurons, and how Tau malfunction precipitates neurodegeneration in AD and other diseases – see also section 1.4.4.

Tau is a member of the microtubule-associated protein (MAP) family, and early studies on Tau focused on understanding its role in microtubule (MT) assembly and stability. Tau interacts with MTs through its microtubule-binding domain (MB), a region composed of either 3 (3R-Tau) or 4 (4R-Tau) repeats of an evolutionarily conserved tubulin binding motif. These isoforms have different binding affinities, with 4R-Tau isoforms presenting a greater affinity for microtubule binding than 3R-Tau isoforms. Tau's dynamic regulation of microtubule stability is in part regulated by its phosphorylation state. Dephosphorylated Tau has a higher affinity for MT binding, promoting its stability and polymerization, while phosphorylation of Tau at specific epitopes can decrease or even completely abolish its MT binding ability. Although Tau phosphorylation regulates its physiological function, the aberrant hyperphosphorylated state, such as is found in disease, is thought to contribute to impaired MT binding and neuronal destabilization and pathology.

Tau is encoded by a single gene present in chromosome 17q21, which contains 16 exons. Full-length Tau protein has 441 amino acids, composed of exons 1-13. Exons 2, 3 and 10 can undergo alternative mRNA splicing, being responsible for the existence of 6 Tau isoforms that differ by the absence or presence of 1 or 2 inserts in the N-terminus, and by the presence of 3 or 4 repeats of the tubulin binding motif at the C-terminus (Andreadis et al., 1992). Adults express all six isoforms of Tau, while in the fetal brain only the shortest isoform (0N3R) is expressed (Bakota et al., 2017). Tau is primarily expressed in the central and peripheral nervous system, where it is most abundant in neurons, though also expressed at lower levels in astrocytes and oligodendrocytes (Götz et al., 2013). Tau is also found in kidney, lung, and testis. In brain sections from mature animals, Tau is primarily observed in the axonal compartment of neurons, with little or no presence in the somatodendritic compartment (Dotti et al., 1987; Götz et al., 2013). However, in cultured hippocampal neurons, Tau compartmentalization does not occur, and Tau is present throughout the dendrites, axons and somata (Dotti et al., 1987). In brain tissue from patients with AD and other tauopathies, Tau loses its axonal

enrichment and redistributes to the soma and dendrites, where it accumulates in the early pathological state. Although this phenomenon is considered aberrant, recent studies have shown that Tau can be locally translated in dendritic spines during physiological events.
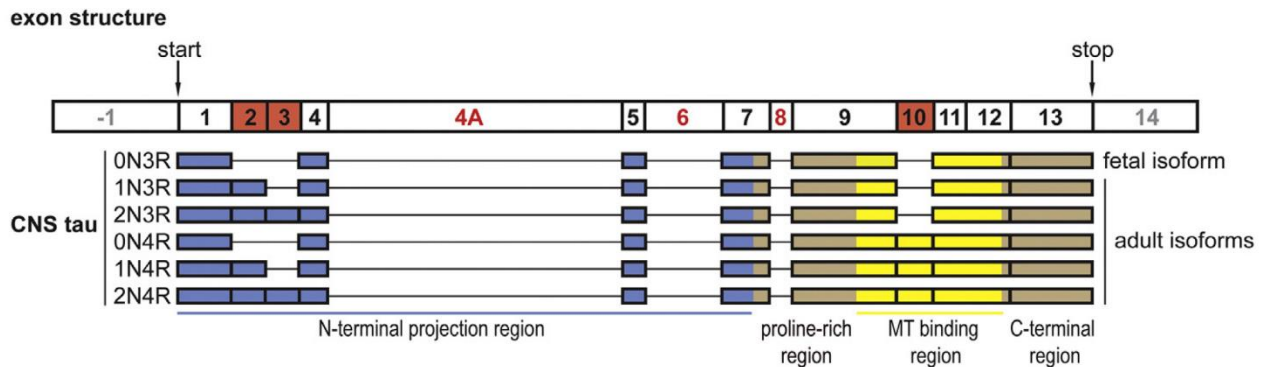
Figure 4. MAPT gene and the Tau splicing isoforms. Alternative splicing leads to the generation of six different Tau isoforms. Tau protein includes two major domains: the N-terminal projection and C-terminal domains. Tau isoforms differ by the absence or presence of one or two N-terminal inserts encoded by exon 2 and 3, as well as the presence of either three or four repeat regions coded by exons 9, 10, 11 and 12 in the C-terminus; adapted from (Bakota et al., 2017).

Although considerable research has focused on the role of Tau in microtubule dynamics, the fact is that Tau has a wide array of functions and interactors that are yet to be uncovered. Indeed, Tau is classified as an intrinsically disordered protein (IDP), with several IDP regions that fail to form a stable structure, providing conformational flexibility and thus a larger area for interaction (Bakota et al., 2017). In the Biological General Repository for Interaction Datasets (BioGRID) database, Tau is predicted to have 118 interactors. The structural instability of the IDP regions facilitates several biological processes, such as alternative splicing and post-translational modifications (PTM). Tau is subject to several PTM, such as phosphorylation, ubiquitination, methylation, acetylation and O-GlcNAc modification (Morris et al., 2015). Since Tau is hyperphosphorylated in neurodegenerative disease states, phosphorylation is the most extensively studied PTM.
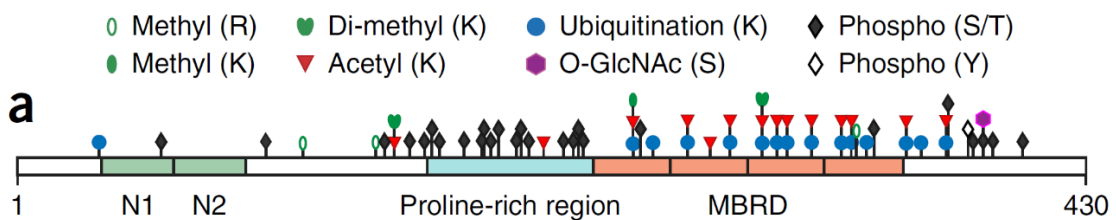
Figure 5. Post-translational modifications of Tau. Post-translational modifications of endogenous Tau identified in the brain of WT-mice; adapted from (Morris et al., 2015).

Besides regulating Tau affinity for microtubules as previously described, Tau phosphorylation also seems to have a critical role on its intracellular distribution. In axons, Tau is found mainly in a dephosphorylated state, while in the soma around 80% of Tau is phosphorylated (Mandell and Banker, 1996). It was recently demonstrated that hyperphosphorylation-mimetic mutants of Tau undergo increased sorting to dendritic spines, while phosphorylation-deficient mutants do not undergo sorting to the synapses (Hoover et al., 2010). Furthermore, phosphorylation of Tau at specific epitopes was shown to be essential for its translocation into dendritic spines, and is regulated by distinct signals including synaptic activity (e.g. phosphorylation at threonine 205) and Aβ (e.g. phosphorylation at serine 404) (Frandemiche et al., 2014). Additionally, it was recently shown that di-phosphorylated Tau in the 386-404 region is enriched at the post-synaptic density (Morris et al., 2015). These studies demonstrate that Tau has specific phosphorylation signatures that regulate its localization and function in neurons, under both physiological and pathological conditions.

Other PTMs have also been shown to modulate Tau function and distribution in the cell. Acetylation of Tau has been shown to impair its degradation and clearance (Min et al., 2010), as well as AMPA receptor trafficking during long-term potentiation (LTP) (Tracy et al., 2016), interfering with microtubule regulation (Cohen et al., 2011) and promoting aggregation. On the other hand, ubiquitination signals Tau degradation, but also weakens its microtubule-binding activity (Min et al., 2013). Ubiquitination and acetylation typically occur on lysine residues, leading to opposite effects on protein fate (Min et al., 2010; Morris et al., 2015), and suggesting that disruption of the balance between ubiquitination and acetylation could lead to Tau accumulation and ultimately to disease states. Indeed, in severe dementia cases, levels of Tau acetylation were elevated compared to those without cognitive impairment. Additionally, ubiquitinated Tau species are found in tangles; however, the effect of ubiquitination on Tau aggregation remains unclear (Min et al., 2013).

Understanding the complex role of Tau within neurons is not an easy task due to its multiple binding partners, each with distinct functions. Thus, it was unexpected when conventional knockout of Tau (Tau-KO) in animal models presented no obvious behavioral or histological alterations in vivo (Dawson et al., 2001; Harada et al., 1994). The lack of effect on neuronal development and cellular function has been attributed to compensatory mechanisms, including the increased expression of certain MAP proteins. However, it was recently shown that aged Tau-KO mice exhibited increased motor impairment compared to control mice, a phenotype that was not observed in younger animals. This motor impairment seemed to result from diminished conductivity in the sciatic nerve due to

degeneration of myelinated fibers and progressive hypomyelination (Lopes et al., 2016a). Thus, further work is needed to better understand the impact of Tau in the nervous system.

1.2.3 Tau proteostasis – a novel target against AD

Accumulating evidence from clinical and animal studies suggests that Tau hyperphosphorylation and pathology correlates with synaptic loss and memory deficits in AD. Thus, reducing Tau levels is suggested as a promising therapeutic strategy in AD since recent experimental evidence shows that Tau reduction attenuates neuronal dysfunction and cognitive deficits in mouse models of AD (Rapoport et al., 2002; Roberson et al., 2007; Zempel et al., 2013). Thus, there is an increasing interest in understanding the mechanisms of Tau proteostasis, which regulate the balance between degradation and accumulation of Tau in the brain, since they may underlie disease-related Tau accumulation and aggregation in brain.

Clearance of both physiological and pathological forms of Tau can occur through the proteasomal and autophagic degradative systems. Ubiquitination, wherein the small protein ubiquitin is conjugated to lysine residues on target proteins, is the major signal for protein degradation in the cell (Piper et al., 2014). Polyubiquitin chains, in which ubiquitin moieties are added to the initial ubiquitin at specific lysine residues, have specific biochemical signatures that can determine the protein's degradative fate. For instance, the most extensively characterized polyubiquitination chains, formed via ubiquitylation of lysine at position 48 (K48) or position 63 (K63), lead to proteasome-mediated degradation (K48) (Chesser et al., 2013), or degradation via the endocytic and autophagy pathways (K63) (Piper et al., 2014). Monoubiquitinated and polyubiquitinated forms of Tau have been found to accumulate in NFTs, suggesting impaired removal of proteins tagged for degradation (Wang and Mandelkow, 2012). Although polyubiquitinated Tau was initially identified mainly in the K48-linked form, new studies have also demonstrated the presence of K6-, K11- and K63-linked polyubiquitinated Tau, suggesting the involvement of multiple degradative pathways (Min et al., 2013; Wang and Mandelkow, 2012).

The proteasomal pathway represents a major form of clearance for damaged or misfolded proteins. The canonical ubiquitin-proteasomal pathway (UPS) degrades substrates that are covalently tagged with polyubiquitin chains, and targeted to the 26S proteasome for proteolysis. Although Tau should represent an ideal UPS substrate, being a relatively small and unfolded protein, its proteasomal

degradation is somewhat controversial (Wang and Mandelkow, 2012). While several cellular studies show that Tau is a substrate of the UPS under physiological conditions (David et al., 2002; Dickey et al., 2007; Shimura et al., 2004), others have contrastingly shown that the role of the UPS in Tau degradation is negligible (Blard et al., 2005; Brown et al., 2005; Delobel et al., 2005). Interestingly, studies performed in both the mouse neuroblastoma cell line (N2a) or in primary cultured neurons (Brown et al., 2005; Delobel et al., 2005; Krüger et al., 2012) have shown little impact of the proteasome on Tau degradation. For instance, suppressing proteasomal activity in primary cultured neurons led to decreased, rather than increased, Tau levels (Krüger et al., 2012). Moreover, hyperphosphorylated Tau aggregates have been shown to be inaccessible to the narrow pore of the proteasome, and thus cannot be degraded through the UPS.

Autophagy is a clearance mechanism for both long-lived proteins as well as aggregates and organelles, which are catabolized in the lysosome. Three types of autophagy have been described: macroautophagy, microautophagy and chaperone-mediated autophagy. The most common type is macroautophagy, which involves the formation of a double membrane phagophore to sequester the substrate, followed by the formation of an autophagosome that can fuse with the lysosome for degradation. Macroautophagy inhibition through 3-methyladenine treatment has been shown to increase levels of both soluble and insoluble Tau (Kaushik et al., 2009), while autophagy inducers enhance Tau clearance (Congdon et al., 2012; Krüger et al., 2012) and reduce the levels of Tau aggregates in Tauopathy mouse models (Lavenir et al., 2012). Impairment of lysosomal function has also been found to increase Tau accumulation and slow its degradation (Chesser et al., 2013; Hamano et al., 2008). However, the lysosome is the converging degradative organelle for several pathways, and its dysfunction does not represent unequivocal evidence of Tau degradation via macroautophagy. Another lysosomal degradative pathway is chaperone-mediate autophagy (CMA), in which cytosolic proteins are directly selected for lysosomal degradation through Hsc70 recognition of a conserved KFERQ motif, followed by translocation into the lysosome via LAMP2A binding (Min et al., 2013; Wang and Mandelkow, 2012). Tau contains two versions of this KFERQ targeting motif, and has been shown to undergo CMA; however, this pathway can also promote Tau aggregation due to the failure of some Tau mutants to undergo translocation, leading to generation of aggregation-prone Tau fragments (Kaushik et al., 2009).

Previous work indicated that Tau degradation mainly relies on the UPS and autophagic systems. However, little research has been done to understand the potential role of another major cellular

degradative system, the endosomal-lysosomal pathway. In this study, we focused on unraveling the importance of intracellular endosomal and lysosomal trafficking for Tau proteostasis.

1.3 The endosomal-lysosomal system – an essential player in neuronal proteostasis

Intracellular membrane dynamics play a vital role in eukaryotic cell physiology, compartmentalizing the cell in different processing hubs, each with specialized roles. The endolysosomal system is a fundamental component of every cell, regulating the sorting, recycling and degradation of different cargos from the plasma membrane to the lysosome. Given its importance, many of the proteins involved in the regulation of this complex system are highly conserved and can be detected even in the earliest eukaryotic ancestors (Schmid et al., 2014). Although this pathway has mainly been studied as an intermediate for degradation, it participates in other cellular functions such as cell signaling, recycling, and cell polarity, among others (Maxfield, 2014).
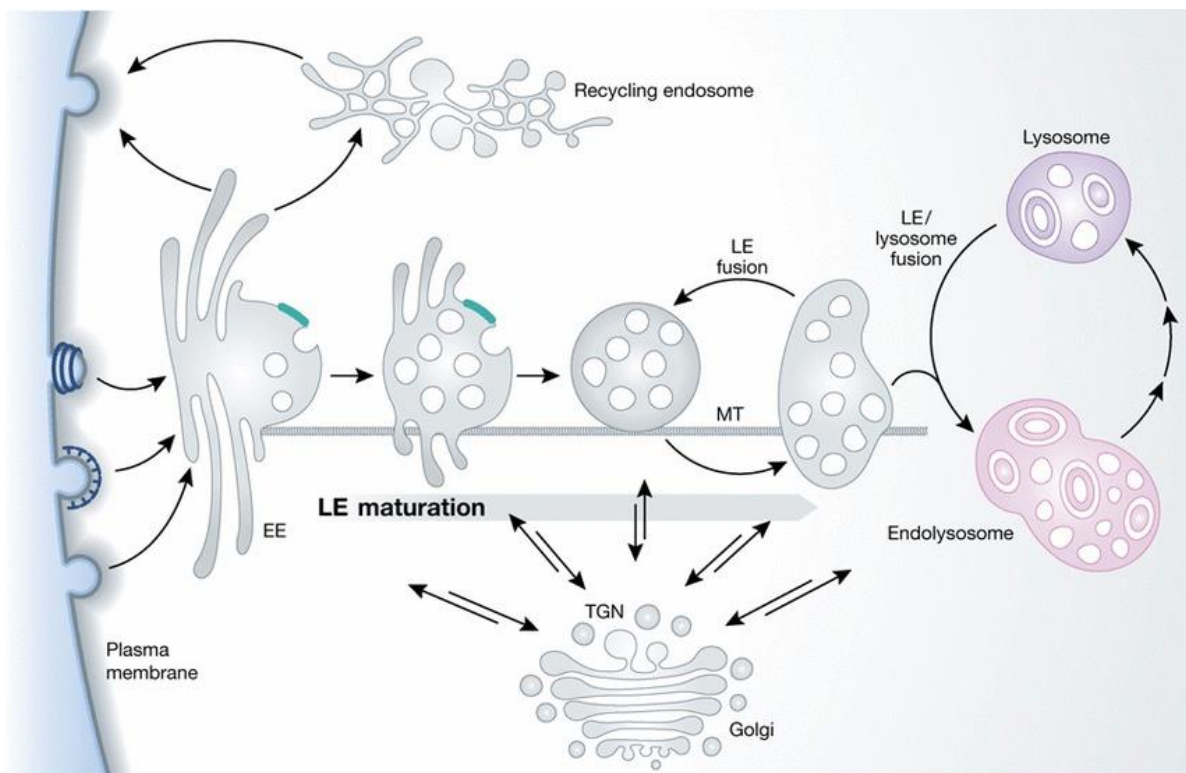

Figure 6. The endosomal-lysosomal system. Upon internalization, recently formed endocytic vesicles are directed for the tubulovesicular EE, where cargo can be sorted for recycling back to the plasma membrane

either directly or through recycling endosomes, or it can be selected for progression through the endolysosomal pathway, thus being directed to LE. In LE/MVBs, cargo is trapped inside ILVs, which fuse with the lysosomes for degradation. Alternatively, LE/MVBs can fuse with the PM, releasing their contents in the form of exosomes (not shown). Constant crosstalk between the TGN and the different endocytic compartments occurs, providing the pathway with essential components for its normal function and serving as an additional recycling pathway for internalized cargo; adapted from Huotari and Helenius, 2011.

The endolysosomal system can be roughly divided into three intracellular components: early endosomes, late endosomes, and lysosomes, with cargo being sorted and transported sequentially through the different compartments. Endocytosis is the primary step in the pathway, wherein small endocytic vesicles are formed from invaginations of the plasma membrane, thus internalizing not only the components present at the membrane, but also nutrients and molecules from the extracellular environment (Maxfield, 2014). The internalized cargo is transported and fused with the early endosomes (EE), a network of dynamic tubulovesicular structures located at the cell's periphery, resulting in the transfer of cargo and addition of membrane from endocytic vesicles into this structure (Klumperman and Raposo, 2014). The EE functions as a key sorting station, where proteins and lipids can be recycled to back the plasma membrane either directly or indirectly via the recycling endosomal compartment, while other molecules can undergo retrograde transport to the trans-Golgi Network (TGN) or be routed towards the lysosome (Scott et al., 2014). The small GTPase Rab5 is the master regulator of EE membrane dynamics, being involved in biogenesis, fusion and normal functioning. Recently, it was shown that knockdown of Rab5 to negligible levels leads to a dramatic decrease in the number of EEs, and a consequent reduction of late endosomes and lysosomes (Zeigerer et al., 2012).

Late endosomes (LE) function as a second trafficking hub and sorting station in the endolysosomal pathway. The transition between EE and LE is thought to occur progressively, through fission of tubular elements that are routed for recycling and the constant invagination of the endosomal membrane, to form intraluminal vesicles (ILVs). These steps lead to endosomal remodeling from a tubular into a globular-shaped, 250-1000 nm, endosome with distinctive lipid and protein compositions and the presence of small <50nm ILVs. A single endocytic compartment is suggested to mature through the different stages of the endocytic pathway. Indeed, it has been shown that individual endosomes can mature from EEs into LEs through the exchange of Rab5 for Rab7, a LE marker (Poteryaev et al., 2010; Rink et al., 2005). This hypothesis has been further supported by studies looking at LDL, showing that conversion of EEs into LEs is the major mode of its trafficking (Foret et al., 2012). However, other models, such as endocytic transport between heterotypic

compartments, have also been proposed. During the maturation process, LEs progressively accumulate ILVs, and thus many electron microscopy studies use the accumulation of ILVs as a tool to distinguish between EEs and LEs (Futter et al., 1996). The high number of ILVs gives a distinctive appearance to LEs, which are also termed multivesicular bodies (MVBs). ILVs main function is to sequester ubiquitinated cargo tagged for degradation (Williams and Urbé, 2007). The major complex regulating all the steps, from cargo sorting to membrane budding and fission, is the Endosomal Sorting Complex Requires for Transport (ESCRT), which will be discussed in greater detail below. Mature LEs can fuse to lysosomes, delivering their intraluminal content for degradation. Additionally, LEs are also important for the function of lysosomes, since they deliver essential proteins for lysosomal function, such as hydrolases, that arrive in a constant influx from the TGN (Huotari and Helenius, 2011). However, another fate is possible for this endocytic compartment: fusion with the PM, thus releasing its intraluminal contents in the form of small signaling vesicles, termed exosomes.

Lysosomes are responsible for the degradation of incoming cargo for metabolic reuse, representing the 'point of no return' for many macromolecules, such as proteins, carbohydrates, nucleic acids and lipids. Lysosomes are typically spherical organelles with diameters between 200 nm and >1µm (Klumperman and Raposo, 2014) and an acidic pH (approximately 4.5-5), essential for the proper activity of their many hydrolases. Disruption of lysosomal function leads to the accumulation of cellular waste, compromising the function of the whole cell. As such, disruption of endosomal-lysosomal trafficking is implicated in several proteinopathies, including neurodegenerative diseases, due to the accumulation of dysfunctional proteins. Indeed, abnormalities of the endosomal-lysosomal system, including endosomal enlargement and high levels of lysosomal hydrolases, are reported as the earliest intracellular features of AD, before the emergence of Aβ plaques or NFTs and the appearance of symptoms. Additionally, in lysosomal storage disorders such as Niemann-Pick disease type C (NPC), where a common pathological hallmark is the accumulation of lysosomal substrates, NFTs accumulate in the brains of patients, suggesting that Tau pathology can occur with disruption of the lysosomal pathway.

1.3.1 Endosomal Sorting Complex Required for Transport

The ESCRT pathway is composed of a series of four protein complexes (ESCRT-0, -I, -II and -III) that are sequentially recruited to the endosomal membrane, regulating both cargo sorting and membrane budding dynamics.

Ubiquitination serves as a sorting signal throughout the endocytic system, redirecting proteins from the recycling pathway to the degradative pathway (Piper et al., 2014). Multiple-monoubiquitinated and K63-linked polyubiquitinated proteins are recognized and sorted by the ESCRT complex, which concentrates cargo in endosomal clathrin microdomains before being internalized into ILVs, thus preventing the cargo from re-entering the recycling endosome or fusing with the PM (Piper et al., 2014). Components of the ESCRT-0, -I and -II contain ubiquitin-interacting motifs, being the major complexes involved in cargo sorting.
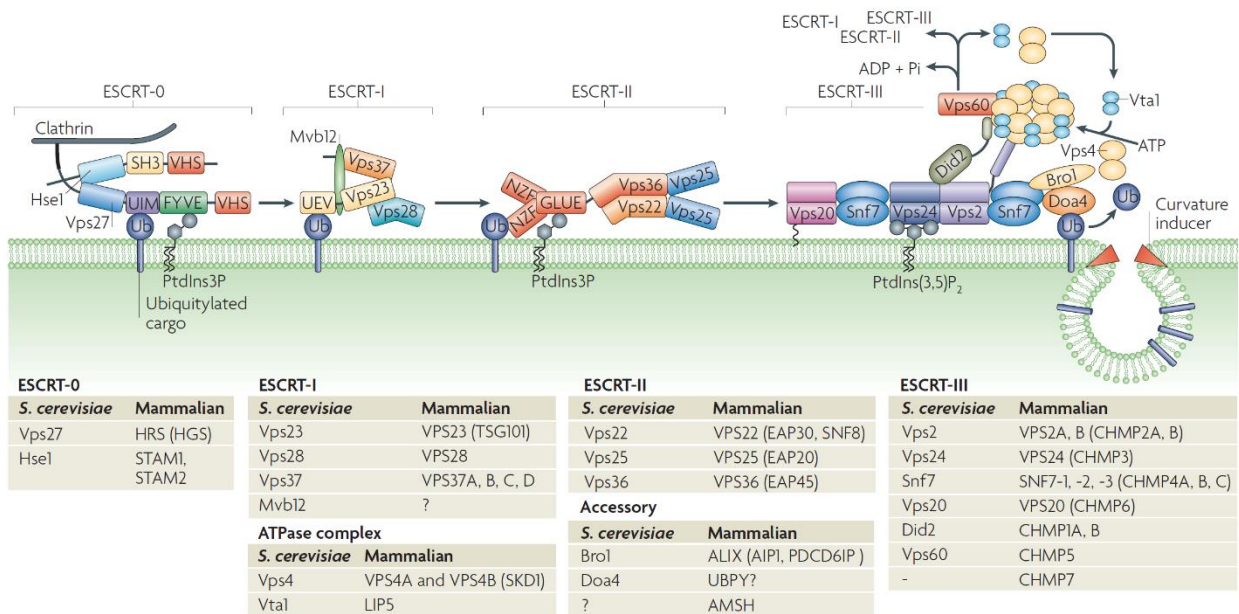
Figure 7. ESCRT machinery involved in cargo sorting through the endosomal-lysosomal pathway. The four ESCRT complexes are recruited to endosomal membrane by their interactions with membranes, clathrin, ubiquitin and/or each other; adapted from Urbe 2007.

ESCRT-0 component hepatocyte growth factor (HGF)-regulated tyrosine kinase substrate (Hrs) is the first protein of this complex network to be recruited to the endosomal membrane, since it contains a FYVE domain, a lipid-binding motif that interacts with phosphatidylinositol 3-phosphate (PI3P), which is enriched on early endosomes. ESCRT-0 is essential for the initial selection of ubiquitinated cargo. Additionally, Hrs participates in the recruitment of downstream ESCRT proteins by direct interaction with ESCRT-I component, Tumor susceptibility gene 101 (TSG101) (Williams and Urbé, 2007).

Besides its structural function, TSG101 also possesses ubiquitin interacting domains that participate in the recognition of ubiquitinated cargo. Indeed, in vitro studies have demonstrated that

depletion of TSG101 has a strong inhibitory effect on cargo degradation and alters endosomal morphology, supporting its importance for the proper functioning of this system. Proteins of the ESCRT-III complex are mainly involved in the formation of ILVs through membrane deformation and recruitment of accessory proteins for membrane budding and fission (Williams and Urbé, 2007).

1.3.2 Rab35 – a star among Rab GTPases

Rab GTPases are the largest family of small GTPases, with approximately 70 members in humans, and are important organizers of membrane trafficking in all eukaryotic cells (Wandinger-ness and Zerial, 2014). Rab GTPases contribute to the structural and functional identity of intracellular membrane compartments. A key aspect of this function is the innate characteristic of Rab GTPases as "molecular switches" that cycle between an active (GTP-bound) and inactive (GDP-bound) state. In GDP-bound form, Rab GTPases are usually cytosolic and chaperoned by Rab GDP dissociation inhibitor (GDI), which stabilizes the inactive state. While in the GTP-bound state, Rab GTPases are usually bound to membranes, recruiting effectors that recognize the activated Rabs and catalyze downstream evens, such as recruitment of signaling pathways, vesicle trafficking, and membrane fusion, among others (Sheehan and Waites, 2017). This reversible association with membranes may be due to the presence of a hydrophobic geranylgeranyl group (Stenmark, 2009), essential for mediating Rab GTPases function by allowing changes in membrane composition and intracellular fate of organelles, as in the previously discussed example of Rab5 exchange for Rab7.
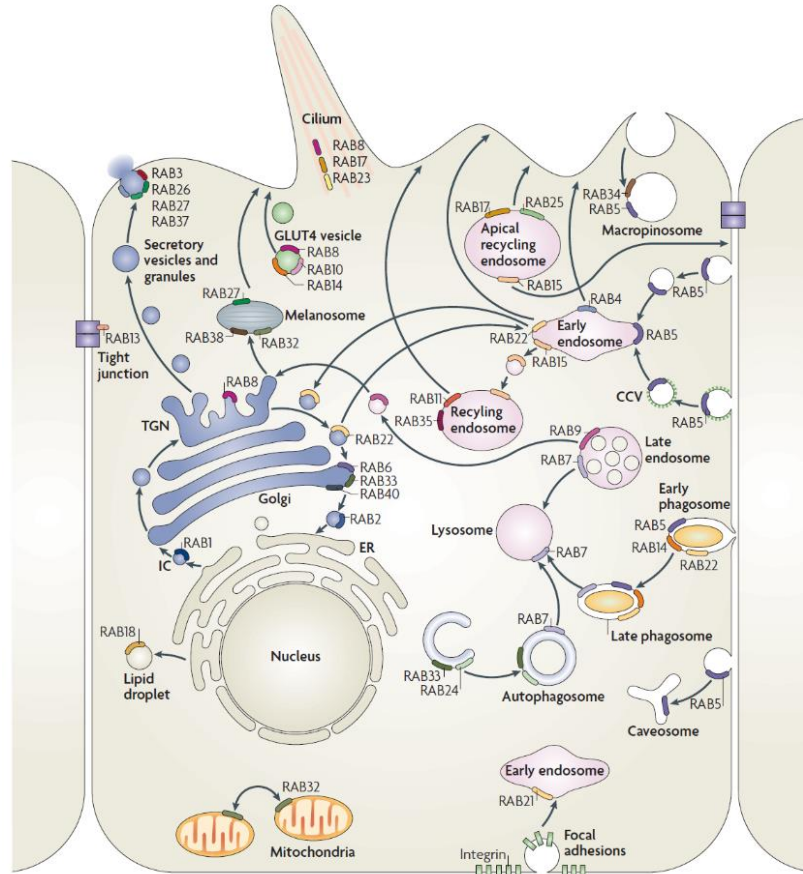
Figure 8. Overview of Rab GTPases and its intracellular distribution. Rab GTPases are distributed across most intracellular membranes, contributing to their identity and function. Rab5 is localized to early endosomes, regulating endocytosis and endosomal fusion of clathrin-coated vesicles. Rab11 is involved in the protein recycling through the recycling endosomes. Rab7 is associated to late endosomes, mediating their maturarion and fusion with lysosomes. Rab35 is known to regulate protein recycling to the plasma membrane, retrograde trafficking to the trans-Golgi Network, as well as regulating protein sorting and degradation through the endolysosomal pathway (adapted from (Stenmark, 2009)).

In these PhD studies, we focused on a specific Rab GTPase, Rab35. Rab35 was shown to be involved in the regulation of synaptic vesicle protein degradation through the regulation of the ESCRT complex (Sheehan et al., 2016; Uytterhoeven et al., 2011). Indeed, it was found that Hrs is an effector of Rab35, and is recruited upon Rab35 activation and subsequently serves to recruit downstream ESCRT pathway components (Sheehan et al., 2016). Interestingly, Rab35 and subsequent synaptic vesicle degradation was shown to be promoted by neuronal activity, consistent with its essential role in the maintenance of neuronal physiology and health (Sheehan et al., 2016).

Additional functions have been described for Rab35, such as regulation of a fast recycling pathway from early endosomes to the PM (Kouranti et al., 2006) and regulation of endocytic recycling (Kouranti et al., 2006). Furthermore, Rab35 regulates trafficking into the retrograde pathway, a

recycling pathway from endocytic compartments back to the TGN (Cauvin et al., 2016). Specifically, Rab35 activation was shown to increase the retrograde trafficking of Mannose-6-Phosphate Receptor, an important protein that mediates the delivery of enzymes to lysosomes. Interestingly, genes identified as risk factors for late-onset AD, namely VPS35 and VPS26, encode proteins that regulate the retrograde pathway (Small, 2008; Small et al., 2005).

Recent studies have begun to focus on the role of Rabs in neurodegenerative diseases including AD. Indeed, a subset of Rab GTPases, including Rab5 and Rab11, have been recently linked to AD neuropathology, through the regulation of APP amyloidogenic processing in endosomes (Ginsberg et al., 2012; Udayar et al., 2013). Additionally, it has been found that levels of specific Rab GTPases are altered in human patients with AD, highlighting the involvement of intracellular trafficking dynamics in disease pathophysiology (Ginsberg et al., 2010a, 2010b).

1.4 Chronic stress – a key precipitant of brain malfunction and AD

AD is increasingly accepted as a multifactorial disorder, with many risk factors suggested to precipitate AD. Recent attention has been given to the detrimental role of prolonged exposure to lifetime stress, as clinical studies suggest that stress may be causally related to AD. But how is stress defined and perceived by organisms?

1.4.1 Stress and the HPA axis

Nature seeks balance and equilibrium in its mechanisms. As such, living organisms tend to maintain their integrity and homeostatic balance with the internal and external environment. Stress is considered to be a disruption to homeostasis after the exposure to endogenous or exogenous challenges or "stressors", which are considered unpleasant or threatening to the system (Kloet et al., 2008; McEwen, 2003). The organism's response to stress represents an attempt to maintain its balance through the challenges presented, adapting and restoring homeostasis by generating a cascade of complex events. Effective coping requires the generation of a stress response upon exposure to a stressor, as well as its termination after stressor removal (Kloet et al., 2005). In organisms such as humans, maladaptive modifications can occur when the stress response is inappropriate and/or extended in time, leading to pathology in different systems, including the

nervous and immune systems (Sorrells and Sapolsky, 2007). The perception of stress challenges, as well as the persistence of their consequences, are very diverse among different individuals (Koolhaas et al., 2011).
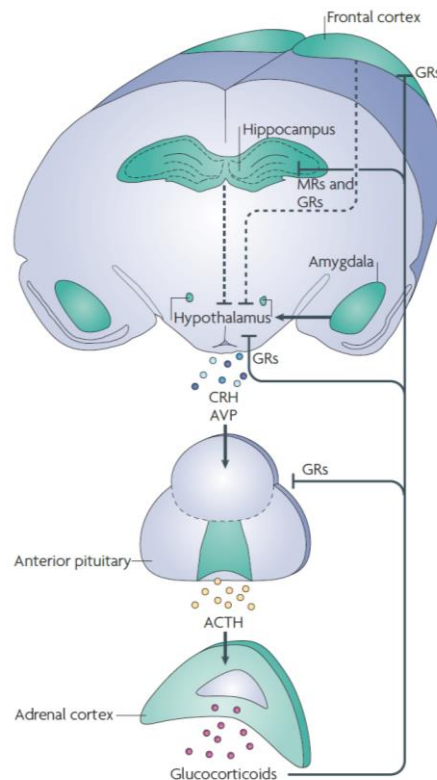
Figure 9. Schematic representation of the HPA axis. Upon stress exposure, CRH is released by the hypothalamus triggering ACTH release by the pituitary into the bloodstream. ACTH stimulates corticosteroid secretion by the adrenal cortex, which function as a negative feedback signal to the hypothalamus and

The physiological response to stress can be separated into two different phases, the fast and the delayed response phase. During the fast phase, also known as the "fight or flight" phase, activation of the autonomic nervous system (SNA) occurs, leading to the release of catecholamines such as adrenaline and noradrenaline from the adrenal medulla. This action heightens the body's responsiveness to the situation at hand by increasing respiratory frequency and heart rate, blood flow to vital organs, as well as blood pressure and basal metabolic rate. During the delayed response phase, activation of the hypothalamus-pituitary-adrenal (HPA) axis stimulates release of corticotropin-releasing hormone (CRH) in the paraventricular nucleus of the hypothalamus (PVN), which in turn promotes the release of adrenocorticotropic hormone (ACTH) from the pituitary, culminating in the secretion of glucocorticoids, the "stress hormones", by the cortex of the adrenal gland (Lupien et al., 2009). Glucocorticoids (GC) function as an inhibitory signal to the hypothalamus and pituitary, in a negative feedback loop of the HPA axis that is essential to prevent chronic hypersecretion of hormones, which could have deleterious effects such as loss of body mass and impaired immunity.

GC travel through the circulatory system, reaching every system in the human body and initiating adaptations to stressful events. GC are small, lipophilic molecules that can penetrate plasma membranes and the blood-brain barrier, exerting their effects on the brain through binding to glucocorticoid receptors (GR) and/or mineralocorticoids receptors (MR) within the cells (Kloet et al., 2005). Interestingly, corticosteroids show a higher affinity for MR, with GR demonstrating almost 10 fold lower affinity (Joëls and Baram, 2009). The difference in receptor affinity leads to preferential binding of GC to the MR, even at low levels, while the GR is only partially occupied under these conditions (Kloet et al., 2008). Thus, GR become increasingly activated as GC levels start to increase, which allows for a proper response and adaptation to stress. Upon entering the cell, GC bind to the GR, resulting in its homodimerization and translocation to the nucleus where it regulates gene transcription, thus affecting many cellular pathways and leading to an adaptative response to stress (Joëls and Baram, 2009). The GR initial activation by GC and translocation from cytoplasm to nucleus requires the involvement of molecular chaperones that bind to GR, such as Hsp90, Hsp70 and Hop. These are essential for opening of the GR binding cleft, enabling its steroid-binding activity (Murphy et al., 2003).

1.4.2. Stress action in the brain

GR are ubiquitously and abundantly expressed throughout the brain, exhibiting broad effects and making them important targets of stress exposure, while MR expression is restricted to specific brain areas such as the hippocampus and amygdala (Joëls and Baram, 2009). Together, both receptors regulate the brain's sensitivity for stress, and determine its adaptation and coping ability. Interestingly, it has been shown that changes in GR expression are involved in the brain's susceptibility to stress, as well as the development of neuropsychiatric disorders.

The hippocampus is a crucial area involved in memory formation and retrieval. Under normal conditions, GC are involved in synaptic plasticity regulation, modulating long-term potentiation (LTP), which is an essential event in memory formation (Diamond et al., 1992). However, under stressful situations and high GC levels, LTP is impaired, while long-term depression, leading to weakening of neuronal synapses, is facilitated. Furthermore, GC have also been implicated in adult neurogenesis, regulation of dendrite dynamics, glutamate transmission and neuronal calcium influx, likely through N-methyl-d-aspartate (NMDA) receptors (Cameron and Gould, 1994; Kim et al., 2002).

1.4.3. Chronic stress and brain pathology

Acute stress is usually adaptive and beneficial, having a crucial role in the maintenance of mental and physical health (Kloet et al., 2005). However, chronic exposure to stress can lead to maladaptive coping mechanisms, elevated levels of GC, and eventual brain damage. The effects of stress and the stress response vary among individuals, depending on personal coping strategies and stress sensitivity, making it difficult to understand the complete consequences of its exposure. However, some mechanisms and effects of chronic stress exposure are well documented.

Stress affects neuronal structural remodeling, altering brain morphology in a region-specific manner. Studies have shown that chronic stress induces a decrease in hippocampal and prefrontal cortex volume (Cerqueira et al., 2007a, 2007b; Pinto et al., 2014). Here, chronic stress leads to synaptic loss, as well as atrophy of apical, but not basal, dendrites of the hippocampal area CA3 and CA1 pyramidal neurons (Pinto et al., 2014; Sotiropoulos et al., 2008a). In humans, a positive correlation between elevated blood cortisol levels, reduced hippocampal size and impaired cognition has been observed, which is reversible following the decrease of corticosteroid levels. Interestingly, in other brain areas, such as the amygdala and nucleus accumbens, prolonged exposure to stress leads to an increase in dendritic arborization (Campioni et al., 2009; Sapolsky, 2003). Additionally, GC have been proposed to induce cell death of pyramidal neurons in the hippocampus, due to increased calcium influx and excitotoxicity. In more recent studies with animal models of stress, cell death was rarely found and happened only in the most extreme cases.

Stress and GC also significantly reduce adult neurogenesis in the dentate gyrus of the hippocampus, thus leading to a decreased number of newly generated neurons (Krishnan and Nestler, 2008). These new cells are functional, integrating into the hippocampal circuitry and being involved in memory formation. Altogether, these findings support a critical role of GC and stress in the regulation of brain morphology and function. However, the underlying molecular mechanism regulating these complex events are still not well understood.

	Prenatal stress	Postnatal stress	Stress in adolescence	Stress in adulthood	Stress in aging
Effect on HPA axis	Programming effects	Differentiation effects	Potentiation/ incubation effects	Maintenance/ manifestation effects	Maintenance/ manifestation effects
Outcome	↑ Glucocorticoids	↑ Glucocorticoids (maternal separation)	↑↑ Glucocorticoids	↑ Glucocorticoids (depression)	↑ Glucocorticoids (cognitive decline)
		↓ Glucocorticoids (severe trauma)	↓↓ Glucocorticoids	↓ Glucocorticoids (PTSD)	↓ Glucocorticoids (PTSD)

Figure 10. The influence of stress in the brain along the life cycle. Stress exposure influences brain in a variety of ways at different stages in life. Notably, brain areas that present a rapid decline with ageing are highly susceptible to the effect of stress exposure during adulthood and aging (red bars); adapted from (Lupien et al., 2009).

1.4.4 Chronic stress and AD neurodegeneration

Aged individuals have a compromised ability to cope with stress, and are at greater risk of suffering from maladaptive effects of excessive stress exposure. Inappropriate stress responses include exaggerated or prolonged GC release, indicating a deregulation of the HPA axis feedback mechanisms. Multiple links between chronic stress and AD neurodegenerative pathology have been described. Indeed, both AD and chronic stress cause synaptic loss and dendritic atrophy, leading to cognitive impairments (Sotiropoulos et al., 2008a). The GC negative feedback loop has also been shown to be reduced in AD patients as a major part of the AD patients exhibit dysregulation of HPA axis followed by elevated cortisol levels (Elgh et al., 2006). The latter positively correlates with the severity of cognitive impairment in these patients (Elgh et al., 2006). Furthermore, two transgenic AD mouse models exhibit altered corticosteroid secretion, although it is difficult to know whether this is cause or consequence of the disease (Green et al., 2006; Touma et al., 2004). Chronic stress also exacerbates memory deficits in AD transgenic mouse models, suggesting that stress accelerates disease progression (Jeong et al., 2006).

Additional evidence has revealed a close relationship between chronic stress/GC and AD disease mechanisms at the molecular level. Several studies demonstrate that chronic stress and GC promote APP processing through the amyloidogenic pathway, leading to increased C99 levels and Aβ

production (Catania et al., 2009a). In these studies, GC was shown to up-regulate APP and BACE1 transcription through GR binding, since both APP and BACE have glucocorticoid response elements (GRE) in their promoter regions (Green et al., 2006). Other reports also demonstrate increased levels of γ-secretase complex, such as Nicastrin, by chronic stress. Interestingly, it has been shown that GC potentiate APP misprocessing and Aβ production in AD models that were previously stressed, which is a finding of major importance, since stressful situations usually occur intermittently throughout life, instead of being the result of a single event (Catania et al., 2009a). Together, these studies suggest that stress has a cumulative effect on AD progression and that exposure to different events throughout live can potentiate the development of disease pathology.

Chronic stress and GC also aggravate Tau pathology, another key pathological mechanism of AD. Previous studies in animal models demonstrate that stress triggers Tau hyperphosphorylation and accumulation in neuronal cell bodies, affecting Tau phosphorylation at specific epitopes correlated with cytoskeletal pathology, synaptic loss, and hippocampal atrophy in AD patients (Sotiropoulos et al., 2011a). More recently, it has been demonstrated that GC and chronic stress are also responsible for the missorting and build-up of Tau in dendritic spines, leading to the accumulation of Tau with specific phosphorylation signatures (Pinheiro et al., 2016). In contrast to APP and BACE, the effect of GC on Tau levels is not dependent on its synthesis, since GC does not affect Tau expression levels (Sotiropoulos et al., 2008b). However, previous cellular and animal studies demonstrated that chronic stress and high GC levels trigger different aspects of Tau pathology, such as Tau hyperphosphorylation at different phospho-epitopes, truncation of Tau protein, as well as accumulation and aggregation of Tau into neurotoxic inclusions ((Sierra-fonseca and Gosselink, 2018; Sotiropoulos et al., 2011b)). Interestingly, recent studies also show that stress and GC cause missorting of Tau to synapses, triggering GluN2B-related excitotoxic signaling (Lopes et al., 2016b). Importantly, knockdown of Tau blocks stress-induced brain pathology, preventing neuronal dendritic atrophy and synaptic loss as well as memory and mood impairments (Lopes et al., 2016b). The above studies conclusively show that APP misprocessing and Tau accumulation represent key neuronal mechanisms through which chronic stress and elevated GC levels trigger neuronal malfunction, synaptic loss and memory impairment precipitating AD pathology. However, it remains unclear how stress and GC trigger the APP misprocessing and the generation of Aβ as well as the accumulation of hyperphosphorylated Tau and which mechanisms may participate in the intraneuronal processing and trafficking of both APP and Tau that facilitates the overproduction of Aβ and Tau accumulation in AD neurons. Based on the suggested critical role of Rab GTPases as master regulators of protein trafficking and proteostasis,

these PhD studies explore the role of Rabs in Aβ & Tau proteostasis and their significance in AD (etio)pathogenesis.
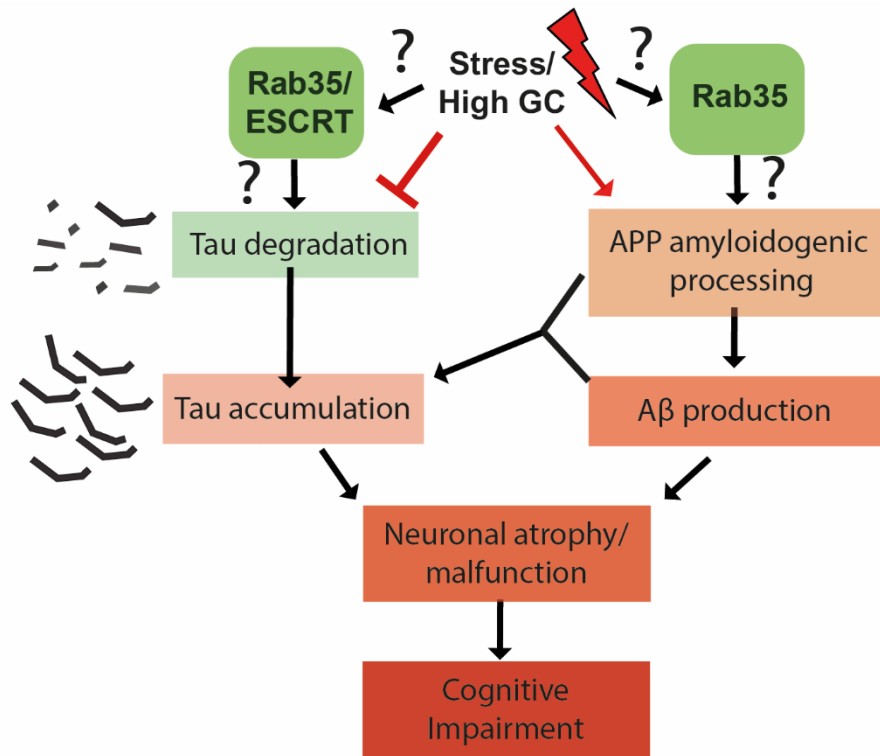
Figure 11. Schematic representation of the working hypothesis of these PhD studies monitoring the role of Rabs on intraneuronal mechanisms of trafficking and proteostasis related to APP misprocessing and Tau accumulation in stress and AD brain pathology.

Aims

Over the last decade, many research efforts have focused on elucidating the intracellular mechanisms that underlie Alzheimer's disease (AD), including Amyloid Precursor Protein (APP) misprocessing and accumulation of hyperphosphorylated Tau. However, our knowledge about the intracellular trafficking and processing of APP and Tau in both healthy and diseased neurons remains limited.

Rab GTPases are master regulators of endosomal protein trafficking, contributing to the structural and functional identity of intracellular membrane compartments. Given the critical roles of Rab GTPases in endosomal trafficking and in light of the growing awareness that endolysosomal defects are linked to the pathogenesis of neurodegenerative diseases, the main goal of this PhD thesis is to understand the role of the Rabs and endosomal-lysosomal system in the regulation of APP and Tau proteostasis, and its involvement in the intraneuronal mechanisms through which chronic stress and GC trigger APP misprocessing and Tau accumulation towards the precipitation of AD pathology. In particular, the objectives of this PhD thesis are summarized below:

- study the role of endolysosomal pathway in APP intracellular trafficking and proteostasis
- understand the involvement of Rab GTPases in Aβ generation under pathological conditions;
- clarify the potential involvement of ESCRT pathway and Rab GTPases in Tau degradation
- investigate the impact of chronic stress and main stress hormones, GC, on Rab GTPases and endolysosomal degradation as part of Tau accumulation and pathology;
- monitor the therapeutic potential of Rab35 against pathological conditions related to Tau accumulation and downstream neuronal malfunction and atrophy.

REFERENCES

Agostinho, P., and Pli, A. (2015). Localization and Trafficking of Amyloid-b Protein Precursor and Secretases: Impact on Alzheimer's Disease. J. Alzheimer's Dis. *45*, 329–347.

Alzheimer Europe (2013). Dementia in Europe Yearbook.

Andreadis, A., Brown, W.M., and Kosik, K.S. (1992). Structure and Novel Exons of the human Tau gene. Biochemistry 10626–10633.

Bakota, L., Ussif, A., Jeserich, G., and Brandt, R. (2017). Molecular and Cellular Neuroscience Systemic and network functions of the microtubule-associated protein tau : Implications for tau-based therapies. Mol. Cell. Neurosci.

Blard, O., Lecourtois, M., and Fre, T. (2005). Tau Is Not Normally Degraded by the Proteasome. J. Neurosci. Res. *405*, 400–405.

Brown, M.R., Bondada, V., Keller, J.N., and Thorpe, J. (2005). Proteasome or calpain inhibition does not alter cellular tau levels in neuroblastoma cells or primary neurons. J. Alzheimer's Dis. *7*, 15–24.

Cameron, H.A., and Gould, E. (1994). Adult neurogenesis is regulated by adrenal steroids in the dentate gyrus. Neuroscience *61*, 203–209.

Campioni, M.R., Xu, M., and Mcgehee, D.S. (2009). Stress-Induced Changes in Stress-induced changes in Nucleus Accumbens Glutamate Synaptic Plasticity. J Neurophysiol 3192–3198.

Catania, C., Sotiropoulos, I., Silva, R., Onofri, C., Breen, K.C., Sousa, N., and Almeida, O.F.X. (2009a). The amyloidogenic potential and behavioral correlates of stress. Mol. Psychiatry *14*, 95–105.

Catania, C., Sotiropoulos, I., Silva, R., Onofri, C., Breen, K.C., Sousa, N., and Almeida, O.F.X. (2009b). The amyloidogenic potential and behavioral correlates of stress. Mol. Psychiatry *14*, 95–105.

Cauvin, C., Rosendale, M., Gupta-Rossi, N., Rocancourt, M., Larraufie, P., Salomon, R., Perrais, D., and Echard, A. (2016). Rab35 GTPase Triggers Switch-like Recruitment of the Lowe Syndrome Lipid Phosphatase OCRL on Newborn Endosomes. Curr. Biol. *26*, 120–128.

Cerqueira, J., Taipa, R., and Uylings, H.B.M. (2007a). Specific Configuration of Dendritic Degeneration in Pyramidal Neurons of the Medial Prefrontal Cortex Induced by Differing Corticosteroid Regimens. Cereb. Cortex.

Cerqueira, J.J., Mailliet, F., Almeida, O.F.X., Jay, T.M., and Sousa, N. (2007b). The prefrontal cortex as a key target of the maladaptive response to stress. J. Neurosci. *27*, 2781–2787.

Chesser, A.S., Pritchard, S.M., and Johnson, G.V.W. (2013). Tau clearance mechanisms and their possible role in the pathogenesis of Alzheimer disease. Front. Neurol. *4 SEP*, 122.

Cirrito, J.R., Yamada, K. a, Finn, M.B., Sloviter, R.S., Bales, K.R., May, P.C., Schoepp, D.D., Paul, S.M., Mennerick, S., and Holtzman, D.M. (2005). Synaptic activity regulates interstitial fluid amyloid-beta levels in vivo. Neuron *48*, 913–922.

Cohen, T.J., Guo, J.L., Hurtado, D.E., Kwong, L.K., Mills, I.P., Trojanowski, J.Q., and Lee, V.M.Y. (2011). The acetylation of tau inhibits its function and promotes pathological tau aggregation. Nat. Commun. *2*, 252–259.

Congdon, E.E., Wu, J.W., Myeku, N., Figueroa, Y.H., Marinec, P.S., Gestwicki, J.E., Dickey, C.A., Yu, W.H., Duff, K.E., Congdon, E.E., et al. (2012). Methylthioninium chloride (methylene blue) induces autophagy and attenuates tauopathy in vitro and in vivo. Autophagy *8627*.

David, D.C., Layfield, R., Serpell, L., Narain, Y., Goedert, M., and Spillantini, M.G. (2002). Proteasomal degradation of tau protein. J. Neurochem. 176–185.

Dawson, H.N., Ferreira, A., Eyster, M. V, Ghoshal, N., Binder, L.I., and Vitek, M.P. (2001). Inhibition of neuronal maturation in primary hippocampal neurons from tau deficient mice. J. Cell Sci.

Delobel, P., Leroy, O., Hamdane, M., Sambo, A. V, Delacourte, A., and Bue, L. (2005). Proteasome inhibition and Tau proteolysis: an unexpected regulation. FEBS Lett. *579*, 1–5.

Diamond, D.M., Bennett, M.C., Fleshner, M., and Rose, G.M. (1992). Inverted-U Relationship Between the Level of Peripheral Corticosterone and the Magnitude of Hippocampal Primed Burst Potentiation. Hippocampus *2*, 421–430.

Dickey, C.A., Burrows, F., Petrucelli, L., Dickey, C.A., Kamal, A., Lundgren, K., Klosak, N., Bailey, R.M., Dunmore, J., Ash, P., et al. (2007). The high-affinity HSP90-CHIP complex recognizes and selectively degrades phosphorylated tau client proteins Find the latest version : The high-affinity HSP90-CHIP complex recognizes and selectively degrades phosphorylated tau client proteins. J. Clin. Invest. *117*, 648–658.

Dotti, C., Banker, G., and Binder, L. (1987). The expression and distribution of the microtubule-associated proteins Tau and Microtubule-associated protein 2 in hippocampal neurons in the rat in situ and in cell culture. Neuroscience *23*, 121–130.

Edgar, J.R., Wille, K., Gouras, G.K., and Futter, C.E. (2015). ESCRTs regulate amyloid precursor protein sorting in multivesicular bodies and intracellular amyloid- β accumulation. J. Cell Sci. 2520–2528.

Elgh, E., Lindqvist Åstot, A., Fagerlund, M., Eriksson, S., Olsson, T., and Näsman, B. (2006). Cognitive dysfunction, hippocampal atrophy and glucocorticoid feedback in Alzheimer's disease. Biol. Psychiatry *59*, 155–161.

Foret, L., Dawson, J.E., Collinet, C., Deutsch, A., Brusch, L., Zerial, M., and Kalaidzidis, Y. (2012). A General Theoretical Framework to Infer Endosomal Network Dynamics from Quantitative Image Analysis. 1381–1390.

Frandemiche, M.L., Seranno, S. De, Rush, T., Borel, E., Arnal, I., Fourier, J., Institut, G., and Cedex, G. (2014). Activity-Dependent Tau Protein Translocation to Excitatory Synapse Is Disrupted by Exposure to Amyloid-Beta Oligomers. J. Neurosci. *34*, 6084–6097.

Futter, C.E., Pearse, A., and Hewlett, L.J. (1996). Multivesicular Endosomes Containing Internalized EGF-EGF Receptor Complexes Mature and Then Fuse Directly with Lysosomes. *132*, 1011–1023.

Giannakopoulos, P., and Herrmann, F.R. (2003). Tangle and neuron numbers, but not amyloid load, predict cognitive status in Alzheimer's disease. Neurology.

Ginsberg, S.D., Alldred, M.J., Counts, S.E., Cataldo, A.M., Neve, R.L., Jiang, Y., Wuu, J., Chao, M. V., Mufson, E.J., Nixon, R.A., et al. (2010a). Microarray analysis of hippocampal CA1 neurons implicates early endosomal dysfunction during Alzheimer's disease progression. Biol. Psychiatry *68*, 885–893.

Ginsberg, S.D., Mufson, E.J., Counts, S.E., Wuu, J., Alldred, M.J., Nixon, R.A., and Che, S. (2010b). Regional selectivity of rab5 and rab7 protein upregulation in mild cognitive impairment and Alzheimer's disease. J. Alzheimer's Dis. *22*, 631–639.

Ginsberg, S.D., Mufson, E.J., Alldred, M.J., Counts, S.E., Wuu, J., Nixon, R.A., and Che, S. (2012). Upregulation of select rab GTPases in cholinergic basal forebrain neurons in mild cognitive impairment and Alzheimer's disease. J Chem Neuroanat. *42*, 102–110.

Gomez-isla, T., Hollister, R., West, H., Mui, S., Growdon, J.H., Petersen, R.C., Parisi, J.E., and Hyman, B.T. (1997). Neuronal loss correlates with but exceeds neurofibrillary tangles in Alzheimer's Disease. Ann Neurol 17–24.

Götz, J., Xia, D., Leinenga, G., Chew, Y.L., and Nicholas, H.R. (2013). What renders TAU toxic. Front. Neurol. *4*, 1–10.

Green, K.N., Billings, L.M., Roozendaal, B., McGaugh, J.L., and LaFerla, F.M. (2006). Glucocorticoids increase amyloid-beta and tau pathology in a mouse model of Alzheimer's disease. J. Neurosci. *26*, 9047–9056.

Haass, C., Koo, E.H., Mellon, A., Hung, A.Y., and Selkoe, D.J. (1992). Targeting of cell-surface p -

amyloid precursor protein to lysosomes : alternative processing into amyloid-bearing fragments g Lysate I. Nature *357*, 9–12.

Haass, C., Kaether, C., Thinakaran, G., and Sisodia, S. (2012). Trafficking and Proteolytic Processing of APP. Cold Spring Harb. Perspect. Biol. 1–26.

Hamano, T., Gendron, T.F., Causevic, E., Yen, S., Lin, W., Isidoro, C., Deture, M., and Ko, L. (2008). Autophagic-lysosomal perturbation enhances tau aggregation in transfectants with induced wild-type tau expression. Eur. J. Neurosci. *27*, 1119–1130.

Harada, A., Oguchi, K., Okabe, S., Kuno, J., Terada, S., Ohshima, T., Sato-Yoshitake, R., Takei, Y., Noda, T., and Hirokawa, N. (1994). Altered microtubule organization in small-calibre axons of mice lacking tau protein. Nature.

Hoover, B.R., Reed, M.N., Su, J., Penrod, R.D., Kotilinek, L.A., Grant, M.K., Pitstick, R., Carlson, G.A., Lanier, L.M., Yuan, L., et al. (2010). Article Tau Mislocalization to Dendritic Spines Mediates Synaptic Dysfunction Independently of Neurodegeneration. Neuron *68*, 1067–1081.

Huotari, J., and Helenius, A. (2011). Endosome maturation. EMBO J. *30*, 3481–3500.
Ingelsson, M., Fukumoto, H., and Newell, K.L. (2004). Early Aβ accumulation and progressive synaptic loss, gliosis, and tangle formation in AD brain. Neurology.

Jeong, Y.H., Park, C.H., Yoo, J., Shin, K.Y., Ahn, S., Kim, H., Lee, S.H., Emson, P.C., Suh, Y., Creative, N., et al. (2006). Chronic stress accelerates learning and memory impairments and increases amyloid deposition in APP. *22*, 1–22.

Joëls, M., and Baram, T.Z. (2009). The neuro-symphony of stress. Nat. Rev. Neurosci. *10*, 459–466.
Kaushik, S., Wong, E., Wang, Y., Martinez-vicente, M., Kru, U., Mandelkow, E., Cuervo, A.M., and Mandelkow, E. (2009). Tau fragmentation , aggregation and clearance: the dual role of lysosomal processing. Hum. Mol. Genet. *18*, 4153–4170.

Kim, J.J., Diamond, D.M., Haven, N., and Blvd, B.B.D. (2002). The stressed hippocampus, synaptic plasticity and lost memories. Nat. Rev. Neurosci. *3*.

Kloet, E.R. De, Joëls, M., and Holsboer, F. (2005). Stress and the brain: from adaption to disease. Nat. Rev. Neurosci. 463–475.

Kloet, E.R. De, Karst, H., and Joe, M. (2008). Corticosteroid hormones in the central stress response : Quick-and-slow. Front. Neuroendocrinol. *29*, 268–272.

Klumperman, J., and Raposo, G. (2014). The Complex Ultrastructure of the Endolysosomal system. Cold Spring Harb. Perspect. Biol.

Koolhaas, J.M., Bartolomucci, A., Buwalda, B., Boer, S.F. De, Flügge, G., Korte, S.M., Meerlo, P., Murison, R., Olivier, B., Palanza, P., et al. (2011). Stress revisited : A critical evaluation of the stress concept. Neurosci. Biobehav. Rev. *35*, 1291–1301.

Kouranti, I., Sachse, M., Arouche, N., Goud, B., and Echard, A. (2006). Rab35 Regulates an Endocytic Recycling Pathway Essential for the Terminal Steps of Cytokinesis. Curr. Biol. *16*, 1719–1725.

Krishnan, V., and Nestler, E.J. (2008). The molecular neurobiology of depression. Nature *455*.

Krüger, U., Wang, Y., Kumar, S., and Mandelkow, E. (2012). Autophagic degradation of tau in primary neurons and its enhancement by trehalose. Neurobiol. Aging *33*, 2291–2305.

Lavenir, I., Ozcelik, S., Tolnay, M., Winkler, D.T., and Goedert, M. (2012). Stimulation of autophagy reduces neurodegeneration in a mouse model of human tauopathy. Brain 2169–2177.

Lloret, A., Fuchsberger, T., Giraldo, E., and Viña, J. (2015). Free Radical Biology and Medicine Molecular mechanisms linking amyloid β toxicity and Tau hyperphosphorylation in Alzheimer ' s disease. Free Radic. Biol. Med. *83*, 186–191.

Lopes, S., Lopes, A., Guimaraes, M.R., Sardinha, V.M., Duarte-silva, S., Pinheiro, S., Oliveira, F., Sousa, N., Leite-almeida, H., and Sotiropoulos, I. (2016a). Absence of Tau triggers age-dependent sciatic nerve morphofunctional deficits and motor impairment. Aging Cell 208–216.

Lopes, S., Vaz-Silva, J., Pinto, V., Dalla, C., Kokras, N., Bedenk, B., Mack, N., Czisch, M., Almeida, O.F.X., Sousa, N., et al. (2016b). Tau protein is essential for stress-induced brain pathology. Proc. Natl. Acad. Sci. *113*, E3755–E3763.

Lupien, S.J., Mcewen, B.S., Gunnar, M.R., and Heim, C. (2009). Effects of stress throughout the lifespan on the brain, behaviour and cognition. Nat. Rev. Neurosci. *10*.

Mandell, J.W., and Banker, G.A. (1996). A Spatial Gradient of Tau Protein Phosphorylation in Nascent Axons. J. Neurosci. *16*, 5727–5740.

Masters, C.L., and Selkoe, D.J. (2012). Biochemistry of Amyloid b -Protein and Amyloid Deposits in Alzheimer Disease. Cold Spring Harb. Perspect. Med.

Maxfield, F.R. (2014). Role of Endosomes and Lysosomes in Human Disease.

Mayeux, R., and Stern, Y. (2012). Epidemiology of Alzheimer Disease.

McEwen, B.S. (2003). Mood Disorders and Allostatic Load. Biol. Psychiatry.

Min, Q., Lee, J., Hoon, J., and Rubinsztein, D.C. (2013). Tau degradation : The ubiquitin – proteasome system versus the autophagy-lysosome system. Prog. Neurobiol. 1–11.

Min, S., Cho, S., Zhou, Y., Schroeder, S., Haroutunian, V., Seeley, W.W., Huang, E.J., Shen, Y., Masliah, E., Mukherjee, C., et al. (2010). Acetylation of Tau Inhibits Its Degradation and Contributes to Tauopathy. Neuron *67*, 953–966.

Moore, S., Evans, L.D.B., Andersson, T., Portelius, E., Smith, J., Dias, T.B., Saurat, N., McGlade, A., Kirwan, P., Blennow, K., et al. (2015). APP Metabolism Regulates Tau Proteostasis in Human Cerebral Cortex Neurons. Cell Rep. *11*, 689–696.

Morris, M., Knudsen, G.M., Maeda, S., Trinidad, J.C., Ioanoviciu, A., Burlingame, A.L., and Mucke, L. (2015). Tau post-translational modifications in wild-type and human amyloid precursor protein transgenic mice. Nat. Neurosci.

Mucke, L., and Selkoe, D.J. (2012). Neurotoxicity of amyloid-b protein. Cold Spring Harb. Perspect. Med. 1–18.

Murphy, P.J.M., Morishima, Y., Chen, H., Galigniana, M.D., Mansfield, J.F., Simons, S.S., and Pratt, W.B. (2003). Visualization and Mechanism of Assembly of a Glucocorticoid Receptor Hsp70 Complex That Is Primed for Subsequent Hsp90-dependent Opening of the Steroid Binding Cleft. J. Biol. Chem. *278*, 34764–34773.

Nelson, P.T., Alafuzoff, I., Bigio, E.H., Bouras, C., Braak, H., Cairns, N.J., Castellani, R.J., Crain, B.J., Davies, P., Tredici, K. Del, et al. (2012). Correlation of Alzheimer Disease Neuropathologic Changes With Cognitive Status : A Review of the Literature. J Neuropathol Exp Neurol *71*, 362–381.
OECD Indicators (2017). Health at a Glance 2017.

Palop, J.J., and Mucke, L. (2010). Disease : From Synapses toward Neural Networks. Nat. Neurosci. *13*, 812–818.

Pinheiro, S., Silva, J., Mota, C., Vaz-silva, J., and Veloso, A. (2016). Tau Mislocation in Glucocorticoid-Triggered Hippocampal Pathology. Mol. Neurobiol. 4745–4753.

Pinto, V., Costa, J.C., Morgado, P., Mota, C., Miranda, A., Bravo, F. V, Oliveira, T.G., Cerqueira, J.J., and Sousa, N. (2014). Differential impact of chronic stress along the hippocampal dorsal – ventral axis. Brain Struct Func.

Piper, R.C., Dikic, I., and Lukacs, G.L. (2014). Ubiquitin-Dependent Sorting in Endocytosis. Cold Spring Harb. Perspect. Med.
Poteryaev, D., Datta, S., Ackema, K., Zerial, M., and Spang, A. (2010). Identification of the Switch in

Early-to-Late Endosome Transition. Cell *141*, 497–508.

Qiu, C., and Kivipelto, M. (2009). Epidemiology of Alzheimer's disease: occurrence, determinants, and strategies toward intervention. Dialogues Clin. Neurosci. 111–128.

Querfurth, H.W., and Laferla, F.M. (2010). Alzheimer's Disease. N. Engl. J. Med. 329–344.
Rapoport, M., Dawson, H.N., Binder, L.I., Vitek, M.P., and Ferreira, A. (2002). Tau is essential to Beta-amyloid-induced neurotoxicity. Proc. Natl. Acad. Sci.

Rink, J., Ghigo, E., Kalaidzidis, Y., and Zerial, M. (2005). Rab Conversion as a Mechanism of Progression from Early to Late Endosomes. Cell *122*, 735–749.

Roberson, E.D., Scearce-Levie, K., Palop, J.J., Yan, F., Cheng, I.H., Wu, T., Gerstein, H., Yu, G.-Q., and Mucke, L. (2007). Reducing endogenous tau ameliorates amyloid beta-induced deficits in an Alzheimer's disease mouse model. Science *316*, 750–754.

Sapolsky, R.M. (2003). Stress and Plasticity in the Limbic System. Neurochem. Res. *28*, 1735–1742.
Schmid, S.L., Sorkin, A., Zerial, M., and Lewis, W.H. (2014). Endocytosis : Past , Present , and Future. *2*.

Scott, C.C., Vacca, F., and Gruenberg, J. (2014). Seminars in Cell & Developmental Biology Endosome maturation , transport and functions. Semin. Cell Dev. Biol. *31*, 2–10.

Serrano-pozo, A., Frosch, M.P., Masliah, E., and Hyman, B.T. (2011). Neuropathological Alterations in Alzheimer Disease. 1–24.

Sheehan, P., and Waites, C.L. (2017). Coordination of synaptic vesicle trafficking and turnover by the Rab35 signaling network. Small GTPases *0*, 1–10.

Sheehan, P., Zhu, M., Beskow, A., Vollmer, C., and Waites, C.L. (2016). Activity-Dependent Degradation of Synaptic Vesicle Proteins Requires Rab35 and the ESCRT Pathway. J. Neurosci. *36*, 8668–8686.

Shimura, H., Schwartz, D., Gygi, S.P., and Kosik, K.S. (2004). CHIP-Hsc70 Complex Ubiquitinates Phosphorylated Tau and Enhances Cell Survival *. J. Biol. Chem. *279*, 4869–4876.

Sierra-fonseca, J.A., and Gosselink, K.L. (2018). Tauopathy and neurodegeneration : A role for stress. Neurobiol. Stress *9*, 105–112.

Small, S.A. (2008). Retromer Sorting: A Pathogenic Pathway in Late-Onset Alzheimer Disease. Arch. Neurol. *65*, 323–328.

Small, D.H., Mok, S.S., and Bornstein, J.C. (2001). Alzheimer's disease and Aβ toxicity: from top to bottom. Nat. Rev. Neurosci.

Small, S.A., Kent, K., Pierce, A., Leung, C., Kang, M.S., Okada, H., Honig, L., Vonsattel, J.P., and Kim, T.W. (2005). Model-guided microarray implicates the retromer complex in Alzheimer's disease. Ann. Neurol. *58*, 909–919.

Small, S.A., Simoes-Spassov, S., Mayeux, R., and Petsko, G.A. (2017). Endosomal Traffic Jams Represent a Pathogenic Hub and Therapeutic Target in Alzheimer's Disease. Trends Mol. Med. *40*, 592–602.

Sorrells, S.F., and Sapolsky, R.M. (2007). An Inflammatory Review of Glucocorticoid Actions in the CNS. Brain Behav Immun *21*, 259–272.

Sotiropoulos, I., Cerqueira, J.J., Catania, C., Takashima, a., Sousa, N., and Almeida, O.F.X. (2008a). Stress and glucocorticoid footprints in the brain-The path from depression to Alzheimer's disease. Neurosci. Biobehav. Rev. *32*, 1161–1173.

Sotiropoulos, I., Catania, C., Riedemann, T., Fry, J., Breen, K., Michaelidis, T., and Almeida, O. (2008b). Glucocorticoids trigger Alzheimer disease-like pathobiochemistry in rat neuronal cells expressing human tau. J. Neurochem. 385–397.

Sotiropoulos, I., Catania, C., Pinto, L.G., Silva, R., Pollerberg, G.E., Takashima, A., Sousa, N., and Almeida, O.F.X. (2011a). Stress acts cumulatively to precipitate Alzheimer's disease-like tau pathology and cognitive deficits. J. Neurosci. *31*, 7840–7847.

Sotiropoulos, I., Catania, C., Pinto, L.G., Silva, R., Pollerberg, G.E., Takashima, A., Sousa, N., and Almeida, O.F.X. (2011b). Stress acts cumulatively to precipitate Alzheimer's disease-like tau pathology and cognitive deficits. J. Neurosci. *31*, 7840–7847.

Spires-jones, T.L., and Hyman, B.T. (2014). The Intersection of Amyloid Beta and Tau at Synapses in Alzheimer ' s Disease. Neuron *82*, 756–771.

Stenmark, H. (2009). Rab GTPases as coordinators of vesicle traffic. Nat. Rev. Mol. Cell Biol. *10*, 513–525.

Touma, C., Ambrée, O., Görtz, N., Keyvani, K., Lewejohann, L., Palme, R., Paulus, W., Schwarze-eicker, K., and Sachser, N. (2004). Age- and sex-dependent development of adrenocortical hyperactivity in a transgenic mouse model of Alzheimer ' s disease. Neurobiol. Aging *25*, 893–904.

Tracy, T.E., Sohn, P.D., Minami, S.S., Ellerby, L.M., Huganir, R.L., Gan, L., Tracy, T.E., Sohn, P.D., Minami, S.S., Wang, C., et al. (2016). Acetylated Tau Obstructs KIBRA-Mediated Signaling Related

Memory Loss Article Acetylated Tau Obstructs KIBRA-Mediated Signaling in Synaptic Plasticity and Promotes Tauopathy-Related Memory Loss. Neuron *90*, 245–260.

Tseng, B.P., Green, K.N., Chan, J.L., Blurton-Jones, M., and LaFerla, F.M. (2008). Ab inhibits the proteasome and enhances amyloid and tau accumulation. Neurobiol. Aging *29*, 1607–1618.

Ubelmann, F., Burrinha, T., Salavessa, L., Gomes, R., and Ferreira, C. (2017). Bin1 and CD2AP polarise the endocytic generation of beta-amyloid. EMBO Rep. *18*, 102–122.

Udayar, V., Buggia-Prévot, V., Guerreiro, R.L., Siegel, G., Rambabu, N., Soohoo, A.L., Ponnusamy, M., Siegenthaler, B., Bali, J., Simons, M., et al. (2013). A paired RNAi and RabGAP overexpression screen identifies Rab11 as a regulator of β-amyloid production. Cell Rep. *5*, 1536–1551.

Uytterhoeven, V., Kuenen, S., Kasprowicz, J., Miskiewicz, K., and Verstreken, P. (2011). Loss of skywalker reveals synaptic endosomes as sorting stations for synaptic vesicle proteins. Cell *145*, 117–132.

Wandinger-ness, A., and Zerial, M. (2014). Rab Proteins and the Compartmentalization of the Endosomal System.

Wang, Y., and Mandelkow, E. (2012). Degradation of tau protein by autophagy and proteasomal pathways. Biochem. Soc. Trans. *40*, 644–652.

Williams, R.L., and Urbé, S. (2007). The emerging shape of the ESCRT machinery. *8*, 355–368.
Zeigerer, A., Gilleron, J., Bogorad, R.L., Marsico, G., Nonaka, H., Seifert, S., Epstein-barash, H., Kuchimanchi, S., Peng, C.G., Ruda, V.M., et al. (2012). Rab5 is necessary for the biogenesis of the endolysosomal system in vivo. Nature *485*, 465–470.

Zempel, H., Luedtke, J., Kumar, Y., Biernat, J., Dawson, H., Mandelkow, E., and Mandelkow, E. (2013). Amyloid- b oligomers induce synaptic damage via and spastin. EMBO J. *32*, 2920–2937.

CHAPTER 2

EXPERIMENTAL WORK

Chapter 2.1

João Vaz-Silva, Gomes P, Jin Q, Zhu M, Zhuravleva V, Quintremil S, Meira T, Silva J, Dioli C, Soares-Cunha C, Daskalakis NP, Sousa N, Ioannis Sotiropoulos & Clarissa L Waites

Endolysosomal degradation of Tau and its role in

glucocorticoid-driven hippocampal malfunction

SOURCE DATA TRANSPARENT PROCESS

THE EMBO JOURNAL

Article

Endolysosomal degradation of Tau and its role in glucocorticoid-driven hippocampal malfunction

João Vaz-Silva[1,2,3] (iD), Patrícia Gomes[1,2,†], Qi Jin[3,†], Mei Zhu[3,†], Viktoriya Zhuravleva[3,4,†], Sebastian Quintremil[3] (iD), Torcato Meira[1,2,5], Joana Silva[1,2], Chrysoula Dioli[1,2] (iD), Carina Soares-Cunha[1,2], Nikolaos P Daskalakis[6], Nuno Sousa[1,2], Ioannis Sotiropoulos[1,2,‡] (iD) & Clarissa L Waites[3,5,*,‡] (iD)

Abstract

Emerging studies implicate Tau as an essential mediator of neuronal atrophy and cognitive impairment in Alzheimer's disease (AD), yet the factors that precipitate Tau dysfunction in AD are poorly understood. Chronic environmental stress and elevated glucocorticoids (GC), the major stress hormones, are associated with increased risk of AD and have been shown to trigger intracellular Tau accumulation and downstream Tau-dependent neuronal dysfunction. However, the mechanisms through which stress and GC disrupt Tau clearance and degradation in neurons remain unclear. Here, we demonstrate that Tau undergoes degradation via endolysosomal sorting in a pathway requiring the small GTPase Rab35 and the endosomal sorting complex required for transport (ESCRT) machinery. Furthermore, we find that GC impair Tau degradation by decreasing Rab35 levels, and that AAV-mediated expression of Rab35 in the hippocampus rescues GC-induced Tau accumulation and related neurostructural deficits. These studies indicate that the Rab35/ESCRT pathway is essential for Tau clearance and part of the mechanism through which GC precipitate brain pathology.

Introduction

Intraneuronal accumulation of Tau protein represents a central pathogenic process in Alzheimer's disease (AD) and is hypothesized to mediate the detrimental effects of amyloid-beta (Aβ) on neuronal

function and cognitive performance (Roberson *et al*, 2007; Ittner *et al*, 2010; Guo *et al*, 2017). Tau accumulation and hyperphosphorylation is linked to synaptic atrophy, neuronal dysfunction, and cognitive deficits (Kimura *et al*, 2007; Yin *et al*, 2016), and triggers these events by disrupting axonal trafficking (Vossel *et al*, 2010), promoting GluN2B-related excitotoxicity (Ittner *et al*, 2010; Zempel *et al*, 2010), and suppressing nuclear CREB-mediated synthesis of synapse- and memory-related proteins (Yin *et al*, 2016), among other effects. Furthermore, emerging studies support a crucial role for Tau in diverse brain pathologies (for review, see Sotiropoulos *et al*, 2017) including prolonged exposure to stressful conditions, a known risk factor for AD and major depressive disorder (Vyas *et al*, 2016). In particular, recent studies demonstrate that exposure to chronic environmental stress or the major stress hormones, glucocorticoids (GC), triggers the accumulation of Tau and its synaptic missorting, precipitating dendritic atrophy and synaptic dysfunction in a Tau-dependent manner (Pinheiro *et al*, 2015; Lopes *et al*, 2016a,b; Pallas-Bazarra *et al*, 2016; Dioli *et al*, 2017). However, the cellular mechanisms responsible for stress/GC-induced accumulation of Tau remain unclear.

A major cause of Tau accumulation is the dysfunction of its degradative pathways (Khanna *et al*, 2016). Tau degradation has been shown to occur through two distinct mechanisms, the ubiquitin–proteasome system and the autophagy–lysosome pathway (Lee *et al*, 2013; Zhang *et al*, 2017a). Indeed, proteasome and lysosome inhibitors can delay Tau turnover and promote Tau-driven neuropathology (Zhang *et al*, 2005; Hamano *et al*, 2008). However, dysfunction of a third degradative pathway, the endolysosomal system, is also linked to AD and other neurodegenerative conditions that exhibit Tau accumulation, including Parkinson's disease (Rivero-Rios *et al*, 2015; Kett & Dauer, 2016; Small *et al*, 2017). Nevertheless, the role of the endolysosomal pathway in the clearance of Tau is almost completely unexplored.

Here, we report that the small GTPase Rab35 and the endosomal sorting complex required for transport (ESCRT) machinery mediate

1 Life and Health Sciences Research Institute (ICVS), School of Medicine, University of Minho, Braga, Portugal
2 ICVS/3B's - PT Government Associate Laboratory, Braga, Portugal
3 Department of Pathology and Cell Biology, Taub Institute for Research on Alzheimer's Disease and the Aging Brain, Columbia University Medical Center, New York, NY, USA
4 Neurobiology and Behavior Graduate Program, Columbia University, New York, NY, USA
5 Department of Neuroscience, Columbia University, New York, NY, USA
6 Department of Psychiatry, McLean Hospital, Harvard Medical School, Belmont, MA, USA
   *Corresponding author. Tel: +1 212 305 6025; E-mail: cw2622@cumc.columbia.edu
   †These authors contributed equally to this work
   ‡These authors contributed equally to this work

the delivery of Tau to lysosomes via early endosomes and multi-vesicular bodies (MVBs). We further demonstrate that this pathway is negatively regulated by GC, which suppress Rab35 transcription, thereby inhibiting Tau degradation and promoting its accumulation. Finally, we show that *in vitro* and *in vivo* overexpression of Rab35 can rescue GC-induced Tau accumulation and neurostructural deficits in hippocampal neurons. These findings demonstrate Rab35's critical role as a regulator of Tau clearance under physiological and pathological conditions.

Results

The ESCRT pathway is necessary and sufficient for Tau degradation

Despite its primarily axonal and microtubule-related distribution, Tau is also found in the somatodendritic compartment and associated with lipid membranes (Pooler & Hanger, 2010; Georgieva *et al*, 2014). To determine whether Tau undergoes endosomal sorting, we looked for Tau immunoreactivity in multivesicular bodies (MVBs), late endosomal structures that deliver cargo to lysosomes. Immuno-electron microscopy in rat hippocampal tissue revealed MVBs that contain Tau immunogold labeling (Figs 1A and EV1A), indicating that Tau is sorted into MVBs and can potentially undergo degradation via the endocytic pathway. MVB biogenesis is catalyzed by the endosomal sorting complex required for transport (ESCRT) system, a series of protein complexes that recruit ubiquitylated cargo destined for degradation and facilitate the formation of intraluminal vesicles (Raiborg & Stenmark, 2009). The initial component of the ESCRT-0 complex, Hrs, is essential for binding and recruitment of ubiquity-lated cargo into MVBs (Raiborg & Stenmark, 2009; Frankel & Audhya, 2017). To examine whether Hrs interacts with Tau, we performed the proximity ligation assay (PLA; see Fig 1B) in N2a cells overexpressing mCh-tagged Hrs (Figs 1C and EV1B). Here, we detected fluorescent puncta, representing close (20–50 nm) proximity of Hrs and Tau, that were associated with Hrs-positive early endosomes (Fig 1C) and increased upon overexpression of GFP-tagged wild-type Tau (GFP-wtTau; 0N4R isoform; Hoover *et al*, 2010; Fig EV1C and D), demonstrating specificity of the PLA signal for the Hrs/Tau interaction. This interaction was confirmed by coimmuno-precipitation (IP) experiments in N2a cells overexpressing FLAG-Hrs and either GFP or GFP-wtTau, wherein Hrs was specifically pulled down by GFP-wtTau (Fig EV1E). Treatment with a deubiquitylating enzyme (DUB) inhibitor to increase ubiquitylated Tau species further increased the Hrs/Tau interaction as measured by both co-IP and PLA (Fig EV1F–I), indicating that ubiquitylation promotes Tau's association with Hrs and subsequent entry into the ESCRT pathway. Using super-resolution fluorescence microscopy, we also identified Tau in both membranes and lumen of Hrs-, EEA1-, and Rab5-positive early endosomes in N2a cells (Fig 1D and E). These findings demonstrate the presence of Tau in endosomal compartments at both early and late stages of the endolysosomal pathway.

Rab35 promotes Tau degradation through the ESCRT pathway

To assess the role of the ESCRT pathway in Tau clearance (Fig 2A), we measured Tau degradation in primary hippocampal neurons

lentivirally transduced with an shRNA against TSG101, an essential component of the ESCRT-I complex. Depletion of TSG101 is a common mechanism for blocking degradation of ESCRT pathway cargo (Edgar *et al*, 2015; Maminska *et al*, 2016), and our shTSG101 hairpin reliably reduces TSG101 levels by ~60% (Fig EV2A and B). Using a previously described cycloheximide (CHX)-chase assay to measure the fold change in Tau degradation (Sheehan *et al*, 2016), we found that shTSG101 decreased this value by 30% (Fig 2B and C), indicating its ability to inhibit Tau degradation. Conversely, activation of the ESCRT pathway by TSG101 overexpression increased Tau degradation by ~30% (Fig 2D and E). Together, these findings indicate that the ESCRT pathway is both necessary and sufficient for mediating Tau degradation.

In recent work, we demonstrated that ESCRT-0 protein Hrs is an effector of the small GTPase Rab35 and is recruited by active Rab35 to catalyze downstream ESCRT recruitment and MVB formation (Sheehan *et al*, 2016). Therefore, we investigated whether Rab35 is also a key regulator of Tau degradation. Again using the CHX-chase assay, we measured Tau degradation in neurons transduced with a previously characterized shRNA to knockdown Rab35 (shRab35; Fig EV2C and D; Sheehan *et al*, 2016). We found that shRab35 decreased Tau degradation by ~30% (Fig 2F and G), indicative of Rab35's role in this process. Moreover, overexpression/gain-of-function of mCherry-tagged Rab35 increased Tau degradation by nearly 50% compared to mCh control (Fig 2H and I), demonstrating that Rab35 is a potent regulator of Tau turnover.

We further confirmed the effect of Rab35 on Tau with a flow cytometry assay using N2a cells transfected with HA-Rab35 and medium fluorescent timer (FT)-tagged wtTau (FT-Tau). The emission of medium FT changes from blue to red as it matures, with half-maximal red fluorescence at 3.9 h (Fig 2J; Subach *et al*, 2009), and this fluorophore has previously been used to monitor protein degradation based on the intensities of red ("older") vs. blue ("younger") fluorescent protein in cells (Fernandes *et al*, 2014). We found that the ratio of red:blue (old:new) FT-Tau was significantly lower in N2a cells co-expressing HA-Rab35 compared to HA vector control (Fig 2K), indicating faster Tau degradation. Rab35 overexpression did not alter the red:blue ratio when FT alone was expressed in N2a cells (Fig EV2E), confirming that Rab35 specifically stimulates Tau degradation. Given that Tau hyperphosphorylation is a key pathogenic event in AD and other tauopathies (Guo *et al*, 2017), we also evaluated whether Rab35 could stimulate the degradation of hyperphosphorylated Tau, using the phospho-mimetic E14 Tau mutant, in which 14 serine and threonine residues are replaced with glutamic acid (Hoover *et al*, 2010). The ratio of red:blue FT-TauE14 was again significantly lower in HA-Rab35-expressing N2a cells (Fig 2L), indicating Rab35's ability to mediate the degradation of phosphorylated Tau.

Since Tau is phosphorylated at multiple sites, we used antibodies against several phospho-Tau epitopes related to pathogenic Tau activity, including Ser396/404, Ser262, and Ser202, to determine which Tau species were sensitive to Rab35/ESCRT-mediated degradation. Interestingly, we found that degradation of both pSer396/404-Tau and pSer262-Tau (measured by CHX-chase assay) was significantly slowed by knockdown of Rab35, while pSer202-Tau was unaffected (Fig 3A and B). We saw similar results with knockdown of TSG101 (Fig EV2F and G). To further verify that Rab35 stimulates Tau degradation through the ESCRT
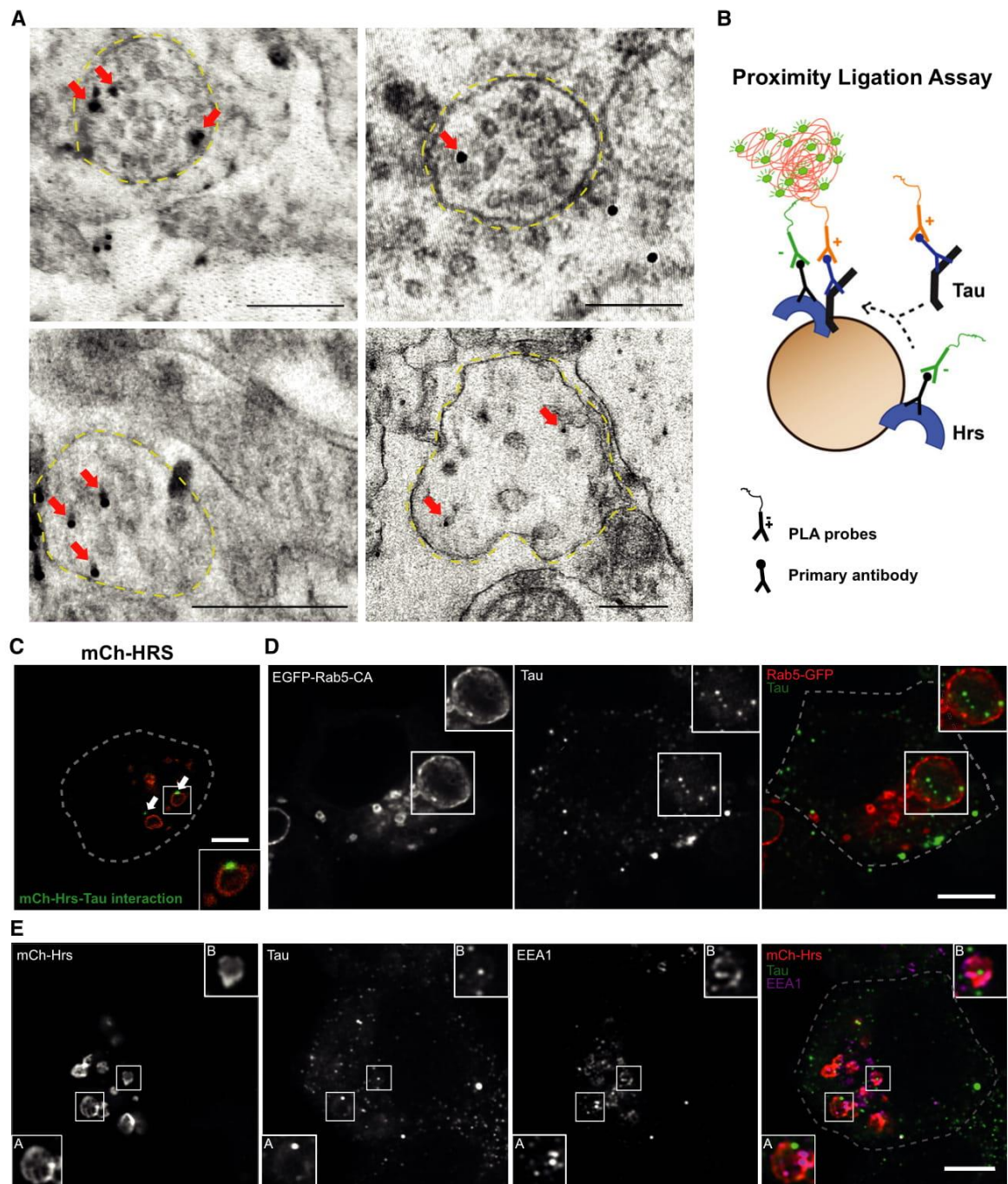
Figure 1. Tau protein localizes to early endosomes and MVBs.

A   Electron micrographs of immunogold-labeled Tau (arrows) in multivesicular bodies (yellow dashed lines) of rat hippocampus (scale bar: 250 nm).

B   Schematic diagram of proximity ligation assay (PLA), wherein primary antibodies against Hrs or Tau are detected by secondary antibodies conjugated to DNA. Ligation and amplification of DNA, resulting in green signal, only occurs when proteins are in close (20–50 nm) proximity.

C   PLA signal (green) for Hrs/Tau interaction (arrows) on an mCh-Hrs-labeled endosome (red) in N2a cells; scale bar: 5 μm (see also Fig EV1).

D   Super-resolution images of N2a cells transfected with constitutively active Rab5 (EGFP-Rab5-CA) and immunostained for Tau, revealing the presence of Tau in both membranes and lumen of early endosomes (scale bar: 5 μm).

E   Super-resolution images of N2a cells transfected with mCh-Hrs and immunostained for Tau and EEA1. Higher-magnification insets (A and B) show Hrs- and EEA1-positive endosomes with juxtaposed Tau puncta present both in the membrane and lumen; scale bar: 5 μm.
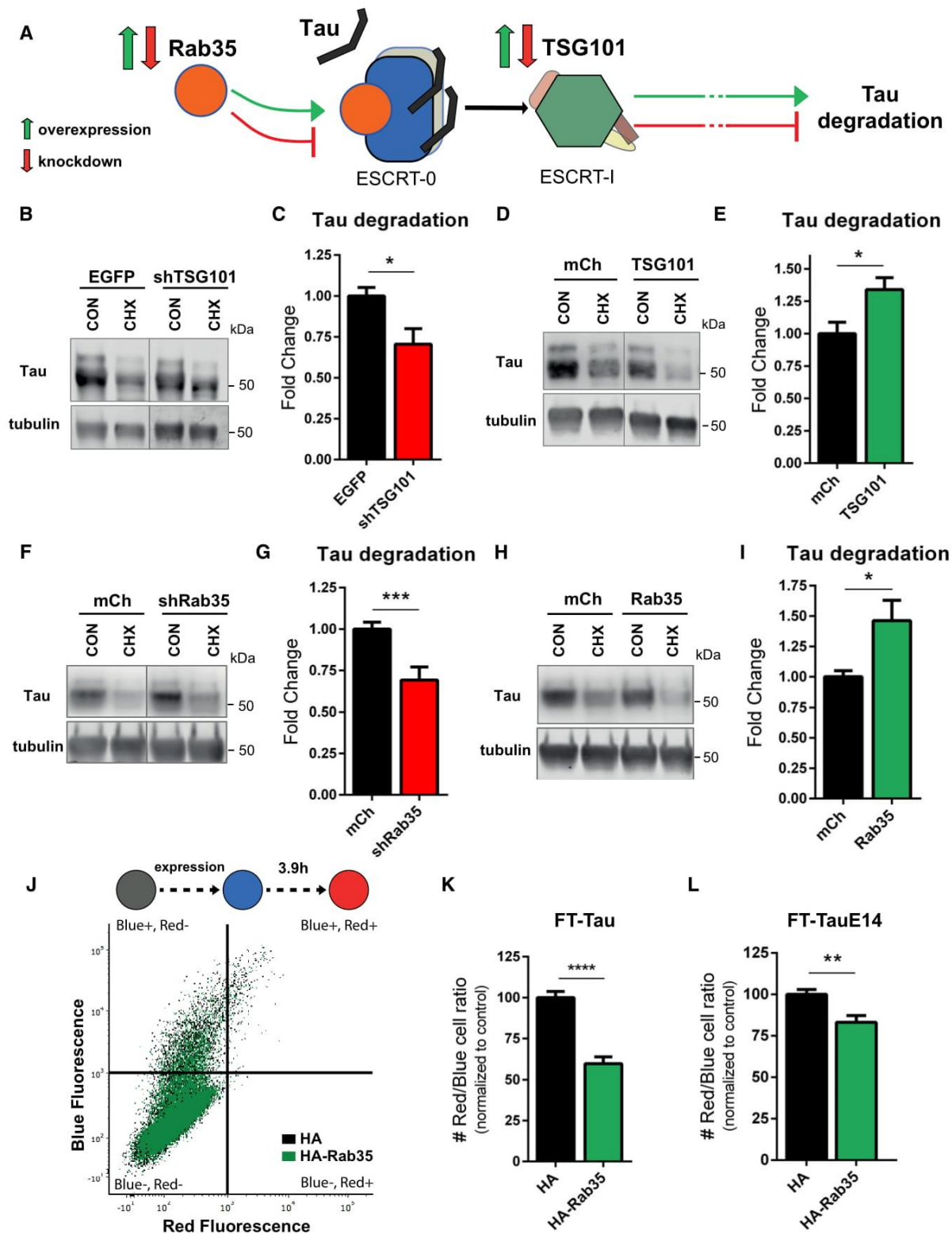
Figure 2.

44

◀

Figure 2. Tau degradation occurs through the Rab35/ESCRT pathway.

A Schematic diagram of the Rab35/ESCRT pathway, indicating the manipulation of targets (Rab35 and TSG101) used in our studies, and the final readout of Tau degradation; green and red arrows represent overexpression and knockdown of the target proteins, respectively.

B, C Representative immunoblots (B) and quantification of Tau degradation (C) from 14 DIV primary neurons transduced with EGFP or shTSG101, treated for 24 h with either DMSO (CON) or cycloheximide (CHX), and probed for Tau and tubulin. shTSG101-expressing neurons exhibit markedly decreased Tau degradation compared to EGFP-expressing controls (*n* = 18–19 per condition, unpaired Student's *t*-test, *P = 0.0108).

D, E Representative immunoblots (D) and quantification of Tau degradation (E) from 14 DIV neurons transduced with mCh or mCh-TSG101, treated for 24 h with either DMSO (CON) or cycloheximide (CHX), and probed for Tau and tubulin. Overexpression of TSG101 increases Tau degradation (*n* = 17/condition, unpaired Student's *t*-test, *P = 0.0115).

F, G Representative immunoblots (F) and quantification of Tau degradation (G) from 14 DIV neurons transduced with mCh or shRab35, treated for 24 h with either DMSO (CON) or cycloheximide (CHX), and probed for Tau and tubulin. shRab35-expressing neurons exhibit markedly decreased Tau degradation compared to mCh-expressing controls (*n* = 23–26 per condition, unpaired Student's *t*-test, ***P = 0.0008).

H, I Representative immunoblots (H) and quantification of Tau degradation (I) from 14 DIV neurons transduced with mCh or mCh-Rab35, treated for 24 h with either DMSO (CON) or cycloheximide (CHX), and probed for Tau or tubulin. Rab35 overexpression increases Tau degradation (*n* = 18 per condition, unpaired Student's *t*-test, *P = 0.0126).

J Flow cytometry distribution of N2a cells co-transfected with either HA vector (black) or HA-Rab35 (green) and medium fluorescence timer-tagged wild-type Tau (FT-Tau); blue fluorescence (*y* axis) indicates "younger" Tau protein, while red fluorescence (*x* axis) indicates "older" Tau.

K The ratio of cells expressing red to blue (older:younger) FT-Tau is reduced in cells overexpressing Rab35, indicating faster Tau turnover (*n* = 9/condition, unpaired Student's *t*-test, ****P < 0.0001).

L The ratio of cells expressing red to blue (older:younger) FT-tagged phospho-mimetic E14 Tau (FT-TauE14) is also reduced in cells overexpressing Rab35, indicating that Rab35 also triggers degradation of phosphorylated Tau (*n* = 10/condition, unpaired Student's *t*-test, *P = 0.0032).

Data information: All numeric data represent mean ± SEM.
Source data are available online for this figure.

pathway, we assessed the effect of Rab35 on Hrs/Tau interaction by PLA. Here, N2a cells were co-transfected with FLAG-Hrs and mCherry or mCh-Rab35, and PLA performed with antibodies against FLAG and either total or phospho-Tau epitopes. For total Tau, as well as pSer396/404-Tau and pSer262-Tau, Rab35 expression significantly increased the number of fluorescent puncta per cell (Fig 3C and D), representing increased interaction of these Tau species with Hrs and thus their subsequent sorting into the ESCRT pathway. In contrast, Rab35 had no effect on PLA puncta number for pSer202-Tau (Fig 3C and D). Consistent with our CHX-chase assay findings, these PLA data suggest that Rab35 promotes the degradation of Tau protein through the ESCRT pathway, with some preference for Tau phosphorylated at pSer262 and pSer396/404, but not pSer202.

To verify that the Rab35/ESCRT pathway mediates Tau degradation through lysosomes, we next treated hippocampal neurons with bafilomycin (to block acidification and trap lysosome contents) in the presence of mCh-tagged TSG101 or Rab35 to stimulate Tau sorting into this pathway (Fig 4A). We found that bafilomycin led to a significant accumulation of Tau in lysosomes of neurons expressing either TSG101 or Rab35 vs. mCh control, assessed by the fraction of Tau colocalization with LAMP1 (Fig 4A and B). Furthermore, through sucrose-based fractionation of primary neurons, we found that Rab35 overexpression increased the fraction of Tau in endosomal/lysosomal (Rab35- and LAMP1-enriched) fractions (Fig EV3), providing further support for the stimulating role of Rab35 on Tau sorting into the endolysosomal pathway. We also evaluated the effects of Rab35 gain-of-function on Tau stability in different neuronal compartments, using CHX treatment combined with immunofluorescence microscopy in hippocampal neurons expressing mCh or mCh-Rab35, as previously described (Sheehan *et al*, 2016). Although both Rab35 and Tau are enriched in axons, Rab35 overexpression reduced Tau fluorescence in both axons and neuronal somata by between 25 and 50%, demonstrating the ability of Rab35 to stimulate Tau degradation in distinct neuronal compartments (Fig 4C and D).

Glucocorticoids decrease Rab35 levels *in vitro* and *in vivo*

Clinical studies suggest that stressful life events and high GC levels are risk factors for AD (Johansson *et al*, 2010; Machado *et al*, 2014); and animal studies demonstrate that prolonged exposure to environmental stress and/or elevated GC levels trigger Tau accumulation (Lopes *et al*, 2016b,c; Vyas *et al*, 2016). Based on our findings identifying the Rab35/ESCRT pathway as a critical regulator of Tau degradation, we next examined whether GC treatment altered the levels of Rab35 or ESCRT pathway proteins. Primary neurons were treated with GC and the levels of ESCRT proteins (Hrs, TSG101, CHMP2b) and Rab35 measured. Interestingly, we found that GC treatment selectively reduced Rab35 protein levels without altering the levels of other ESCRT proteins (Fig 5A and B). GC are known to regulate gene transcription via activation of the glucocorticoid receptor (GR), which binds glucocorticoid response elements (GRE) within the promoter regions of genes (Vyas *et al*, 2016). We therefore used qPCR to measure Rab35 mRNA levels in hippocampal neurons and N2a cells, and found that GC treatment led to a significant reduction in Rab35 mRNA in both cell types (Fig 5C). Consistent with the concept that GC regulate Rab35 transcription, we found that the *Rab35* gene contains 14 non-redundant GREs (Table 1). We subsequently measured the levels of Rab35 and other endocytic Rab GTPases in the hippocampi of rats that received GC injections for 15 days (Fig 5D). The hippocampus displays overt lesions in both stress- and Tau-related pathologies and is one of the earliest brain regions to show signs of neurodegeneration (Vyas *et al*, 2016). In line with our *in vitro* findings, Rab35 levels were significantly decreased in GC-injected animals, whereas none of the other Rab GTPases analyzed had significantly altered levels as assessed by immunoblot analysis (Fig 5E and F). We observed a similar ~25% decrease in immunofluorescence staining of Rab35 in the dorsal CA1 area of hippocampus in GC-treated vs. control animals (Figs 5G and H, and EV4A). Altogether, these *in vitro* and *in vivo* results suggest that GC specifically decrease Rab35 transcription,
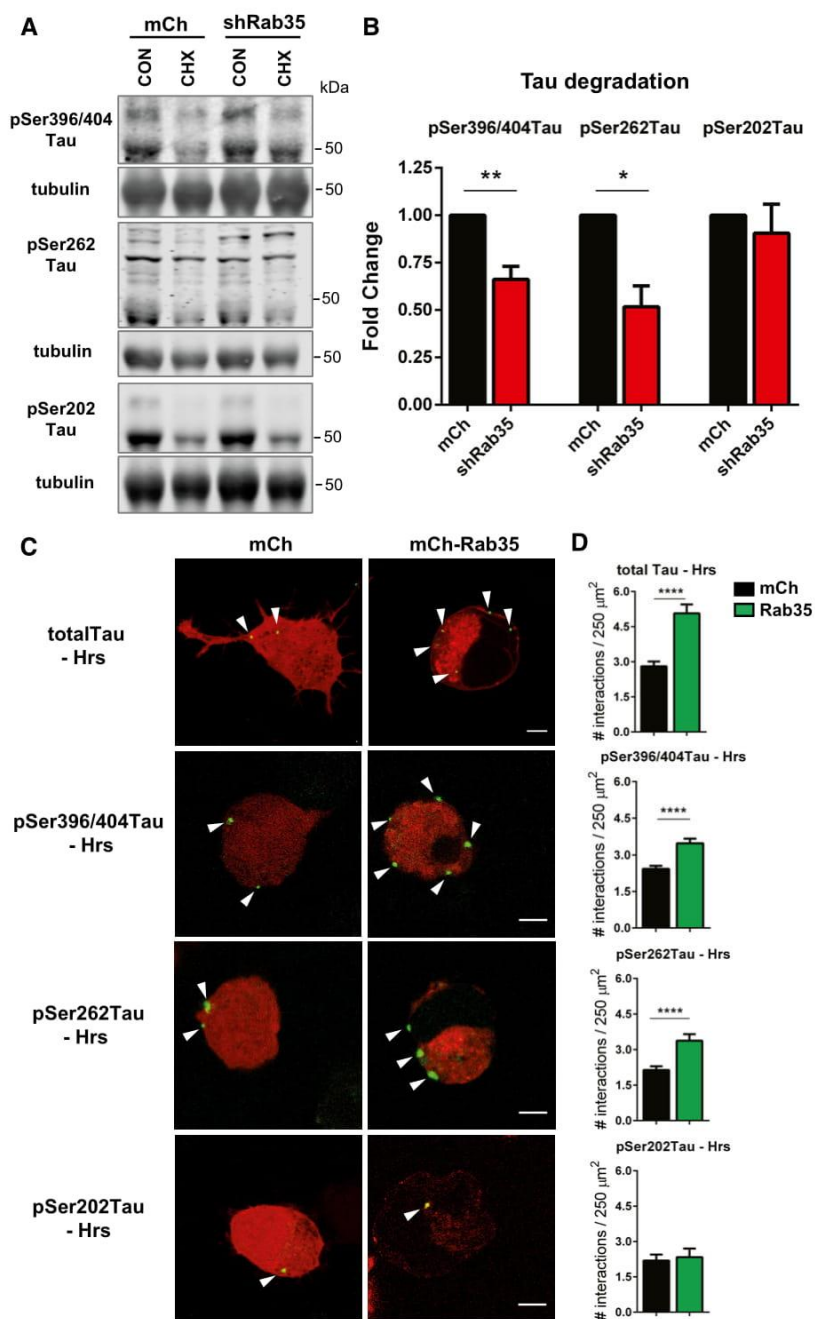
Figure 3. Phospho-dependent selectivity of Tau sorting into the Rab35/ESCRT pathway.

A, B   Representative immunoblots (A) and quantification of Tau degradation (B) from 14 DIV primary neurons transduced with mCh or shRab35, treated for 24 h with either DMSO (CON) or cycloheximide (CHX), and probed for pSer396/404-Tau (PHF1), pSer262-Tau, or pSer202-Tau (CP13) and tubulin. shRab35-expressing neurons exhibit markedly decreased pSer262- and p396/404-Tau degradation compared to mCh-expressing controls, while pSer202-Tau degradation is unaffected (n = 4 per condition for pSer396/404-Tau and pSer202-Tau, n = 3 for pSer262-Tau, unpaired Student's t-test, **P = 0.0027, *P = 0.0120).

C   Images of PLA signal (green) for Hrs/Tau interaction in N2a cells co-transfected with FLAG-Hrs and either mCh or mCh-Rab35 (red), and probed with antibodies against FLAG and total (DA9) or phospho-Tau species (pSer396/404-Tau, pSer262-Tau, or pSer202-Tau); scale bar: 5 μm.

D   Rab35 overexpression significantly increases PLA puncta for total, pSer396/404-Tau, pSer262-Tau but not pSer202-Tau (n = 121–132 cells for total Tau, 178–195 cells for pSer396/404-Tau, 71–98 cells for pSer262-Tau, 25–29 cells for pSer202-Tau; Mann–Whitney U-test, ****P < 0.0001).

Data information: All numeric data represent mean ± SEM.
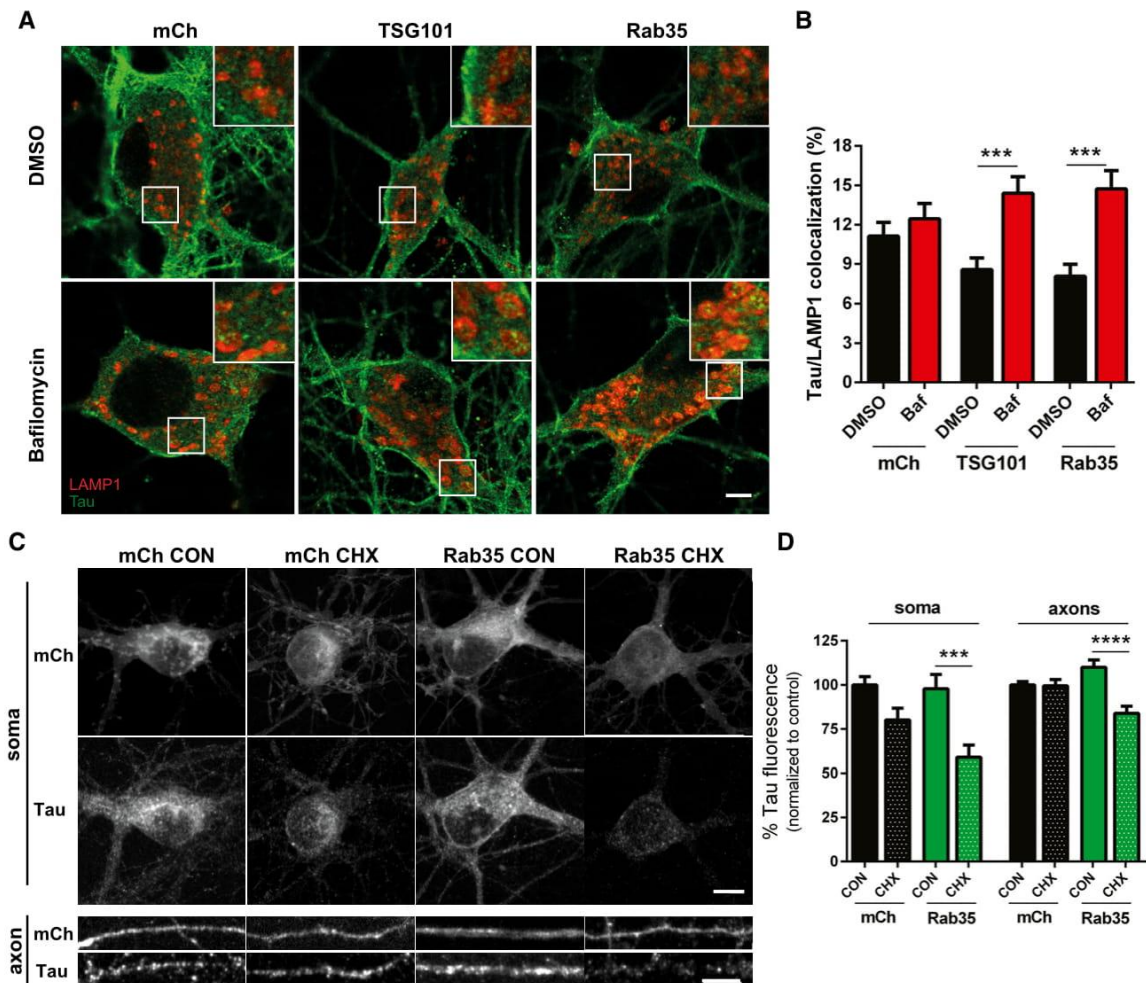Source data are available online for this figure.

46

Figure 4. Rab35/ESCRT pathway promotes Tau degradation via lysosomes.

A, B Representative images and quantification of 14 DIV neurons transduced with mCh, mCh-TSG101, or mCh-Rab35, treated for 5 h with either DMSO (CON) or bafilomycin (Baf) to block lysosomal degradation, and immunostained for Tau and LAMP1. Overexpression of Rab35 or TSG101 increases Tau accumulation in lysosomes of Baf-treated neurons, indicating that Rab35/ESCRT pathway activation stimulates sorting of Tau into lysosomes (scale bar: 5 μm) (n = 25–27 cells/condition; for TSG101, two-way ANOVA, $Baf \times TSG101$ interaction $F_{1,99}$ = 4,075 P = 0.04, overall Baf effect $F_{1,99}$ = 10.30 P = 0.0018, Sidak *post hoc* analysis ***P = 0.0007; for Rab35, two-way ANOVA, $Baf \times Ra35$ interaction $F_{1,101}$ = 5.36 P = 0.02, overall Baf effect $F_{1,101}$ = 12.01 P = 0.0008, Sidak *post hoc* analysis ***P = 0.0001). All numeric data represent mean ± SEM.

C Images of 14 DIV neurons transduced with mCh or mCh-Rab35, treated for 24 h with either DMSO (CON) or cycloheximide (CHX) and immunostained for Tau; scale bar: 10 μm.

D Tau fluorescence intensity is markedly reduced in both soma and axons of CHX-treated neurons overexpressing Rab35 compared to mCh, indicating faster Tau degradation (n = 24/condition; for axons, n = 25–26/condition); for soma, two-way ANOVA, overall CHX effect $F_{1,92}$ = 19.27 P < 0.0001, Sidak *post hoc* analysis ***P = 0.002; for axon, two-way ANOVA, $CHX \times Rab35$ interaction $F_{1,97}$ = 13.27 P = 0.0004, overall CHX effect $F_{1,97}$ = 14.34, P = 0.0003, Sidak *post hoc* analysis ****P < 0.0001).

leading to reduced Rab35 mRNA and protein levels in hippocampal neurons.

Rab35 gain-of-function rescues GC-induced Tau accumulation and neurostructural deficits

Based on our findings that Rab35 mediates Tau turnover, and that exposure to high GC levels downregulates Rab35, we hypothesized that Rab35 overexpression could attenuate GC-induced Tau accumulation and related neuronal atrophy (Green *et al*, 2006; Sotiropoulos *et al*, 2011; Pinheiro *et al*, 2015). To test this hypothesis, we performed the CHX-chase assay in hippocampal neurons transduced with either mCh or mCh-Rab35, and treated with GC or vehicle control. As shown in Fig 6, GC treatment reduced Tau degradation in mCherry-expressing neurons, but this effect was completely blocked by Rab35 overexpression (Fig 6A and B). Similar results
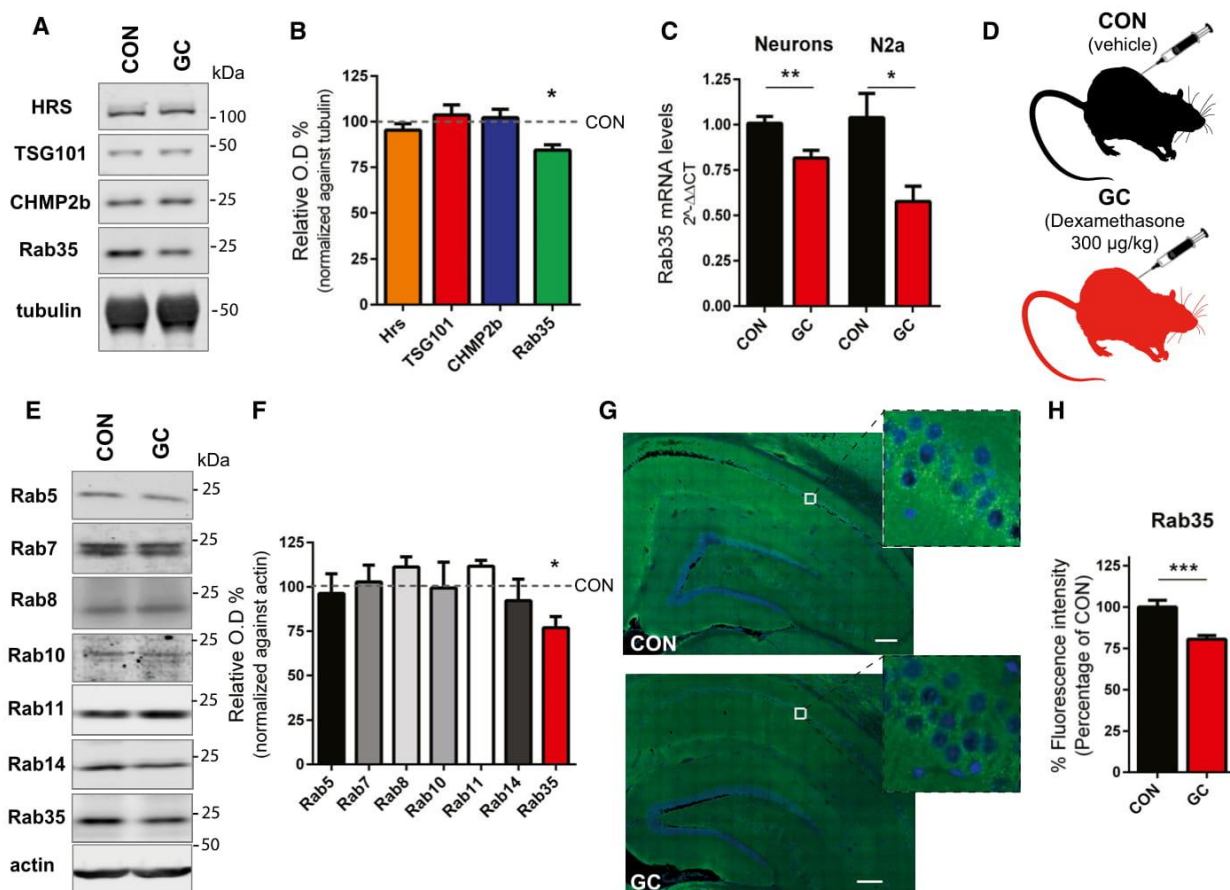
Figure 5. Glucocorticoids decrease Rab35 levels *in vitro* and *in vivo*.

A, B   Representative immunoblots (A) and quantification of Hrs, TSG101, CHMP2b, and Rab35 protein levels (B) from 14 DIV neurons treated with either DMSO (CON) or glucocorticoids (GC). GC treatment selectively decreases Rab35 protein levels without affecting levels of Hrs, TSG101, or CHMP2b (*n* = 9–10/condition, unpaired Student's *t*-test, **P* = 0.0221).

C   Rab35 mRNA levels are decreased by GC in 14 DIV hippocampal neurons and N2a cells (for neurons, *n* = 9/condition, unpaired Student's *t*-test, ***P* = 0.0036; for N2a cells, *n* = 6/condition, unpaired Student's *t*-test, **P* = 0.0138).

D   Schematic diagram of GC and vehicle control (CON) treatment in rats for 15 days.

E, F   Representative immunoblots (E) and quantification of levels of different Rab proteins (F) in hippocampus of GC-treated and CON animals. Protein levels of Rab35, but not other Rabs, are decreased in GC-treated animals compared to CON ones (*n* = 5 animals/condition, unpaired Student's *t*-test, **P* = 0.0257).

G, H   Immunofluorescence staining of Rab35 (green) and DAPI (blue) (G) showing that Rab35 fluorescence intensity is reduced in hippocampal area (CA1) of GC-treated animals (H) (*n* = 15 slices/condition; unpaired Student's *t*-test, ****P* = 0.0003).

Data information: All numeric data represent mean ± SEM.
Source data are available online for this figure.

were seen in N2a cells, where Rab35 overexpression prevented the GC-driven increase in total Tau levels (Fig EV4B and C) and in ubiquitylated Tau species (Fig EV4D–F). Since ubiquitylation is the major signal for cargo sorting into the ESCRT pathway, these findings provide further evidence that Rab35 stimulates the endolysosomal sorting of ubiquitylated Tau.

Previous studies showed that exposure to stress or high GC levels induced Tau accumulation, dendritic atrophy, and synapse loss in animals (Pinheiro *et al*, 2015; Lopes *et al*, 2016b), and that these hippocampal deficits were Tau-dependent (Lopes *et al*, 2016a,b). To test whether Rab35 could protect against these GC-induced effects, we injected middle-aged rats with adeno-associated virus (AAV) to

express EGFP or EGFP-Rab35 in excitatory neurons of the hippocampus under control of the CaMKIIα promoter (Fig 6C). Animals were subsequently treated with GC or vehicle control. Both EGFP- and EGFP-Rab35-injected animals displayed similar body mass loss following GC administration, demonstrating a similar response to high GC levels in the presence or absence of overexpressed Rab35 (Fig EV5A–C). However, in contrast to EGFP animals that exhibited significant GC-induced Tau accumulation in hippocampal synaptosomes, animals expressing EGFP-Rab35 did not show any such accumulation (Fig 6D and E). Furthermore, using Golgi-based 3D neuronal reconstruction of CA1 pyramidal neurons in hippocampus, we found that GC significantly decreased

48

Table 1. Chromosomal position of GR binding sites for *Rab35* gene.

Position	Chromosome	Start	End
1	chr5	115630873	115630972
2	chr5	115631594	115631675
3	chr5	115631971	115632003
4	chr5	115632442	115632541
5	chr5	115632583	115632682
6	chr5	115633507	115633606
7	chr5	115633735	115633834
8	chr5	115635642	115635723
9	chr5	115635734	115635827
10	chr5	115637535	115637616
11	chr5	115640541	115640640
12	chr5	115645909	115646008
13	chr5	115646118	115646217
14	chr5	115647366	115647465

Our analysis identified 14 distinct glucocorticoid response elements associated with the *Rab35* gene, indicating the relevance of glucocorticoids for regulating *Rab35* transcription.

the length of apical dendrites in the EGFP control group, but not in animals expressing EGFP-Rab35 (Fig 6F and G). Notably, EGFP-Rab35 expression alone did not alter apical dendritic length (Fig 6G), and no difference in basal dendrite length was found between the groups (Fig EV5D), consistent with previous work showing selective vulnerability of apical dendrites to GC (Lopes *et al*, 2016b). We also found that GC treatment led to a significant loss of mature spines and concomitant increase in immature spines in EGFP-expressing animals, but no change in mature or immature spine density in EGFP-Rab35 animals (Figs 6H and EV5E). GC-induced neuronal atrophy was further confirmed by Sholl analysis, which measures the number of dendritic intersections as a function of their distance from the soma. As shown in Fig 6I and J, GC reduced the number of distal dendritic intersections in neurons expressing EGFP but not EGFP-Rab35. Altogether, these *in vivo* findings indicate that Rab35 overexpression prevents GC-driven neurostructural deficits, implicating Rab35 as an essential regulator of GC-induced neuronal dysfunction.

Discussion

Impairment of Tau proteostasis is linked to neuronal and synaptic dysfunction in AD animal models and patients (Roberson *et al*, 2007; Ittner *et al*, 2010; Guo *et al*, 2017). Given that Tau accumulation appears to drive neurodegenerative processes in AD and other neurological diseases (see also Introduction), there is growing interest in understanding the mechanisms that mediate Tau clearance, and their selectivity for different forms of Tau. Previous studies have shown that Tau degradation can occur through the ubiquitin–proteasome system (UPS), but that macroautophagy plays an important role in the catabolism of aggregated/insoluble Tau, which is not accessible to the UPS (for review, see Chesser *et al*, 2013). Recent work indicates that chaperone-mediated autophagy and

endosomal microautophagy also contribute differentially to the degradation of wild-type vs. pathogenic mutants forms of Tau (Caballero *et al*, 2017), suggesting that Tau turnover is a complex process regulated by multiple factors and involving distinct degradative pathways.

The current study utilizes *in vitro* and *in vivo* approaches to demonstrate a critical role for the endocytic pathway, and in particular Rab35 and the ESCRT machinery, in the turnover of total Tau and specific phospho-Tau species (see Fig 7). The ESCRT system mediates the degradation of membrane-associated proteins such as epidermal growth factor receptor (Raiborg & Stenmark, 2009), but it has also been implicated in the degradation of cytosolic proteins GAPDH and aldolase (Sahu *et al*, 2011). These findings are of particular relevance for Tau, which has both cytosolic and membrane-associated pools (Pooler & Hanger, 2010; Georgieva *et al*, 2014), and has been shown to localize to different neuronal subcompartments based on its phosphorylation state (Hoover *et al*, 2010; Pinheiro *et al*, 2015). The current study reveals that Tau appears in Hrs-, EEA1-, and Rab5-positive early endosomes (on the membrane and in the lumen), intraluminal vesicles of MVBs, and LAMP1-positive vesicles and membrane fractions, demonstrating its trafficking through the entire endolysosomal pathway. Moreover, we find that Tau interacts with the initial ESCRT protein Hrs, and that this interaction is strengthened by deubiquitylating enzyme inhibitors, indicating its dependence on Tau ubiquitylation. We also observe that the small GTPase Rab35 is a positive regulator of Tau sorting into the ESCRT pathway. Not only does overexpression of Rab35 stimulate Tau's interaction with Hrs and subsequent lysosomal degradation, but Rab35 knockdown significantly slows Tau degradation. Interestingly, while Rab35 stimulates the turnover of phospho-mimetic E14 Tau, not all phosphorylated Tau species are equally susceptible to degradation in the Rab35/ESCRT pathway. In particular, we find that pSer396/404 and pSer262, but not pSer202, phospho-Tau species undergo Rab35-mediated degradation, indicative of preferential sorting of specific phospho-Tau proteins into the Rab35/ESCRT pathway. Such differences might reflect changes in ubiquitylation and/or endosomal membrane association of the various phospho-Tau species. Additional work is needed to clarify the relationship between Tau posttranslational modifications (e.g., phosphorylation and ubiquitylation) and the sorting and clearance of cytosolic vs. membrane-associated pools of Tau, as well as the impact of stress/GC on these processes.

We recently showed that Rab35 and ESCRT proteins (e.g., Hrs, CHMP2b) localize to axons and presynaptic boutons, similar to Tau, and that Rab35 stimulates the degradation of synaptic vesicle proteins by mediating the recruitment of Hrs to SV pools in response to neuronal activity (Sheehan *et al*, 2016). In the current study, we show that Tau interacts with Hrs-positive early endosomes in a Rab35-dependent manner, and that Rab35 stimulates the degradation of both axonal and somatodendritic pools of Tau. Although Tau localizes primarily to axons, many studies (including our own) have shown that it also localizes to the somatodendritic compartment and to dendritic spines under both healthy and pathological conditions, suggesting a synaptic function for Tau (Ittner *et al*, 2010; Mondragon-Rodriguez *et al*, 2012; Frandemiche *et al*, 2014; Pinheiro *et al*, 2015; Lopes *et al*, 2016c). Moreover, recent work demonstrates more complex intraneuronal trafficking of Tau than

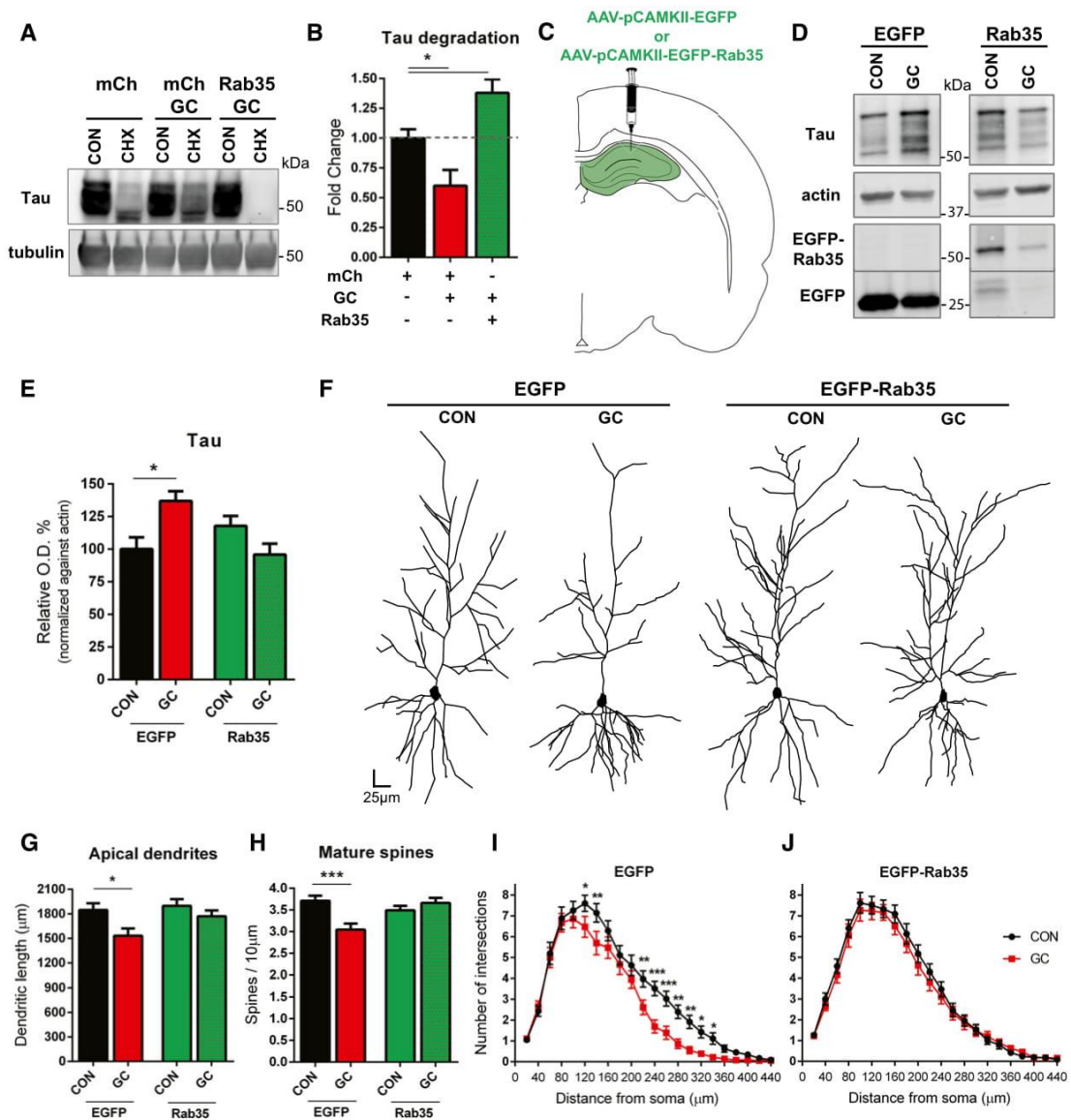Glucocorticoids impair Tau degradation   *João Vaz-Silva et al*

Figure 6. AAV-mediated Rab35 expression rescues glucocorticoid-induced Tau accumulation and associated neuronal atrophy in rat hippocampus.

A, B Representative immunoblots (A) and quantification of Tau degradation (B) in 14 DIV neurons expressing mCh-Rab35 or mCh, treated for 24 h with cycloheximide (CHX) or DMSO (CON) under GC conditions. GC significantly decreases Tau degradation, whereas Rab35 overexpression blocks this effect (n = 12–14/condition; one-way ANOVA, Dunnet *post hoc* analysis, $*P_{mCh\ vs.\ mCh\ GC}$ = 0.0319, $*P_{mCh\ vs.\ Rab35\ GC}$ = 0.047).

C Injection of AAV to express EGFP or EGFP-Rab35, driven by the CaMKIIα promoter, in rat hippocampus prior to GC or vehicle (CON) treatment.

D, E Representative immunoblots (D) and quantification of Tau levels (E) in hippocampal synaptosomes reveal that GC increases total Tau levels in animals expressing EGFP, but not Rab35 (n = 5–6 animals/group, two replicates, two-way ANOVA, *GC* × *Rab35* interaction $F_{1,39}$ = 10.51 P = 0.002; Sidak *post hoc* analysis $*P$ = 0.0168).

F Golgi-based 3D neuronal reconstruction of hippocampal pyramidal neurons (CA1 area).

G GC treatment reduces the length of apical dendrites in animals expressing EGFP, but not EGFP-Rab35 (n = 6–7 animals/group; 6–8 neurons/animal, 2-way ANOVA, *GC* × *Rab35* interaction $F_{1,155}$ = 3.969 P = 0.0481, overall *GC* effect $F_{1,155}$ = 8.998 P = 0.0031, Sidak *post hoc* analysis $**P$ = 0.0021).

H GC treatment reduces mature spine density in animals expressing EGFP, but not EGFP-Rab35 (two-way ANOVA, *GC* × *Rab35* interaction $F_{1,499}$ = 12.33 P = 0.0005, overall *GC* effect $F_{1,499}$ = 4.373 P = 0.0370, Sidak *post hoc* analysis $***P$ = 0.0003; n = 6–7 animals/group; 6–8 neurons per animal).

I, J Sholl analysis of apical dendrites in rat hippocampus shows reduced dendritic intersections after GC treatment in EGFP-expressing animals; however, this effect is not seen in EGFP-Rab35-expressing animals (three-way ANOVA, *GC* × *Rab35* interaction $F_{1,4,212}$ = 14,926 P < 0.0001, simple effect analysis, Sidak test for multiple comparisons $*P_{120}$ = 0.012, $**P_{140}$ = 0.001, $**P_{220}$ = 0.002, $***P_{240}$ < 0.001, $***P_{260}$ < 0.001, $**P_{280}$ = 0.001, $**P_{300}$ = 0.001, $*P_{320}$ = 0.021, $*P_{340}$ = 0.047, n = 6–7 animals/group, 6–8 neurons per animal).

Data information: All numeric data represent mean ± SEM.
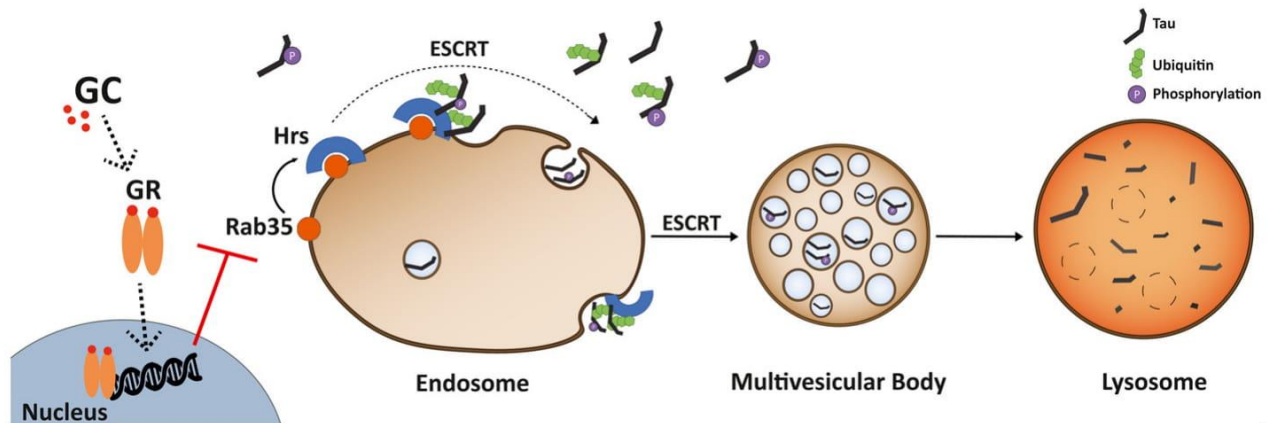Source data are available online for this figure.

50

Figure 7. High glucocorticoid levels suppress Rab/ESCRT-dependent Tau degradation, leading to Tau accumulation.

Working model of Tau degradation through the Rab35/ESCRT pathway, and its inhibition by glucocorticoids (GC). Rab35 mediates Tau clearance via the endolysosomal pathway by recruiting initial ESCRT component Hrs, which recognizes and sorts ubiquitylated Tau into early endosomes for packaging into MVBs. GC suppress transcription of Rab35, which in turn decreases Tau sorting into MVBs and its subsequent degradation by lysosomes, leading to Tau accumulation and related neuronal atrophy.

previously appreciated, including activity-dependent translocation of Tau to excitatory synapses (Frandemiche *et al*, 2014) and AMPA/NMDA receptor-dependent Tau hyperphosphorylation and dendritic Tau mRNA translation (Kobayashi *et al*, 2017). Interestingly, our current findings demonstrate the selective sorting of particular phospho-Tau species into the Rab35/ESCRT pathway, which together with other studies (Pooler & Hanger, 2010; Mondragon-Rodriguez *et al*, 2012; Frandemiche *et al*, 2014; Pinheiro *et al*, 2015) provides novel mechanistic insights into how epitope-specific Tau phosphorylation regulates its trafficking, subcellular localization, and degradation. Our future studies will focus on understanding the role of the Rab35/ESCRT pathway on Tau degradation in different neuronal compartments under pathological conditions, including AD and other tauopathies, wherein Tau is hyperphosphorylated at multiple epitopes (Ittner *et al*, 2010; Zempel *et al*, 2010).

Recent evidence suggests that dysfunction of the ESCRT machinery itself is associated with profound cytopathology, as brain-specific deletion of ESCRT components in mice leads to the accumulation of ubiquitylated proteins, impaired endosomal trafficking, and cell death (Watson *et al*, 2015; Oshima *et al*, 2016). Further, a truncating mutation in ESCRT-III protein CHMP2b causes familial frontotemporal dementia and amyotrophic lateral sclerosis, and at the cellular level induces endolysosomal pathway dysfunction and the accumulation of ubiquitylated proteins (Clayton *et al*, 2015; Zhang *et al*, 2017b). Together with our findings, the above studies support the importance of the endolysosomal pathway, and specifically the ESCRT machinery, in clearance of ubiquitylated proteins such as Tau. Indeed, abnormalities of the endolysosomal pathway, including endosomal enlargement and high levels of lysosomal hydrolases, are reported as the earliest intracellular features of AD (Nixon & Yang, 2011). Intriguingly, these same features are present in Niemann-Pick disease type C (NPC), an inherited lysosomal storage disorder also characterized by Tau pathology (Suzuki *et al*, 1995). These shared pathological features of AD and NPC indicate a strong connection between endolysosomal dysfunction and Tau accumulation,

supporting the importance of this degradative pathway for Tau proteostasis and pathological accumulation.

Multiple cellular pathways are altered by chronic stress, increasing the vulnerability of affected individuals to psychiatric and neurodegenerative diseases such as depression and AD (Sotiropoulos *et al*, 2008b; Ross *et al*, 2017). For example, prolonged exposure to stress or high levels of GC trigger Tau accumulation and hyperphosphorylation accompanied by synaptic missorting of Tau and neuronal atrophy (Green *et al*, 2006; Sotiropoulos *et al*, 2011; Pinheiro *et al*, 2015; Lopes *et al*, 2016c). Importantly, Tau is essential for this stress/GC-driven damage, as Tau ablation was found to be neuroprotective (Lopes *et al*, 2016c; Pallas-Bazarra *et al*, 2016; Dioli *et al*, 2017). While previous *in vitro* studies showed that GC reduce Tau turnover (Sotiropoulos *et al*, 2008a), the underlying molecular mechanisms were unclear. The current study demonstrates that GC impair Tau degradation by downregulating Rab35, thereby suppressing Tau sorting into the ESCRT pathway and leading to the accumulation of ubiquitylated Tau (Fig 7). These results support the concept that ubiquitylation, the major signal for cargo sorting into the ESCRT pathway, represents the first line of cellular defense against Tau accumulation and related neuronal malfunction (Chesser *et al*, 2013; Kontaxi *et al*, 2017). Importantly, we find that Rab35 overexpression blocks Tau accumulation and neuronal atrophy induced by high GC levels. Future studies will clarify the potential interplay between endolysosomal machinery and other degradative pathways such as autophagy under stressful/high GC conditions. Our current findings identify the Rab35/ESCRT pathway as a critical regulator of Tau proteostasis, supporting its involvement in the intraneuronal events through which the primary stress hormones, GC, impair neuronal morphology, and plasticity in the hippocampus (Sousa & Almeida, 2012). Based on the emerging significance of endosomal trafficking defects in AD brain pathology (Small *et al*, 2017), Rab35 and the endolysosomal pathway deserve further investigation for their therapeutic relevance against Tau-dependent neuronal malfunction and pathology.

Materials and Methods

Primary neurons and cell lines

Primary neuronal cultures were prepared from E18 Sprague Dawley rat embryos and maintained for 14 DIV before use, as described previously (Sheehan *et al*, 2016). Neuro2a (N2a) neuroblastoma cells (ATCC CCL-131) and HEK293T cells (Sigma) were grown in DMEM-GlutaMAX (Invitrogen) with 10% FBS (Atlanta Biological) and Anti-Anti (ThermoFisher) and kept at 37°C in 5% CO_2. During dexamethasone treatment in N2a cells, FBS content in the growth media was reduced to 3%.

Pharmacological treatments

Pharmacological agents were used in the following concentrations and time courses: cycloheximide (Calbiochem, 0.2 μg/μl, 24 h or 0.1 μg/μl, 16 h), bicuculline (Sigma, 40 μM, 24 h), 4-aminopyridine (Tocris Bioscience, 50 μM, 24 h), bafilomycin A1 (Millipore, 0.1 μM, 5 h), dexamethasone (Ratiopharm, 10 μM, 48 h), dexamethasone (InvivoGen, 20 μM, 72 h), epoxomicin (Sigma, 0.1 μM) PR-619 (LifeSensors, 50 μM).

Lentivirus production, transduction, and DNA transfection

DNA constructs were described previously (Sheehan *et al*, 2016), with the exception of pRK5-EGFP-Tau (Addgene plasmid #46904), and pAAV-CAMKIIa-EGFP-Rab35, which was created by subcloning EGFP-Rab35 into the pAAV-CAMKIIa-EGFP vector (Addgene plasmid #50469). Both pAAV-CAMKIIa-EGFP-Rab35 and pAAV-CAMKIIa-EGFP were then packaged into AAV8 serotype by the UNC Gene Therapy Center Vector Core (UNC Chapel Hill). Lentivirus was produced as previously described (Sheehan *et al*, 2016). Neurons were transduced with 50–150 μl of lentiviral supernatant per well (12-well plates) or 10–40 μl per coverslip (24-well plates) either at 3 DIV for shRNA transduction or 10 DIV in gain-of-function experiments. Respective controls were transduced on the same day for all experimental conditions. Neurons were collected for immunoblotting or immunocytochemistry at 14 DIV.

Immunofluorescence microscopy

Immunofluorescence staining in neurons and N2a cells was performed as previously described (Sheehan *et al*, 2016). Briefly, cells were fixed with Lorene's Fix (60 mM PIPES, 25 mM HEPES, 10 mM EGTA, 2 mM $MgCl_2$, 0.12 M sucrose, 4% formaldehyde) for 15 min, and primary and secondary antibody incubations were performed in blocking buffer (2% glycine, 2% BSA, 0.2% gelatin, 50 mM NH_4Cl in 1× PBS) overnight at 4°C or for 1 h at room temperature, respectively. For staining of brain slices, coronal vibratome sections (40 μm) of paraformaldehyde-fixed brains were placed in heated citrate buffer for 15 min. Sections were then permeabilized using 0.5% Triton X-100 for 30 min, followed by 5 min blocking with Ultravision Protein Block (Thermoscientific). Primary and secondary antibodies were diluted in 0.5% Triton/0.2% BSA/0.5% FBS in 1× PBS, and incubation was performed overnight at 4°C or for 3 h at

room temperature, respectively. Images were acquired using a Zeiss LSM 800 confocal microscope equipped with Airyscan module, using either a 63× objective (Plan-Apochromat, NA 1.4), for neurons or N2a cell imaging, or a 40× objective (Neofluar, NA 1.4) for imaging of rat brain sections. Primary antibodies are listed in Table EV1.

Proximity ligation assay

Proximity ligation assay (PLA) was performed in N2a cells according to manufacturer's instructions (Duolink, Sigma). Until the PLA probe incubation step, all manipulations were performed as detailed above for the immunocytochemistry procedure. PLA probes were diluted in blocking solution. The primary antibody pairs used were anti-FLAG (Rabbit; Abcam) and DA9 (anti-Total Tau, Mouse, gift from Peter Davies), anti-FLAG (Rabbit, Abcam) and PHF1 (Mouse), anti-FLAG (Rabbit, Abcam) and CP13 (Mouse), anti-FLAG (Mouse, Sigma) and pSer262 Tau (Rabbit, ThermoFisher Scientific), anti-mCherry (Rabbit, Biovision), and DA9 (Mouse, Peter Davies). Additionally, a blocking FLAG peptide (Sigma), used at a 100 μg/ml concentration, was included to evaluate the specificity of the technique. All protocol steps were performed at 37°C in a humidity chamber, except for the washing steps. Coverslips were then mounted using Duolink *In situ* Mounting Media with DAPI.

Tau immunogold staining and electron microscopy

For electron microscope analysis, rat hippocampi were fixed at 4°C with 4% PFA, then transferred to 4% PFA/0.8% glutaraldehyde in 0.1 M of phosphate buffer (PB) for 1 h and afterward, to 0.1 M PB. Vibratome-cut axial sections of the dorsal hippocampus (300 μm thick) were collected, and CA1 hippocampal area was surgically removed. Tissue was then carefully oriented and embedded in Epon resin, and ultrathin sections (500 Å), encompassing the superficial-to-deep axis, were cut onto nickel grids. For Tau immunogold staining, sections were treated with heated citrate buffer (Thermo Scientific) for 30 min and then by 5% BSA. Grids were incubated overnight with Tau5 primary antibody diluted in 1% BSA in PB, followed by secondary gold antibody (Abcam). Grids were imaged on a JEOL JEM-1400 transmission electron microscope equipped with a Orius Sc1000 digital camera.

Image analysis

Images were analyzed and processed using the Fiji software. PLA puncta were counted using the Multi-point tool, and cell area was measured with Polygon selection tool. Fluorescence intensity was measured after performing a Z-projection using the SUM function. For cell bodies, the corrected total cell fluorescence was calculated, by subtracting the average fluorescence of the background of the whole area to the Integrated fluorescence density. For Axons, a mask was created in the mCherry channel, representing the experimental condition, using the same threshold value, and the average fluorescence intensity of the axon was then measure in the other channel. Average fluorescence intensity per slice was measured in images acquired from immunofluorescence stained brain slices.

Coimmunoprecipitation

For coimmunoprecipitation, N2a cells were transfected with Lipofectamine 3000 according to the manufacturer's protocol (Life Technologies). Cell lysates were collected 48 h after transfection, after 3× washes with cold PBS, in Co-IP lysis buffer (0.1% NP-40, 1 mM EDTA in 1× PBS) with protease inhibitor (Roche) and phosphatase inhibitor cocktails II and III (Sigma) and clarified by centrifugation at high speed (10 min, 20,000 *g*). Protein concentration was determined using the BCA protein assay kit (ThermoFisher Scientific), and the same amount of protein was used for each condition. Lysates were pre-cleared using magnetic agarose beads (Chromotek) for 1 h at 4°C. For GFP pull down, lysates were incubated with GFP-Trap Magnetic agarose beads (Chromotek) for 3 h at 4°C. Beads were washed three times with co-IP lysis buffer and then eluted using 2× sample buffer (Bio-Rad) and subject to SDS–PAGE immunoblotting as described below.

Western blotting

For Western blotting experiments, neurons were collected using 2× SDS sample buffer (Bio-Rad). N2a cells were first collected in Lysis Buffer as described previously. Samples were subject to SDS–PAGE, transferred to nitrocellulose membranes using wet or semi-dry apparati (Mini Trans-Blot Cell or Trans-Blot Turbo Blotting System, respectively, Bio-Rad), and probed with primary antibody (Table EV1) in 5% BSA/PBS + 0.1% Tween-20, followed by DyLight 680 or 800 anti-rabbit, anti-mouse (Thermo Scientific) or by HRP-conjugated secondaries (Bio-Rad). Membranes were imaged using an Odyssey Infrared Imager (model 9120, LI-COR Biosciences), and protein intensity was measured using the Image Studio Lite software (LI-COR Biosciences).

Cycloheximide-chase fold change calculation

In cycloheximide-chase experiments, the amount of protein remaining after 24 h of cycloheximide treatment was calculated as a fraction of the amount of protein in the DMSO-treated condition, as previously described (Sheehan *et al*, 2016). Both levels were previously normalized to the tubulin loading control. The fractional degradative amount of each condition was then normalized to the experimental control by dividing the perturbation condition by the control condition.

Subcellular fractionation with sucrose step gradient

For each gradient, two T75 culture flaks of primary cortical neurons (7,500,000 cells each) were used. All procedures were carried out at 4°C post-collection and performed as described previously (de Araujo *et al*, 2008), with slight modifications. Briefly, neurons were detached from the flask with TrypLE Express (Life Technologies) and washed once with ice-cold Neurobasal and twice with ice-cold PBS. Neurons were then subject to hypotonic shock and allowed to swell on ice for 15 min. After cell resuspension in isotonic conditions, neurons were gently lysed with 3× freeze–thaw cycles. The lysates were centrifuged (2,000 × *g*, 10 min, 4°C), and the postnuclear supernatant (PNS) was brought to 40.6% sucrose and loaded in the bottom of a centrifugation tube, overlaid with 35% sucrose,

followed by 25% sucrose and then 8% sucrose solution (in ddH$_2$O, 3 mM imidazole, pH 7.4 with protease and phosphatase inhibitors). After centrifugation in a Beckman centrifuge (3 h, 210,000 × *g*, 4°C), thirteen 100 μl fractions were collected and equal volumes were used for Western blotting, as previously described. Relative protein distribution was calculated after determining the optical density of each fraction and further normalizing against the sum of all fractions. Fractions were divided into different groups according to their respective sucrose gradient.

Real-time RT–PCR

RNA was extracted from either cortical neurons or N2a cells using TRIzol (Thermo Fischer) and purified using the Direct-zol RNA MiniPrep Plus kit (Zymo Research). RT–PCR was performed in a StepOnePlus RealTime PCR instrument, with iTaq™ Universal Probes One-Step Kit (Bio-Rad), using pre-designed TaqMan probes. Amplification conditions were the following: initial denaturing at 95°C for 10 min, 40 cycles of denaturation at 95°C for 15 s and extension at 60°C for 1 min. Rab35 levels were normalized to either β-actin (actb) or TATA-binding protein (tbp). Results presented are normalized to β-actin.

Flow cytometry

N2a cells were detached using TrypLE Express (Life Technologies), for 5 min at 37°C. After washing, cells were resuspended in ice-cold Flow Buffer (0.2% FBS, 0.5 mM EDTA in PBS) and strained through a 35-μm nylon mesh to promote single cell suspensions and kept on ice. Cells were analyzed in a BD Fortessa (BD Biosciences). Unstained cells were used as a control for background fluorescence. Flow Cytometry data were analyzed using FCS Express 6 (DeNovo Software).

Ubiquitylation assay

N2a cells were transfected with vectors encoding GFP-Tau and HA-Ubiquitin with either mCherry or mCh-Rab35. After 48 h, cells were treated with DMSO vehicle or Dexamethasone, and incubated for another 43 h. Cells were then incubated with chloroquine, leupeptin, and epoxomicin for 5 h. Cell lysates were collected, washed 3× with cold PBS in Lysis buffer (50 mm Tris-Base, 150 mm NaCl, 1% Triton X-100, 0.5% deoxycholic acid) with protease inhibitor (Roche) and phosphatase inhibitor cocktails II and III (Sigma), and clarified by centrifugation at high speed (10 min, 20,000 *g*). Subsequent steps were performed as described in the coimmunoprecipitation section.

Animals and AAV injection

Eight- to 10-month-old male Wistar rats (Charles River Laboratories, Spain; *N* = 5 per group) were paired under standard laboratory conditions (8:00 A.M. to 8:00 P.M.; 22°C) with *ad libitum* access to food and drink. Animals received daily subcutaneous injections of the synthetic glucocorticoid, dexamethasone (GC) (300 μg/kg; Sigma D1756; dissolved in sesame oil containing 0.01% ethanol; Sigma S3547) for 14 sequential days, while the other half received daily injections of the vehicle solution (sesame oil with 0.01%

ethanol). All experimental procedures were approved by the local ethical committee of University of Minho and national authority for animal experimentation; all experiments were in accordance with the guidelines for the care and handling of laboratory animals, as described in the Directive 2010/63/EU. For AAV injection experiment ($N = 6$–8 per group), animals were anaesthetized with 75 mg/kg ketamine (Imalgene, Merial) plus 0.5 mg/kg medetomidine (Dorbene, Cymedica). Virus was bilaterally injected into the dorsal and ventral hippocampus (coordinates from bregma, according to Paxinos and Watson 50: −3.0 mm anteroposterior (AP), ±1.6 mm mediolateral (ML), and −3.3 mm dorsoventral (DV) and −6.2 mm AP, ±4.5 mm ML, and −6.0 mm DV, respectively). A total of 2 μl was injected at a rate of 200 nl/min, and the needle was kept in place for 7 min before retraction. Rats were removed from the stereotaxic frame, sutured, and allowed to recover for 3 weeks prior to vehicle or dexamethasone treatment.

Subcellular fractionation

To obtain the synaptosome membrane fraction, a previously described fractionation protocol was used (Lopes *et al*, 2016c). Briefly, hippocampal tissue was homogenized [10 × homogenization buffer (sucrose 9%; 5 mM DTT; 2 mM EDTA; 25 mM Tris, pH 7.4); Complete Protease Inhibitor (Roche), and Phosphatase Inhibitor Mixtures II and III (Sigma)] and centrifuged ($1,000 \times g$). The post-nuclear supernatant was subsequently centrifuged ($12,500 \times g$) to yield crude synaptosomal and synaptosome-depleted fractions. The latter was ultracentrifuged ($176,000 \times g$) to yield a light membrane/Golgi fraction (P3) and a cytoplasmic fraction (S3). The crude synaptosomal fraction was lysed in a hypo-osmotic solution and then centrifuged ($25,000 \times g$) to obtain the synaptosomal fraction (LP1).

Neurostructural analysis

As previously described, half of each rat brain ($N = 6$–7 per group) was immersed in Golgi-Cox solution for 7–10 days. After transfer to tissue protectant solution, vibratome-cut coronal brain sections (200 μm thick) were used. After development, fixation, and dehydration, slides were used to perform three-dimensional morphometric analysis. Dendritic arborization and spines were analyzed in dorsal hippocampus (CA1 area). All neuronal dendritic trees were reconstructed at ×600 (oil) magnification using a motorized microscope (Axioplan2, Zeiss) and Neurolucida software (MBF Bioscience). For spine analysis, proximal and distal apical dendritic segments (30 μm) were randomly selected and spines were counted and further classified in immature (thin) and complex/mature (mushroom, wide/thick, and ramified) categories as previously described (Pinheiro *et al*, 2015). Three different dendritic segments were selected per neuron.

Rab35 glucocorticoid receptor (GR) binding

Binding sites were analyzed with the use of the GTRD database (http://gtrd.biouml.org/; Yevshin *et al*, 2017), which is the largest aggregation of ChIP-seq experiment raw data for the human and mouse genome from publically available sources (including GEO, SRA, Encode) using a unified alignment and ChIP-seq peak calling.

Peaks were merged into clusters and unique metaclusters (~70 M to ensure that transcription factor binding sites are not non-redundant). Our analysis focused on the mouse *Rab35* gene since there is no such comprehensive Chip-seq database for other rodents species. In the search for GR binding sites, we permitted a maximum distance of 1,000 nucleotides from *Rab35*.

Statistical analysis

Graphing and statistics analysis were performed using Prism (GraphPad). Shapiro–Wilk normality test was used to determine whether data sets were modeled by a normal distribution. Unpaired, two-tailed *t*-tests, one-way ANOVA, or two-way ANOVAs were used with values of $P < 0.05$ being considered as significantly different.

Expanded View for this article is available online.

Author contributions

JV-S, IS, and CLW designed the research; JV-S, MZ, QJ, VZ, PG, SQ, TM, JS, CD, CS-C, and NPD performed experiments and analyzed data; NS, IS, and CLW supervised experiments; JV-S, IS, and CLW wrote the manuscript.

Conflict of interest

The authors declare that they have no conflict of interest.

References

de Araujo ME, Huber LA, Stasyk T (2008) Isolation of endocytic organelles by density gradient centrifugation. *Methods Mol Biol* 424: 317–331

Caballero B, Wang Y, Diaz A, Tasset I, Juste YR, Stiller B, Mandelkow EM, Mandelkow E, Cuervo AM (2017) Interplay of pathogenic forms of human tau with different autophagic pathways. *Aging Cell* 17: e12692

Chesser AS, Pritchard SM, Johnson GV (2013) Tau clearance mechanisms and their possible role in the pathogenesis of Alzheimer disease. *Front Neurol* 4: 122

Clayton EL, Mizielinska S, Edgar JR, Nielsen TT, Marshall S, Norona FE, Robbins M, Damirji H, Holm IE, Johannsen P, Nielsen JE, Asante EA,

João Vaz-Silva et al   Glucocorticoids impair Tau degradation   *The EMBO Journal*

Collinge J, FReJA Consortium, Isaacs AM (2015) Frontotemporal dementia caused by CHMP2B mutation is characterised by neuronal lysosomal storage pathology. *Acta Neuropathol* 130: 511−523

Dioli C, Patricio P, Trindade R, Pinto LG, Silva JM, Morais M, Ferreiro E, Borges S, Mateus-Pinheiro A, Rodrigues AJ, Sousa N, Bessa JM, Pinto L, Sotiropoulos I (2017) Tau-dependent suppression of adult neurogenesis in the stressed hippocampus. *Mol Psychiatry* 22: 1110−1118

Edgar JR, Willen K, Gouras GK, Futter CE (2015) ESCRTs regulate amyloid precursor protein sorting in multivesicular bodies and intracellular amyloid-beta accumulation. *J Cell Sci* 128: 2520−2528

Fernandes AC, Uytterhoeven V, Kuenen S, Wang YC, Slabbaert JR, Swerts J, Kasprowicz J, Aerts S, Verstreken P (2014) Reduced synaptic vesicle protein degradation at lysosomes curbs TBC1D24/sky-induced neurodegeneration. *J Cell Biol* 207: 453−462

Frandemiche ML, De Seranno S, Rush T, Borel E, Elie A, Arnal I, Lante F, Buisson A (2014) Activity-dependent tau protein translocation to excitatory synapse is disrupted by exposure to amyloid-beta oligomers. *J Neurosci* 34: 6084−6097

Frankel EB, Audhya A (2017) ESCRT-dependent cargo sorting at multivesicular endosomes. *Semin Cell Dev Biol* 74: 4−10

Georgieva ER, Xiao S, Borbat PP, Freed JH, Eliezer D (2014) Tau binds to lipid membrane surfaces via short amphipathic helices located in its microtubule-binding repeats. *Biophys J* 107: 1441−1452

Green KN, Billings LM, Roozendaal B, McGaugh JL, LaFerla FM (2006) Glucocorticoids increase amyloid-beta and tau pathology in a mouse model of Alzheimer's disease. *J Neurosci* 26: 9047−9056

Guo T, Noble W, Hanger DP (2017) Roles of tau protein in health and disease. *Acta Neuropathol* 133: 665−704

Hamano T, Gendron TF, Causevic E, Yen SH, Lin WL, Isidoro C, Deture M, Ko LW (2008) Autophagic-lysosomal perturbation enhances tau aggregation in transfectants with induced wild-type tau expression. *Eur J Neurosci* 27: 1119−1130

Hoover BR, Reed MN, Su J, Penrod RD, Kotilinek LA, Grant MK, Pitstick R, Carlson GA, Lanier LM, Yuan LL, Ashe KH, Liao D (2010) Tau mislocalization to dendritic spines mediates synaptic dysfunction independently of neurodegeneration. *Neuron* 68: 1067−1081

Ittner LM, Ke YD, Delerue F, Bi M, Gladbach A, van Eersel J, Wolfing H, Chieng BC, Christie MJ, Napier IA, Eckert A, Staufenbiel M, Hardeman E, Gotz J (2010) Dendritic function of tau mediates amyloid-beta toxicity in Alzheimer's disease mouse models. *Cell* 142: 387−397

Johansson L, Guo X, Waern M, Ostling S, Gustafson D, Bengtsson C, Skoog I (2010) Midlife psychological stress and risk of dementia: a 35-year longitudinal population study. *Brain* 133: 2217−2224

Kett LR, Dauer WT (2016) Endolysosomal dysfunction in Parkinson's disease: recent developments and future challenges. *Mov Disord* 31: 1433−1443

Khanna MR, Kovalevich J, Lee VM, Trojanowski JQ, Brunden KR (2016) Therapeutic strategies for the treatment of tauopathies: hopes and challenges. *Alzheimers Dement* 12: 1051−1065

Kimura T, Yamashita S, Fukuda T, Park JM, Murayama M, Mizoroki T, Yoshiike Y, Sahara N, Takashima A (2007) Hyperphosphorylated tau in parahippocampal cortex impairs place learning in aged mice expressing wild-type human tau. *EMBO J* 26: 5143−5152

Kobayashi S, Tanaka T, Soeda Y, Almeida OFX, Takashima A (2017) Local somatodendritic translation and hyperphosphorylation of tau protein triggered by AMPA and NMDA receptor stimulation. *EBioMedicine* 20: 120−126

Kontaxi C, Piccardo P, Gill AC (2017) Lysine-directed post-translational modifications of tau protein in Alzheimer's disease and related tauopathies. *Front Mol Biosci* 4: 56

Lee MJ, Lee JH, Rubinsztein DC (2013) Tau degradation: the ubiquitin-proteasome system versus the autophagy-lysosome system. *Prog Neurobiol* 105: 49−59

Lopes S, Lopes A, Pinto V, Guimaraes MR, Sardinha VM, Duarte-Silva S, Pinheiro S, Pizarro J, Oliveira JF, Sousa N, Leite-Almeida H, Sotiropoulos I (2016a) Absence of Tau triggers age-dependent sciatic nerve morphofunctional deficits and motor impairment. *Aging Cell* 15: 208−216

Lopes S, Teplytska L, Vaz-Silva J, Dioli C, Trindade R, Morais M, Webhofer C, Maccarrone G, Almeida OF, Turck CW, Sousa N, Sotiropoulos I, Filiou MD (2016b) Tau deletion prevents stress-induced dendritic atrophy in prefrontal cortex: role of synaptic mitochondria. *Cereb Cortex* 27: 2580−2591

Lopes S, Vaz-Silva J, Pinto V, Dalla C, Kokras N, Bedenk B, Mack N, Czisch M, Almeida OF, Sousa N, Sotiropoulos I (2016c) Tau protein is essential for stress-induced brain pathology. *Proc Natl Acad Sci USA* 113: E3755−E3763

Machado A, Herrera AJ, de Pablos RM, Espinosa-Oliva AM, Sarmiento M, Ayala A, Venero JL, Santiago M, Villaran RF, Delgado-Cortes MJ, Arguelles S, Cano J (2014) Chronic stress as a risk factor for Alzheimer's disease. *Rev Neurosci* 25: 785−804

Maminska A, Bartosik A, Banach-Orlowska M, Pilecka I, Jastrzebski K, Zdzalik-Bielecka D, Castanon I, Poulain M, Neyen C, Wolinska-Niziol L, Torun A, Szymanska E, Kowalczyk A, Piwocka K, Simonsen A, Stenmark H, Furthauer M, Gonzalez-Gaitan M, Miaczynska M (2016) ESCRT proteins restrict constitutive NF-kappaB signaling by trafficking cytokine receptors. *Sci Signal* 9: ra8

Mondragon-Rodriguez S, Trillaud-Doppia E, Dudilot A, Bourgeois C, Lauzon M, Leclerc N, Boehm J (2012) Interaction of endogenous tau protein with synaptic proteins is regulated by N-methyl-D-aspartate receptor-dependent tau phosphorylation. *J Biol Chem* 287: 32040−32053

Nixon RA, Yang DS (2011) Autophagy failure in Alzheimer's disease−locating the primary defect. *Neurobiol Dis* 43: 38−45

Oshima R, Hasegawa T, Tamai K, Sugeno N, Yoshida S, Kobayashi J, Kikuchi A, Baba T, Futatsugi A, Sato I, Satoh K, Takeda A, Aoki M, Tanaka N (2016) ESCRT-0 dysfunction compromises autophagic degradation of protein aggregates and facilitates ER stress-mediated neurodegeneration via apoptotic and necroptotic pathways. *Sci Rep* 6: 24997

Pallas-Bazarra N, Jurado-Arjona J, Navarrete M, Esteban JA, Hernandez F, Avila J, Llorens-Martin M (2016) Novel function of Tau in regulating the effects of external stimuli on adult hippocampal neurogenesis. *EMBO J* 35: 1417−1436

Pinheiro S, Silva J, Mota C, Vaz-Silva J, Veloso A, Pinto V, Sousa N, Cerqueira J, Sotiropoulos I (2015) Tau mislocation in glucocorticoid-triggered hippocampal pathology. *Mol Neurobiol* 53: 4745−4753

Pooler AM, Hanger DP (2010) Functional implications of the association of tau with the plasma membrane. *Biochem Soc Trans* 38: 1012−1015

Raiborg C, Stenmark H (2009) The ESCRT machinery in endosomal sorting of ubiquitylated membrane proteins. *Nature* 458: 445−452

Rivero-Rios P, Gomez-Suaga P, Fernandez B, Madero-Perez J, Schwab AJ, Ebert AD, Hilfiker S (2015) Alterations in late endocytic trafficking related to the pathobiology of LRRK2-linked Parkinson's disease. *Biochem Soc Trans* 43: 390−395

Roberson ED, Scearce-Levie K, Palop JJ, Yan F, Cheng IH, Wu T, Gerstein H, Yu GQ, Mucke L (2007) Reducing endogenous tau ameliorates amyloid beta-

induced deficits in an Alzheimer's disease mouse model. *Science* 316: 750–754

Ross JA, Gliebus G, Van Bockstaele EJ (2017) Stress induced neural reorganization: a conceptual framework linking depression and Alzheimer's disease. *Prog Neuropsychopharmacol Biol Psychiatry* 85: 136–151

Sahu R, Kaushik S, Clement CC, Cannizzo ES, Scharf B, Follenzi A, Potolicchio I, Nieves E, Cuervo AM, Santambrogio L (2011) Microautophagy of cytosolic proteins by late endosomes. *Dev Cell* 20: 131–139

Sheehan P, Zhu M, Beskow A, Vollmer C, Waites CL (2016) Activity-Dependent Degradation of Synaptic Vesicle Proteins Requires Rab35 and the ESCRT Pathway. *J Neurosci* 36: 8668–8686

Small SA, Simoes-Spassov S, Mayeux R, Petsko GA (2017) Endosomal traffick jams represent a pathogenic hub and therapeutic target in Alzheimer's disease. *Trends Neurosci* 40: 592–602

Sotiropoulos I, Catania C, Riedemann T, Fry JP, Breen KC, Michaelidis TM, Almeida OF (2008a) Glucocorticoids trigger Alzheimer disease-like pathobiochemistry in rat neuronal cells expressing human tau. *J Neurochem* 107: 385–397

Sotiropoulos I, Cerqueira JJ, Catania C, Takashima A, Sousa N, Almeida OF (2008b) Stress and glucocorticoid footprints in the brain-the path from depression to Alzheimer's disease. *Neurosci Biobehav Rev* 32: 1161–1173

Sotiropoulos I, Catania C, Pinto LG, Silva R, Pollerberg GE, Takashima A, Sousa N, Almeida OF (2011) Stress acts cumulatively to precipitate Alzheimer's disease-like tau pathology and cognitive deficits. *J Neurosci* 31: 7840–7847

Sotiropoulos I, Galas MC, Silva JM, Skoulakis E, Wegmann S, Maina MB, Blum D, Sayas CL, Mandelkow EM, Mandelkow E, Spillantini MG, Sousa N, Avila J, Medina M, Mudher A, Buee L (2017) Atypical, non-standard functions of the microtubule associated Tau protein. *Acta Neuropathol Commun* 5: 91

Sousa N, Almeida OF (2012) Disconnection and reconnection: the morphological basis of (mal)adaptation to stress. *Trends Neurosci* 35: 742–751

Subach FV, Subach OM, Gundorov IS, Morozova KS, Piatkevich KD, Cuervo AM, Verkhusha VV (2009) Monomeric fluorescent timers that change color from blue to red report on cellular trafficking. *Nat Chem Biol* 5: 118–126

Suzuki K, Parker CC, Pentchev PG, Katz D, Ghetti B, D'Agostino AN, Carstea ED (1995) Neurofibrillary tangles in Niemann-Pick disease type C. *Acta Neuropathol* 89: 227–238

Vossel KA, Zhang K, Brodbeck J, Daub AC, Sharma P, Finkbeiner S, Cui B, Mucke L (2010) Tau reduction prevents Abeta-induced defects in axonal transport. *Science* 330: 198

Vyas S, Rodrigues AJ, Silva JM, Tronche F, Almeida OF, Sousa N, Sotiropoulos I (2016) Chronic stress and glucocorticoids: from neuronal plasticity to neurodegeneration. *Neural Plast* 2016: 6391686

Watson JA, Bhattacharyya BJ, Vaden JH, Wilson JA, Icyuz M, Howard AD, Phillips E, DeSilva TM, Siegal GP, Bean AJ, King GD, Phillips SE, Miller RJ, Wilson SM (2015) Motor and sensory deficits in the teetering mice result from mutation of the ESCRT component HGS. *PLoS Genet* 11: e1005290

Yevshin I, Sharipov R, Valeev T, Kel A, Kolpakov F (2017) GTRD: a database of transcription factor binding sites identified by ChIP-seq experiments. *Nucleic Acids Res* 45: D61–D67

Yin Y, Gao D, Wang Y, Wang ZH, Wang X, Ye J, Wu D, Fang L, Pi G, Yang Y, Wang XC, Lu C, Ye K, Wang JZ (2016) Tau accumulation induces synaptic impairment and memory deficit by calcineurin-mediated inactivation of nuclear CaMKIV/CREB signaling. *Proc Natl Acad Sci USA* 113: E3773–E3781

Zempel H, Thies E, Mandelkow E, Mandelkow EM (2010) Abeta oligomers cause localized Ca(2+) elevation, missorting of endogenous Tau into dendrites, Tau phosphorylation, and destruction of microtubules and spines. *J Neurosci* 30: 11938–11950

Zhang JY, Liu SJ, Li HL, Wang JZ (2005) Microtubule-associated protein tau is a substrate of ATP/Mg(2+)-dependent proteasome protease system. *J Neural Transm (Vienna)* 112: 547–555

Zhang Y, Chen X, Zhao Y, Ponnusamy M, Liu Y (2017a) The role of ubiquitin proteasomal system and autophagy-lysosome pathway in Alzheimer's disease. *Rev Neurosci* 28: 861–868

Zhang Y, Schmid B, Nikolaisen NK, Rasmussen MA, Aldana BI, Agger M, Calloe K, Stummann TC, Larsen HM, Nielsen TT, Huang J, Xu F, Liu X, Bolund L, Meyer M, Bak LK, Waagepetersen HS, Luo Y, Nielsen JE, FReJA Consortium *et al* (2017b) Patient iPSC-derived neurons for disease modeling of frontotemporal dementia with mutation in CHMP2B. *Stem Cell Reports* 8: 648–658

56

Chapter 2.1.1

João Vaz-Silva, Gomes P, Jin Q, Zhu M, Zhuravleva V, Quintremil S, Meira T, Silva J, Dioli C, Soares-Cunha C, Daskalakis NP, Sousa N, Ioannis Sotiropoulos & Clarissa L Waites

Endolysosomal degradation of Tau and its role in

glucocorticoid-driven hippocampal malfunction

Expanded View Figures

Figure EV1. EM and PLA controls, and the impact of ubiquitylation on Hrs/Tau interaction.

A   EM negative controls for Tau immunogold labeling.

B   As a technical control for specificity of the proximity ligation assay (PLA) to detect mCh-Hrs/Tau interaction, mCh-Hrs was expressed in N2a cells, but only primary antibody against Tau was used, preventing the PLA signal.

C, D   For validation of PLA to detect FLAG-Hrs/Tau interaction (arrows), FLAG-Hrs was expressed in N2a cells alone (left), or together with EGFP-Tau (middle). Higher Tau levels lead to significantly increased PLA signal, indicating specificity of the interaction (scale bar: 5 μm) (n = 23–28 cells per experiment; ****$P < 0.0001$; Mann-Whitney test). Moreover, FLAG-peptide incubation with anti-FLAG antibody prior to the PLA protocol completely abolished PLA signal (right), thus serving as a negative control.

E   Immunoblots of N2a cell lysates expressing FLAG-Hrs and either EGFP-Tau or soluble EGFP, immunoprecipitated with GFP antibodies and probed with FLAG or Tau antibodies. Note that Hrs is pulled down with EGFP-Tau, but not with EGFP alone, demonstrating a specific interaction between Tau and Hrs.

F, G   Immunoblots of N2a cell lysates expressing FLAG-Hrs and either EGFP-Tau or soluble EGFP, ±the deubiquitylating enzyme (DUB) inhibitor PR619, immunoprecipitated with GFP antibodies and probed with FLAG or Tau antibodies. Note that Hrs is pulled down with EGFP-Tau but not EGFP alone, and that this pull down is enhanced in the presence of PR619, demonstrating specificity of the Hrs/Tau and its dependence on ubiquitylation (n = 3/condition; ***$P = 0.0008$; unpaired Student's t-test).

H, I   Incubation of N2a cells with DUB inhibitor PR619 also significantly increases the number of PLA puncta, demonstrating the dependence of Hrs/Tau interaction on ubiquitylation (n = 113–121/condition; **$P = 0.0014$; Mann-Whitney test).

Source data are available online for this figure.

A

B

PLA: mCh-Hrs - Tau
negative control

mCh-HRS
mCh-Hrs-Tau interaction

C

FLAG-Hrs

FLAG-Hrs + GFP-Tau

FLAG-Hrs + FLAG blocking peptide

Tubulin

Tubulin
GFP-Tau

Tubulin

FLAG-Hrs-Tau interaction

FLAG-Hrs-Tau interaction

FLAG-Hrs-Tau interaction

D

total Tau - Hrs

****

| FLAG-Hrs | + | + |
| EGFP-Tau | − | + |

E

F

G

Hrs (IP)

***

H

mCh   PLA   Merge

mCh+
FLAG-Hrs
Control

mCh+
FLAG-Hrs+
DUB
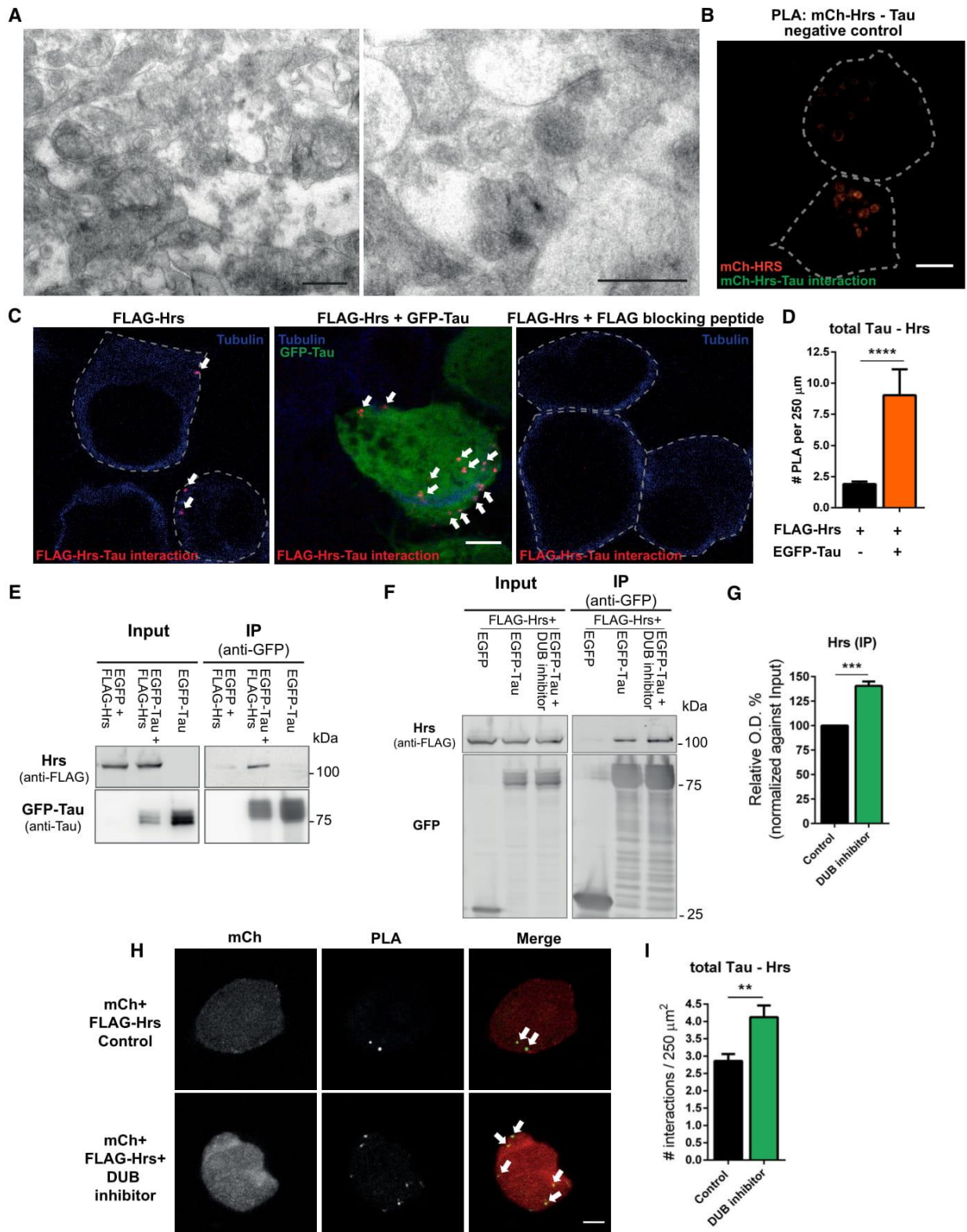inhibitor

I

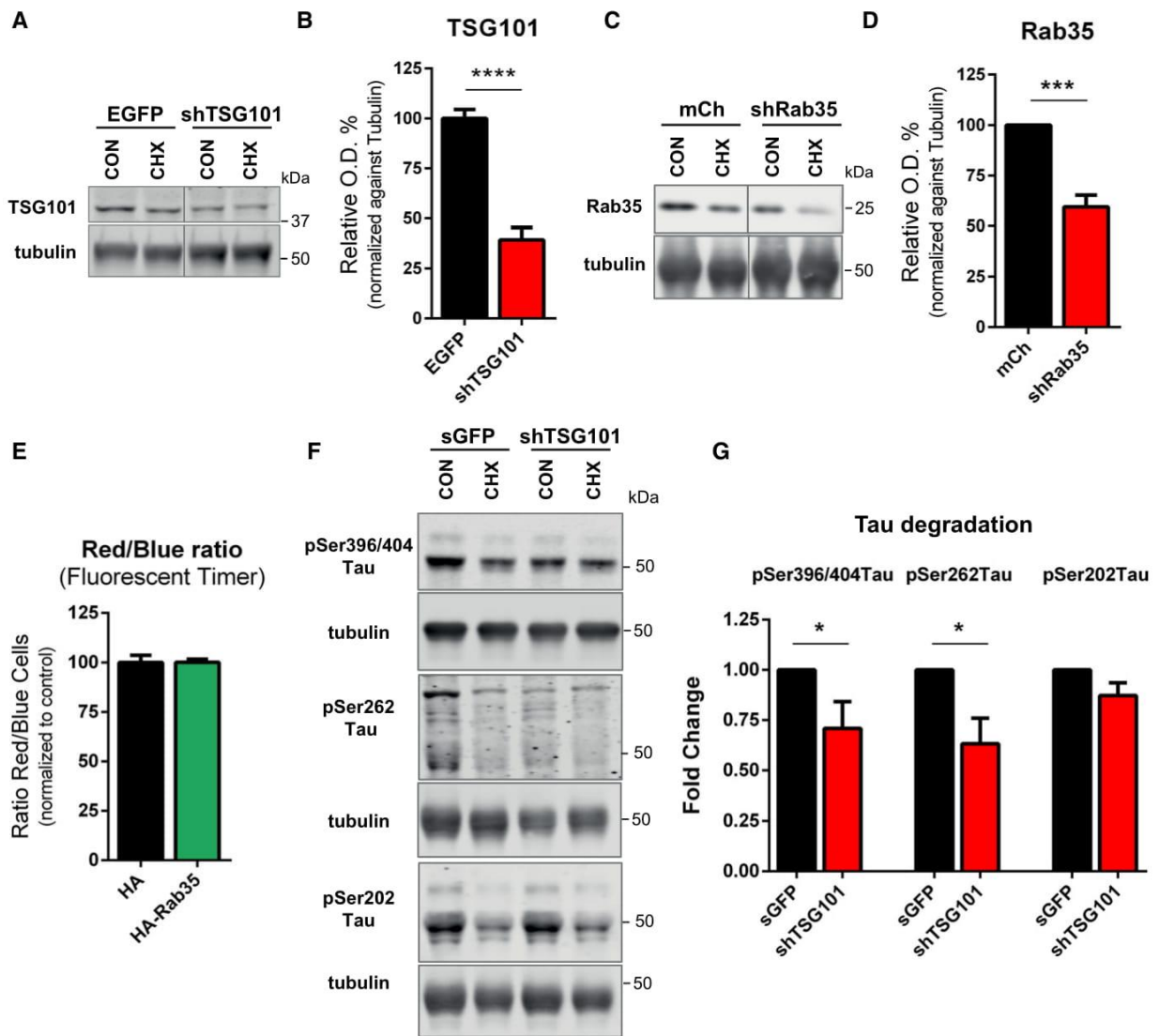total Tau - Hrs

**

Figure EV1.

60

Figure EV2. ESCRT-I component TSG101 mediates degradation of pSer396/404- and pSer262-Tau.

A, B   Representative immunoblots (A) and quantification of TSG101 levels (B) from 14 DIV primary neurons transduced with EGFP or shTSG101, treated for 24 h with either DMSO (CON) or cycloheximide (CHX), and probed for TSG101 and tubulin. (B) shTSG101 significantly decreases TSG101 protein levels (n = 12–14/condition, unpaired Student's t-test, ****P < 0.0001).

C, D   Representative immunoblots (C) and quantification of Rab35 levels (D) from 14 DIV primary neurons transduced with mCherry or shRab35, treated for 24 h with either DMSO (CON) or cycloheximide (CHX), and probed for Rab35 and tubulin. (D) shRab35 significantly decreases Rab35 protein levels (n = 4/condition, unpaired Student's t-test, ***P = 0.0004).

E   Ratio of red:blue N2a cells co-expressing medium FT together with HA vector or HA-Rab35 and analyzed by flow cytometry, showing no effect of Rab35 on the turnover of FT tag alone. These data indicate that Rab35 specifically stimulates the degradation of Tau (n = 6/condition).

F, G   Representative immunoblots (F) and quantification of Tau degradation (G) from 14 DIV primary neurons transduced with EGFP or shTSG101, treated for 24 h with either DMSO (CON) or cycloheximide (CHX), and probed for pSer396/404-Tau (PHF1), pSer262-Tau, or pSer202-Tau (CP13) and tubulin. shTSG101-expressing neurons exhibit markedly decreased pSer262-Tau and pSer396/404-Tau degradation compared to EGFP-expressing controls, while pSer202-Tau degradation is unaffected (n = 8/condition for pSer396/404-Tau, n = 5/condition for pSer262-Tau and pSer202-Tau, *ppSer396/404-Tau = 0.0462, ppSer262-Tau = 0.0199).

Data information: All numeric data represent mean ± SEM.
Source data are available online for this figure.

A

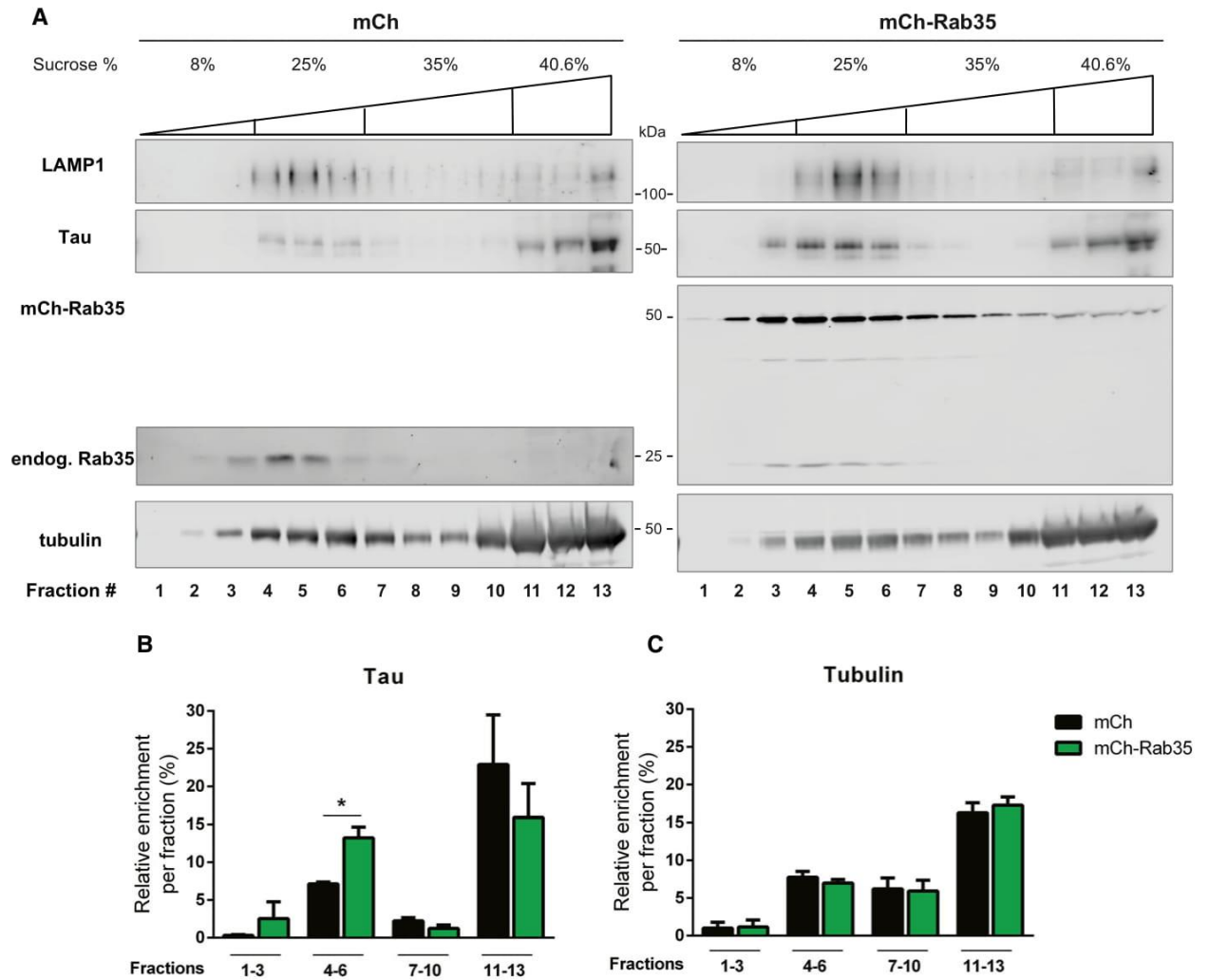**B**   **C**

Figure EV3. Rab35 overexpression increases Tau accumulation in neuronal endolysosomal fractions.

A   Immunoblots of Tau and tubulin in sucrose-gradient-based subcellular fractions of 14 DIV neurons transduced with mCh or mCh-Rab35.

B, C   Quantification of the enrichment per fraction (%) of Tau and tubulin. Rab35-expressing neurons exhibit an increased relative distribution of Tau in fractions 3–6 (endosome/lysosome-enriched fractions) compared to mCh-expressing neurons, while tubulin distribution remained unchanged (*P = 0.0135; unpaired Student's *t*-test; n = 1). LAMP1 was used as a marker of endosome/lysosome fractions.

Data information: All numeric data represent mean ± SEM.
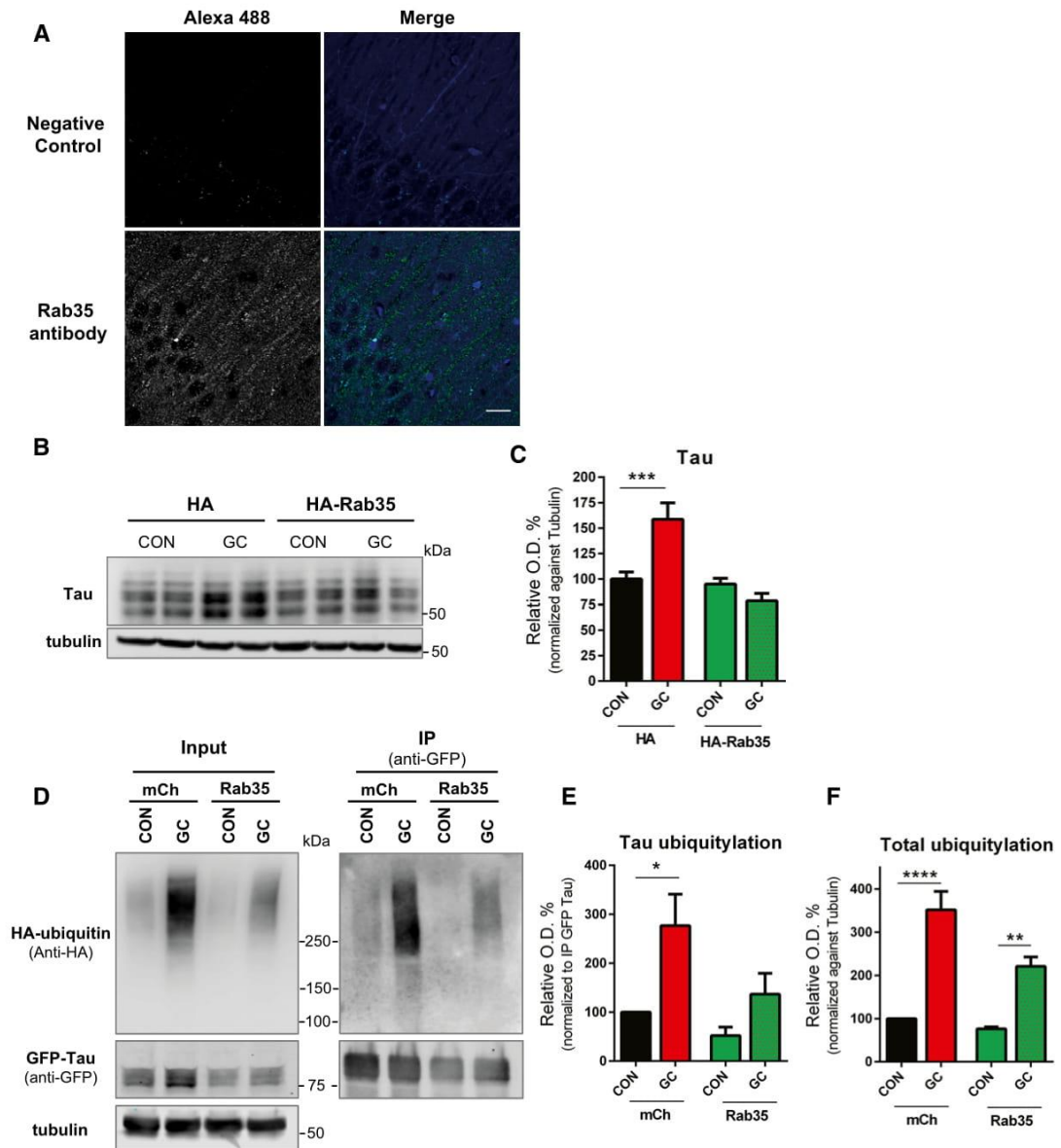Source data are available online for this figure.

62

Figure EV4. Rab35 overexpression prevents GC-induced accumulation of total and ubiquitylated Tau.

A   Rat hippocampal sections incubated with secondary antibody only (negative control) or Rab35 primary antibody, showing specificity for Rab35 immunofluorescence.

B, C   Representative immunoblots and quantification of Tau levels from N2a cells transfected with HA vector or HA-Rab35, treated with vehicle control (CON) or GC, and probed for Tau and tubulin. GC induces significant Tau accumulation in cells expressing the HA vector control, and this effect is completely blocked by Rab35 overexpression (n = 9/condition; 2-way ANOVA, GC × Rab35 interaction $F_{1, 32}$ = 14.40 P = 0.0006, overall GC effect $F_{1, 32}$ = 4.537 P = 0.04, overall Rab35 effect $F_{1, 32}$ = 18.47 P = 0.002, Sidak *post hoc* analysis ***P = 0.0004).

D   Representative blots of cell lysates (input; left) or anti-GFP immunoprecipitates (IP; right) from N2a cells transfected with HA-Ubiquitin, EGFP-Tau, and either mCh or mCh-Rab35 under control and GC conditions.

E   GC induces significant accumulation of ubiquitylated Tau (IP panel from D), and this effect is attenuated by Rab35 overexpression (n = 4/condition; 2-way ANOVA overall GC effect $F_{1, 12}$ = 10,99 P = 0.0062, overall Rab35 effect $F_{1, 12}$ = 5,673 P = 0.0346, Sidak *post hoc* analysis *P = 0.0161).

F   Similarly, GC induces the accumulation of total ubiquitylated proteins (input panel from D), and this effect is attenuated by Rab35 expression (n = 4/condition; 2-way ANOVA, GC × Rab35 interaction $F_{1,12}$ = 4.904 P = 0.0469, overall GC effect $F_{1, 12}$ = 67.25 P < 0.0001, overall Rab35 effect $F_{1, 12}$ = 10.27 P = 0.0076, Sidak *post hoc* analysis **P = 0.0023, ****P < 0.0001).

Data information: All numeric data represent mean ± SEM.
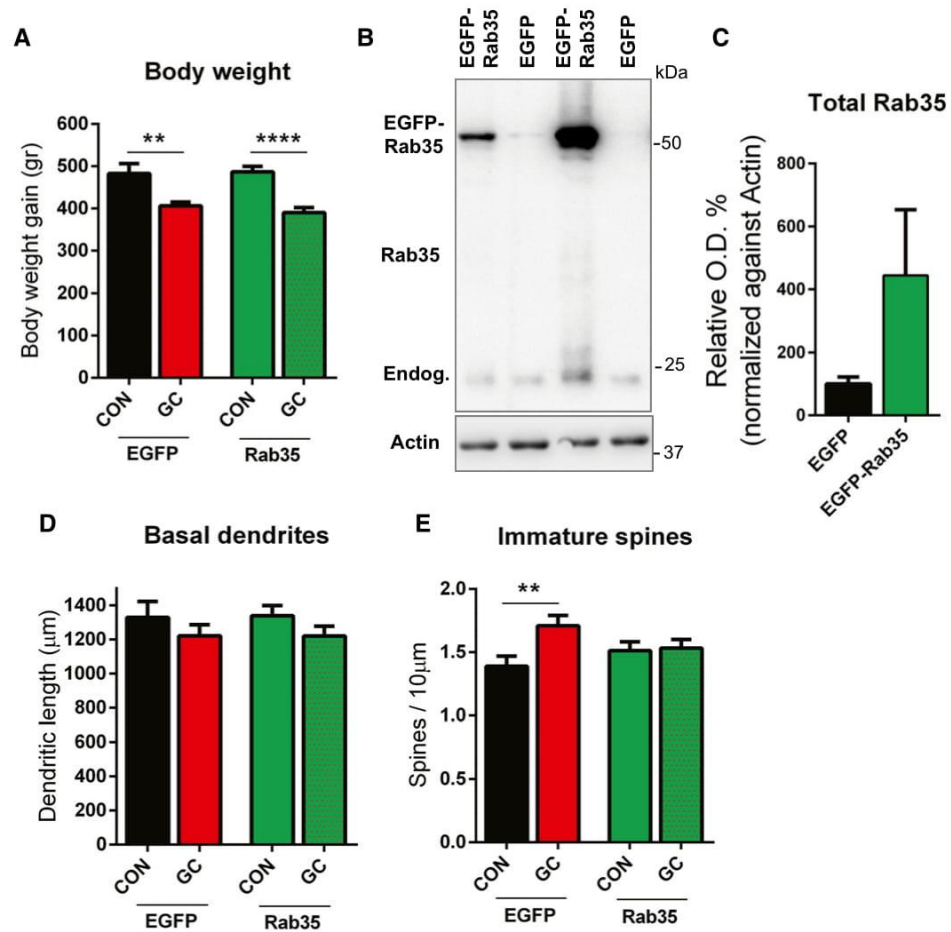Source data are available online for this figure.

Figure EV5. Rab35 overexpression in vivo blocks GC-driven neurostructural changes.

A   Body weight of rats injected with either EGFP or EGFP-Rab35 and treated for 2 weeks with GC or vehicle control (CON). GC-treated groups exhibited reduced body weight, demonstrating the similar systemic effect of GC treatment on both EGFP- and Rab35-expressing animals (n = 6–8 animals; 2-way ANOVA, overall *GC* effect $F_{1,\ 25}$ = 35,63 P < 0.0001, Sidak *post hoc* analysis **P = 0,0031, ****P < 0.0001).

B, C   Blots and quantification of AAV-EGFP-Rab35 overexpression levels in the animals' brains, showing a 4:1 ratio of Rab35 levels in EGFP-Rab35-injected animals (expressing both exogenous and endogenous Rab35) vs. EGFP-injected animals (expressing only endogenous Rab35).

D   The average lengths of basal dendrites of CA1 pyramidal neurons are not altered following GC treatment in either EGFP- or Rab35-expressing animals.

E   Immature spine density increases following GC treatment in EGFP- but not Rab35-expressing animals (n = 6–7 animals/group; 6–8 neurons per animal, 2-way ANOVA, *GC* × *Rab35* interaction $F_{1,\ 499}$ = 4.013 P = 0.045, overall *GC* effect $F_{1,\ 499}$ = 5.142 P = 0.0238, Sidak *post hoc* analysis **P = 0.0072).

Data information: All numeric data represent mean ± SEM.
Source data are available online for this figure.

64

Expanded View Table 1

| Antibody	Source	Species	Catalog no.
Actin	Abcam	Mouse	ab8226
CHMP2b	Abcam	Rabbit	ab33174
CP13 (pSer202)	Gift from Peter Davies	Mouse	
DA9	Gift from Peter Davies	Mouse	
EEA1	Cell Signaling Technology	Rabbit	3288S
FLAG	Sigma	Mouse	F3165
FLAG	Abcam	Rabbit	ab1162
HA	Santa Cruz Biotechnology	Rabbit	y-11 sc805
HA	Santa Cruz Biotechnology	Mouse	f-7 sc7392
Hrs	Abcam	Mouse	ab56468
LAMP1	Abcam	Rabbit	ab24170
MAP2	Abcam	Chicken	ab92434
mCherry	Biovision	Rabbit	5993
PHF1 (pser396/404)	Gift from Peter Davies	Mouse	
pSer262 Tau	ThermoFisher Scientific	Rabbit	44-750G
Rab5	Synaptic Systems	Mouse	108011
Rab7	Abcam	Mouse	ab50533
Rab8	Proteintech	Rabbit	55296-1-AP
Rab10	Santa Cruz Biotechnology	Goat	sc6564
Rab11	Cell Signaling Technology	Rabbit	5589
Rab14	Santa Cruz Biotechnology	Rabbit	sc-98610
Rab35	Proteintech	Rabbit	11329-2-AP
Tau5	Abcam	Mouse	ab80579
Tubulin	Abcam	Rabbit	ab4074
Tubulin	Sigma	Mouse	t9026
TSG101	Santa Cruz Biotechnology	Mouse	sc-7964

Figure 2

Figure 3

3A
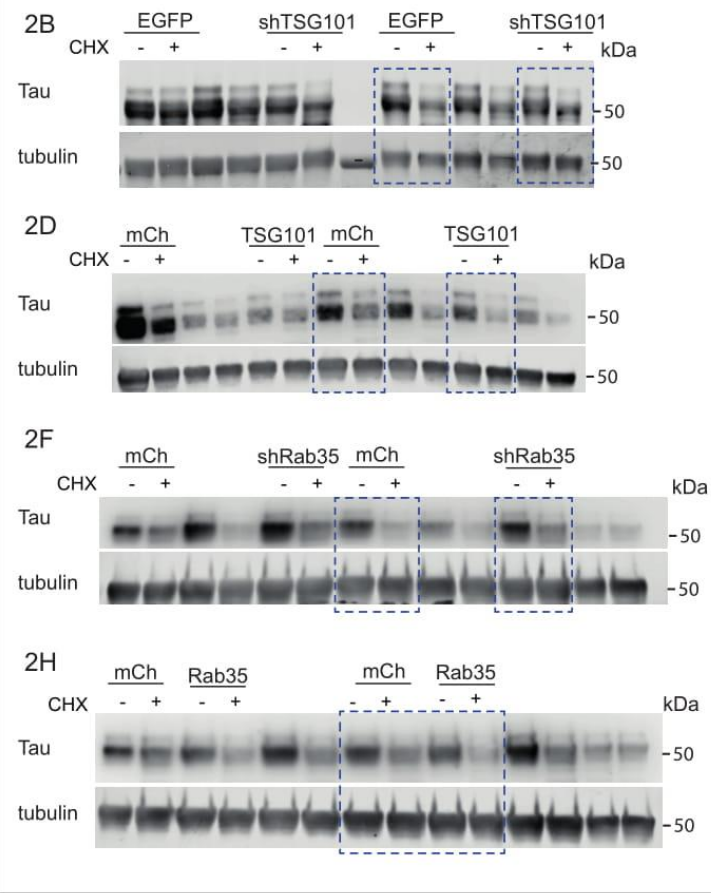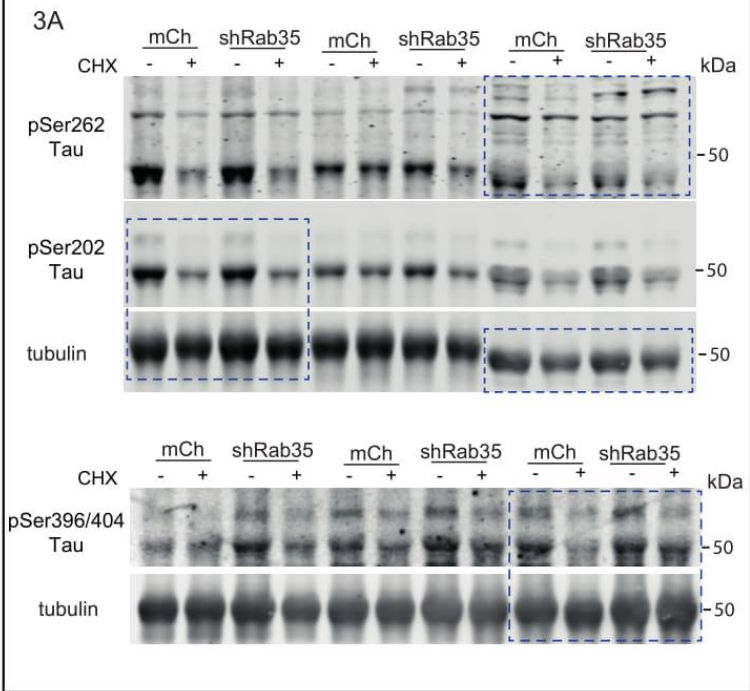
Figure 5

5A

5E

Figure 6

Figure EV1

EV1E

EV1F

70

Figure EV2

EV2A

EV2C

EV2F

Figure EV2

EV2A

EV2C
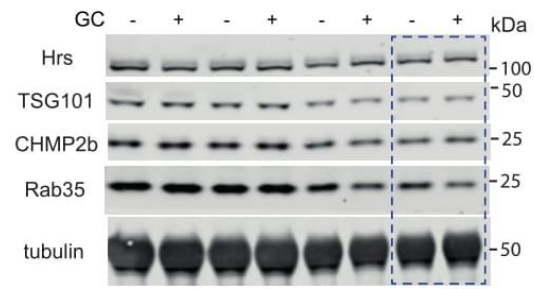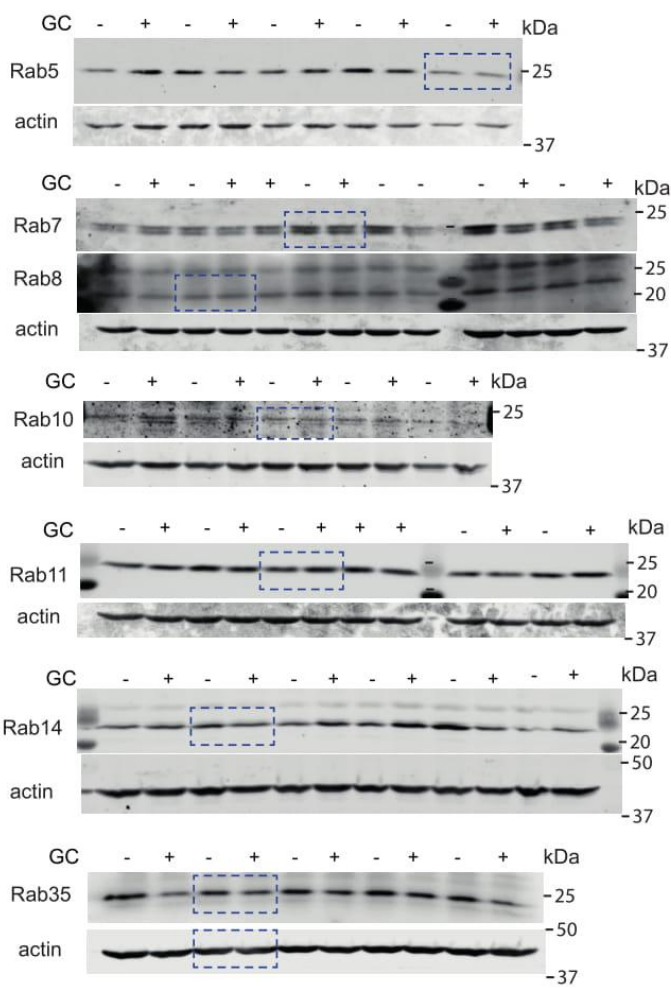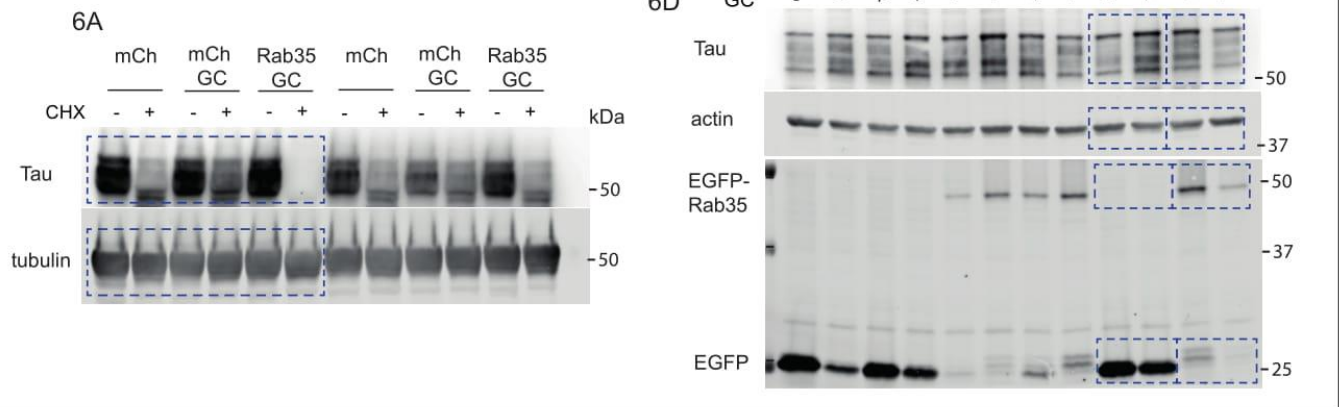
EV2F
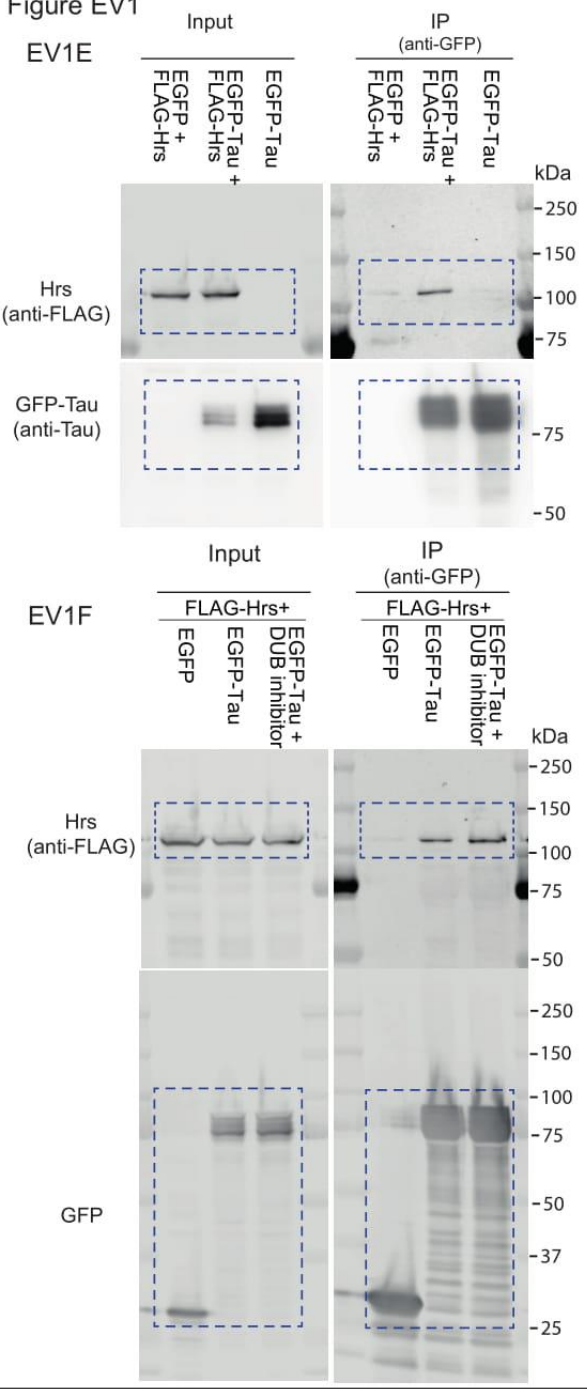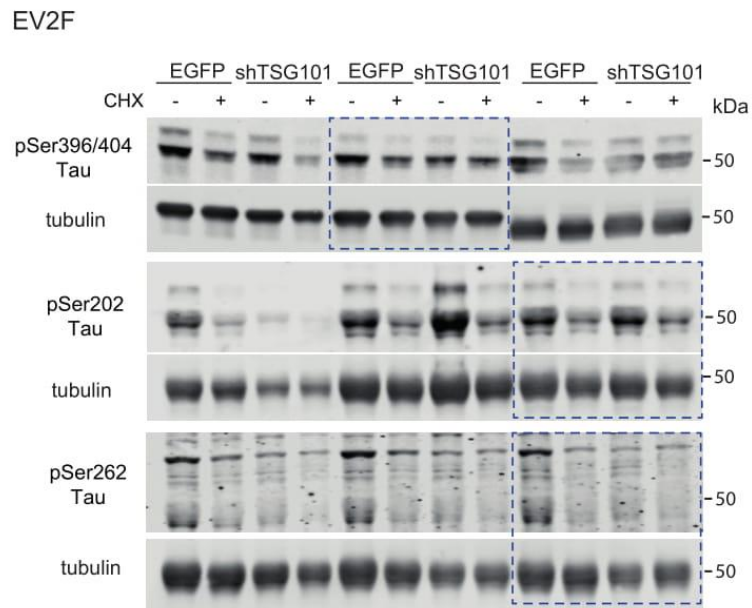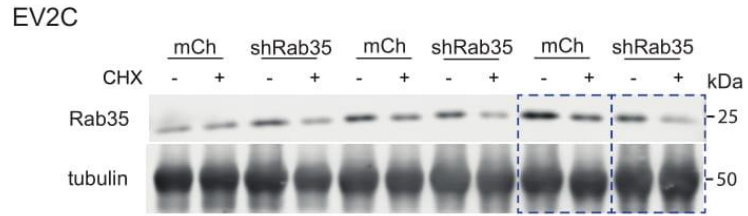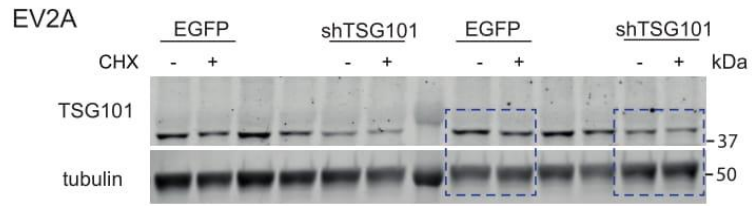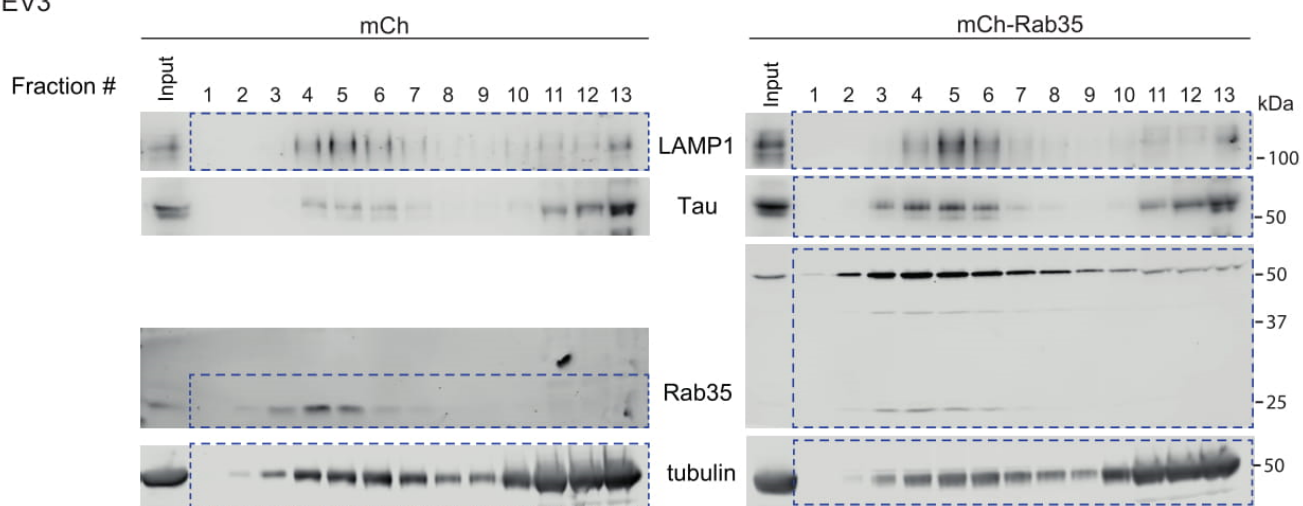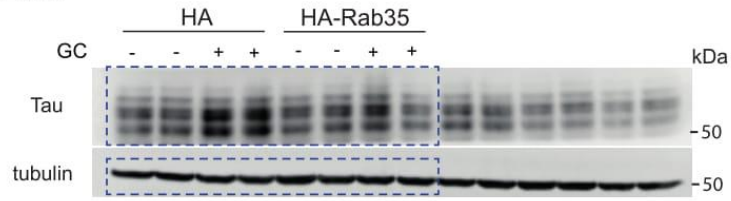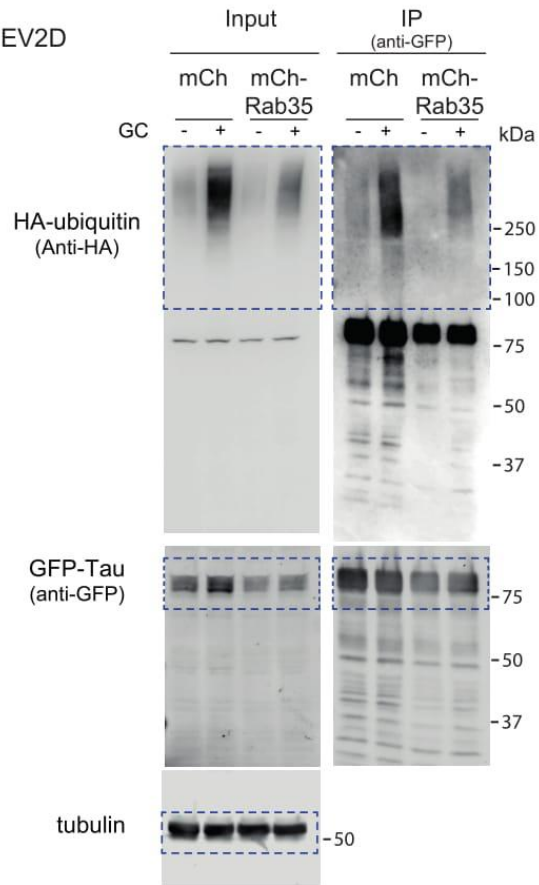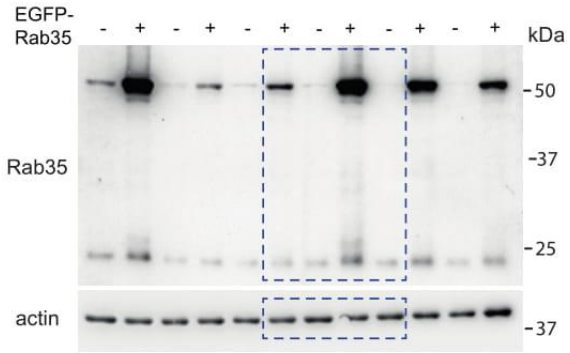
Figure EV3

Figure EV4

EV2B

EV2D

Figure EV5

EV5B

João Vaz-Silva, Zhuravleva V, Zhu M, Jin Q, Sousa N, Ioannis Sotiropoulos & Clarissa L Waites

Identification of Rab35 as a negative regulator of Aβ production

Manuscript under preparation

Identification of Rab35 as a negative regulator of Aβ production

João Vaz-Silva[1,2,3], Zhuravleva V[3,4], Zhu M[3], Rufei Li[3], Jin Q[3], Sousa N[1,2], Ioannis Sotiropoulos[1,2] & Clarissa L Waites[3]

1 Life and Health Sciences Research Institute (ICVS), School of Medicine, University of Minho, Braga, Portugal
2 ICVS/3B's - PT Government Associate Laboratory, Braga, Portugal
3 Department of Pathology and Cell Biology, Taub Institute for Research on Alzheimer's Disease and the Aging Brain, Columbia University Medical Center, New York, NY, USA
4 Neurobiology and Behavior Graduate Program, Columbia University, New York, NY, USA

Disclaimer:

All data presented in figure 1A-B, figure 3 and supplementary figure 1, respective results and figure legend are adapted from Joao Vaz-Silva's Master thesis and should not be considered as constituent part of this PhD thesis, however we could not exclude them from this chapter since this data is an integral part of the submitted manuscript.

Abstract

Cleavage of amyloid precursor protein (APP) into neurotoxic amyloid-β (Aβ) peptide is a key event in Alzheimer's disease pathogenesis, but the intraneuronal mechanisms responsible for Aβ overproduction remain unclear. A series of complex membrane trafficking events regulate APP cleavage by β-secretase (BACE), the rate-limiting step in Aβ production. As master regulators of vesicle biogenesis, transport, and fusion, Rab GTPases catalyze the trafficking of APP and BACE1 throughout the endosomal network, and have recently been implicated in AD etiology. Here, we identify one such endocytic Rab, Rab35, as a potent negative regulator of Aβ production, and find that its levels are downregulated in AD and other pathological conditions promoting APP misprocessing such as exposure to chronic stress, a risk factor of AD. Moreover, we demonstrate that Rab35 attenuates Aβ production by decreasing the trafficking of both APP and BACE1 into the endosomal network, the major site of Aβ production. Mechanistically, Rab35 decreases endosomal APP levels by stimulating its fast recycling to the plasma membrane, and reduces endosomal BACE1 levels by stimulating its trafficking through the retrograde pathway to the trans-Golgi Network. These studies suggest that

Rab35 is a negative regulator of APP and BACE1 intraneuronal trafficking and subsequent Aβ production while deficits in Rab35 may promote AD brain pathology.

Introduction

Alzheimer's disease (AD) is an age-related neurodegenerative disease that causes progressive memory loss and dementia. A pathological hallmark of AD is the presence of cerebral amyloid plaques, composed of aggregated amyloid-β (Aβ) peptides that accumulate following the proteolytic cleavage of Amyloid Precursor Protein (APP) (Querfurth and LaFerla, 2010). While the toxicity of amyloid plaques remains controversial, considerable evidence shows that Aβ peptides are neurotoxic, supporting the 'amyloid cascade' hypothesis that AD is initiated by Aβ production (Mucke and Selkoe, 2012). Indeed, familial early-onset forms of AD are caused by autosomal dominant mutations in APP or presenilin genes that promote amyloidogenic processing of APP into Aβ. However, 95% of AD cases are sporadic and late-onset (LOAD), precipitated by a complex interplay of environmental and genetic risk factors . Intriguingly, many of the recently-identified genetic risk factors for AD are linked to endosomal protein trafficking.

The rate-limiting step for Aβ production is APP cleavage by β-secretase 1 (BACE1); thus, APP and BACE1 trafficking/localization within the cell determine APP cleavage fate (Haass et al., 2012). After synthesis in the endoplasmatic reticulum (ER), APP and BACE1 are transported to the plasma membrane (PM) and subsequently internalized into the endosomal network, which contains the optimal acidic pH for BACE1 activity and has been identified as a major site of Aβ generation (Haass et al., 2012). Indeed, endocytosis of APP and BACE1 is essential for Aβ production (Cirrito et al., 2005; Zou et al., 2007), and AD-linked genes are known to induce endosomal dysfunction and prolong the resident times of APP and/or BACE in endosomal compartments, accelerating Aβ production (Small et al., 2017; Ubelmann et al., 2017).

Rab GTPases are master regulators of endosomal protein trafficking, contributing to the structural and functional identity of intracellular membrane compartments (Stenmark, 2009). Rabs cycle between active (GTP-bound) and inactive (GDP-bound) states, with GTP-bound Rabs recruiting effectors that catalyze downstream events such as membrane fusion and vesicle transport (Stenmark, 2009). Given their critical roles in endosomal trafficking, recent studies have begun to explore the role of Rabs in AD pathogenesis, and have identified a subset linked to AD etiology through their regulation of APP trafficking (Ginsberg et al., 2010, 2012; Udayar et al., 2013). However, the contributions of

Rab GTPases to AD pathophysiology and their molecular mechanisms of action remain poorly understood.

In the current study, we identify a specific Rab GTPase, Rab35, whose levels are significantly decreased under conditions that promote AD pathomechanisms (stress, advanced age), potentially linking it to disease etiology. Indeed, we find that Rab35 is the most potent suppressor of APP/BACE interaction in a gain-of-function screen of Rabs that regulate endocytic protein trafficking. Moreover, Rab35 overexpression decreases Aβ production in Neuro2a cells and human-derived cortical neurons. Mechanistically, we show that Rab35 decreases the localization and trafficking of both APP and BACE to endosomes, by stimulating APP recycling between endosomes and the PM, and BACE retrograde trafficking to the trans-Golgi network. Together, these findings implicate Rab35 as an important regulator of Aβ production, and suggest that inhibition of Rab35 expression or activity could be a precipitating factor in AD pathogenesis.

Results

Rab35 levels are decreased in pathological conditions of APP amyloidogenic processing

Our recent work implicates Rab35 as a critical regulator of Tau pathology downstream of stress and glucocorticoids (GCs), the major stress hormones. Given that stress/GCs also stimulate Aβ production (Green et al., 2006b), and Rab35 is a key regulator of endosomal protein trafficking, we tested whether Rab35 also mediates APP misprocessing. In our previous study, we found that Rab35 levels were downregulated by GCs (Vaz-Silva et al., 2018). Therefore, we first assessed whether Rab35 levels were decreased not only by GCs, but also in response to chronic unpredictable stress, shown to stimulate Aβ production and AD progression in both transgenic animal models and human patients. We found that Rab35 levels were decreased by ~60% in chronically stressed animals compared to controls (Fig. 1C, D), and this decrease was not observed for other Rabs associated with endocytic protein trafficking (Fig. 1E, F). In parallel, we analyzed Rab35 levels in animals infused with Aβ peptides in the hippocampus to mimic early stages of AD. Remarkably, we found that Aβ infusion also dramatically decreased Rab35 levels, and that this effect was again specific for Rab35 (Fig. 1C, D). Since ageing is the highest risk factor for AD, we also compared Rab35 levels between young (4 month old) and aged (22-24 month old) rats. Again, we observed a significant (~25%) decrease in hippocampal Rab35 levels in aged animals (Fig. 1A, B), suggesting dysregulation of Rab35 expression

with age. Together, these experiments suggest a negative correlation between Rab35 levels and conditions favoring Aβ production, potentially implicating Rab35 in APP misprocessing.
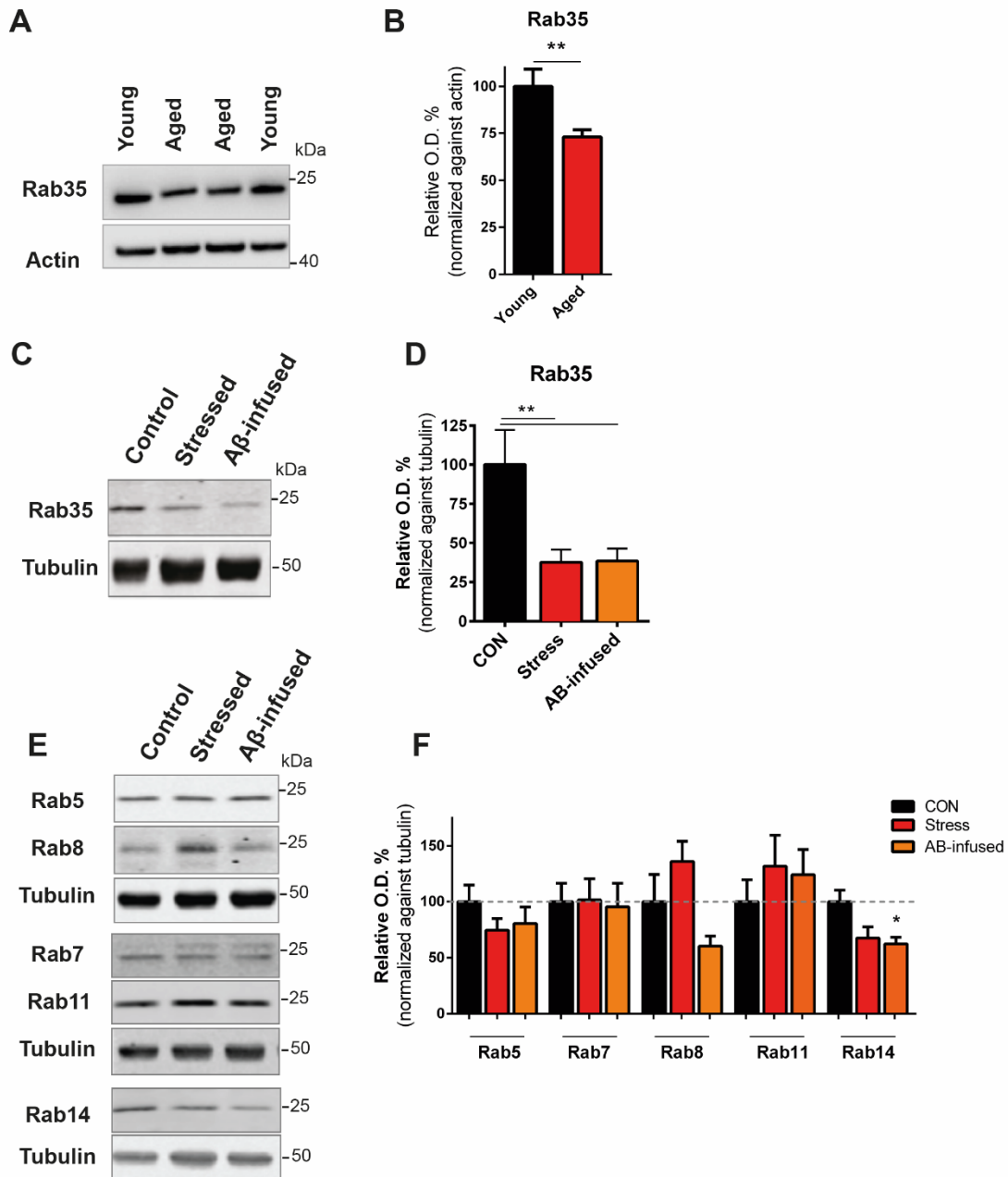
Figure 1. Hippocampal Rab35 levels decrease with ageing, chronic stress and Aβ infusion. A, B) Representative immunoblots (A) and quantification of Rab35 levels (B) in hippocampus of young (4-month-old) and aged (22- to 24-month-old) animals. Protein levels of Rab35 are decreased in aged animals (n = 13–17 per condition, unpaired Student's t-test, **P = 0.0056). C, D) Representative immunoblots (A) and quantification of Rab35 levels (B) in hippocampus of control (CON), stressed and Aβ-infused animals. Both chronic stress and Aβ-infusion decreases Rab35 protein levels in these animals. (n = 8–10 per condition, oneway ANOVA, Dunnet post hoc analysis, **PCON vs. stressed = 0.0075, **PCON vs. Aβ-infused = 0.0069).

E, F) Representative immunoblots (E) and quantification of Rab 5, 7, 8, 11 and 14 levels (F) in hippocampus of control (CON), stressed and Aβ-infused animals. Only Rab14 presented changes by infusion of Aβ (n=8–10 per condition, oneway ANOVA, Dunnet post hoc analysis, *PCON vs. Aβ-infused = 0.0228).

Rab35 suppresses APP amyloidogenic processing through regulation of APP/BACE1 interaction

To assess whether Rab35 has a role in APP processing and Aβ production, we measured the levels of APP and its cleavage products in human induced pluripotent stem cell (iPSC)-derived cortical neurons lentivirally transduced with mCherry-tagged Rab35. Overexpression/gain-of-function of Rab35 did not alter total APP levels (Fig. 2A, B), but decreased the levels of APP C-terminal fragments (CTFs) by ˜25% (Fig. 2A, C), and the levels of secreted Aβ42 and Aβ40 peptides by ˜20% (Fig. 2C, D). The Aβ42/40 ratio was similar between conditions, indicating that production of both Aβ peptides was equally affected. These findings suggest a crucial role for Rab35 in the regulation of APP trafficking through the amyloidogenic pathway.

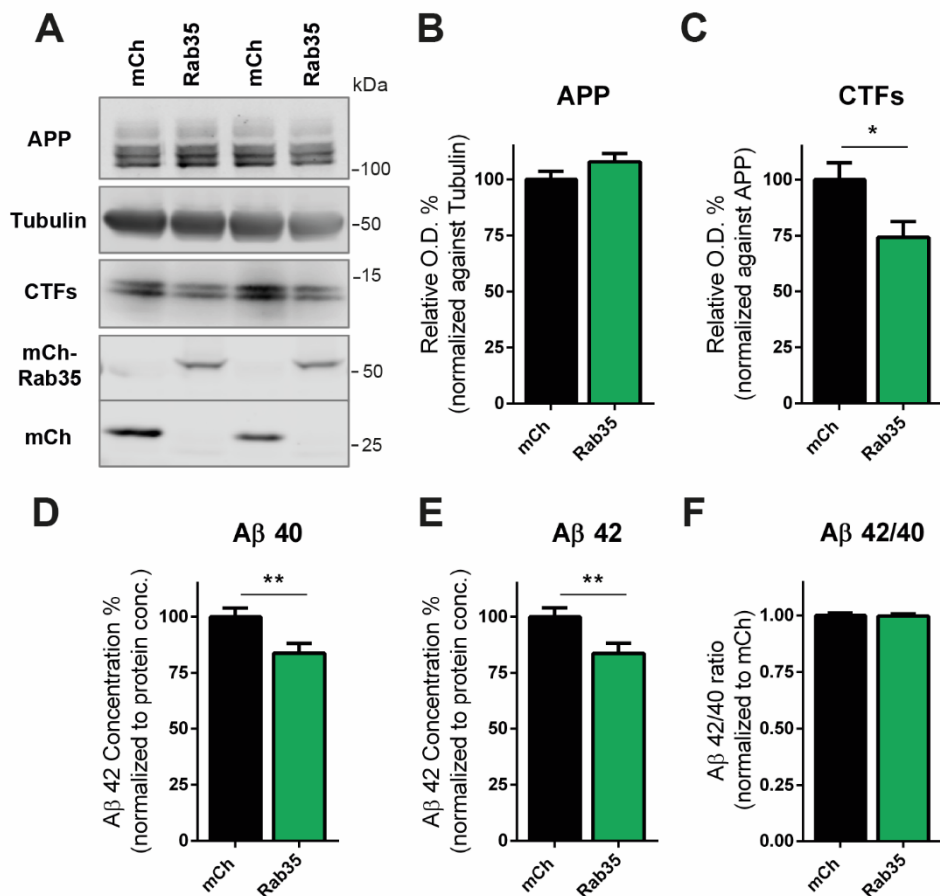**Figure 2. Rab35 suppresses amyloidogenic processing of APP.** A-C) Representative immunoblots (A) and quantification of APP (B) and CTFs (C) from iPSC-derived neurons transduced with mCherry or mCh-Rab35, and probed for APP and CTFs, tubulin and mCherry. Overexpression of Rab35 decreased CTF levels, but did

not alter total APP protein levels (n=19-21 per condition, unpaired Student's t-test, *P = 0.0172). D, E) Measurement of Aβ peptides secreted by iPSC-derived human neurons transduced with mCherry or mCh-Rab35. Rab35 overexpression decreased the levels of both Aβ40 and Aβ42 peptides (n=19-20, (Aβ40) unpaired Student's t-test, **P = 0.0088, (Aβ42) unpaired Student's t-test, **P = 0.0097). F) Ratio of Aβ42/Aβ40 in the culture medium of iPSC-derived neurons, showing no alteration based on Rab35 levels.

Since the rate limiting step for Aβ production is the cleavage of APP by BACE1 protease, we analyzed the effects of Rab35 and other endocytic Rab GTPases on APP/ BACE1 interaction through a previously-described bimolecular fluorescence complementation assay (Das et al., 2016). Here, APP was tagged with the N-terminal fragment of Venus fluorescent protein (VN), and BACE1 with the complementary C-terminal fragment (VC) (Fig.3A). First, we assessed Venus fluorescence expression, indicative of the APP/BACE interaction, in N2a cells co-expressing APP:VN and BACE:VC together with soluble mCherry (Fig. 3B). Next, using flow cytometry, we analyzed the median fluorescence intensity of Venus signal in N2a cells co-expressing APP:VN and BACE:VC together with the HA-tagged Rab GTPases. The HA tag was used to identify Rab-expressing cells in which Venus fluorescence was measured. Of the Rabs analyzed, Rab35 had the strongest suppressive effect on Venus fluorescence, indicating its ability to negatively regulate APP/BACE1 interaction and amyloidogenic APP processing. To confirm these findings, we performed fluorescence microscopy on N2a cells co-transfected with APP:VN and BACE:VC together with mCh or mCh-Rab35. Cells overexpressing Rab35 exhibited significantly less Venus fluorescence compared to mCh-expressing controls (Suppl. Fig.1A-B), confirming that Rab35 is an important regulator of amyloidogenic APP processing. Moreover, we assessed the effect of Rab35 on endogenous APP/BACE interaction, using the proximity ligation assay (PLA) in primary hippocampal neurons transduced either with mCh or mCh-Rab35. Consistent with our previous experiments, we found that Rab35 gain-of-function significantly decreased the number of PLA puncta, representing colocalized APP/BACE1, in neuronal cell bodies (Fig. 3D-E). Finally, since elevated GC levels are known to trigger amyloidogenic processing of APP (Green et al., 2006b) and to reduce Rab35 expression (Vaz-Silva et al., 2018), we hypothesized that stress/GC may influence APP/BACE interaction through Rab35. To test this concept, we performed the Venus fluorescence complementation assay in N2a cells transfected with mCh or mCh-Rab35 and treated with either DMSO (CON) or dexamethasone (GC), a synthetic glucocorticoid. Here, we found that GC treatment significantly increased Venus intensity in control mCh-expressing N2a cells, but not in Rab35-expressing cells (Suppl Fig. 1E-F; Rab35 x GC interaction (F1, 291=5,989, p=0,015), overall effect of Rab35 (F1, 291= 41,35, p<0,0001), an overall effect of GC (F1, 291= 12,19, p=0,0006; Two-way

ANOVA). These findings suggest that Rab35 gain-of-function can suppress GC-induced amyloidogenic processing of APP.
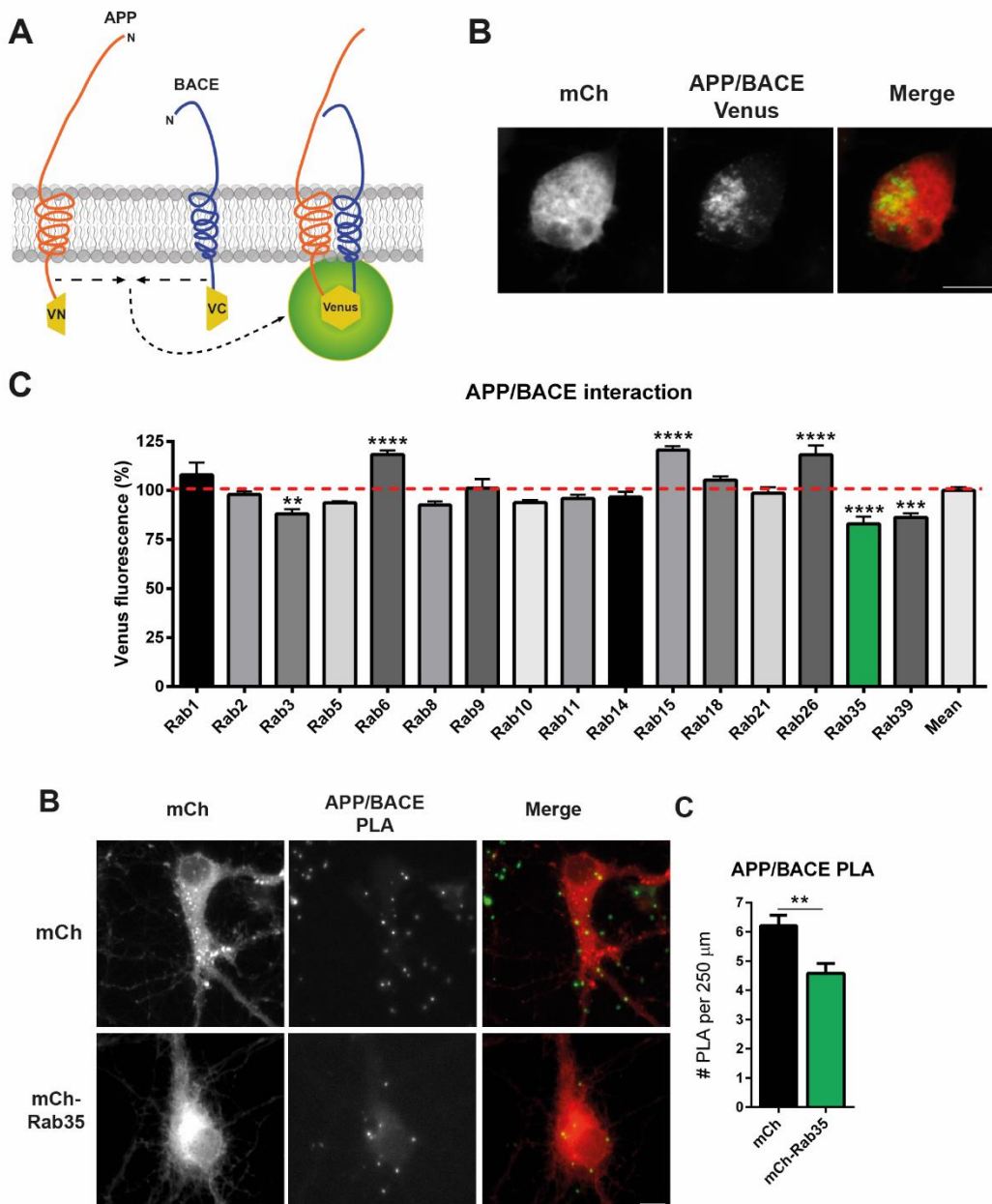
Figure 3. Rab35 is a negative regulator of APP/BACE interaction. A) Schematic of bimolecular fluorescence complementation assay with APP and BACE tagged with complementary (VN- or VC-) fragments of Venus fluorescence protein (VFP). Interaction between APP and BACE leads to reconstitution of VFP, allowing the identification of this interaction through analysis of fluorescence intensity. B) Representative immunofluorescence images of VFP signal, representing APP and BACE interaction, in N2a cells co-transfected with APP:VN and BACE:VC, as well as mCherry for cell labeling. C) Screening results for the effects of Rab GTPase gain-of-function on VFP fluorescence intensity (representing APP/BACE interaction) in N2a cells

analyzed through flow cytometry. Rabs 6, 15 and 26 were identified as positive regulators, and Rabs 3, 35 and 39 as negative regulators of this interaction (**p<0.01, ***p<0.001, ****p<0.0001 One-way ANOVA, Dunnet post-hoc analysis, n=2 experiments). D, E) Proximity ligation assay (PLA) for APP/BACE interaction in primary hippocampal neurons transduced with either mCh or mCh-Rab35. Rab35 gain-of-function decreased the number of PLA puncta, representing endogenous APP and BACE interaction, in neuronal cell bodies compared to mCh control (**p<0.01, unpaired student's t-test, n=2 experiments).
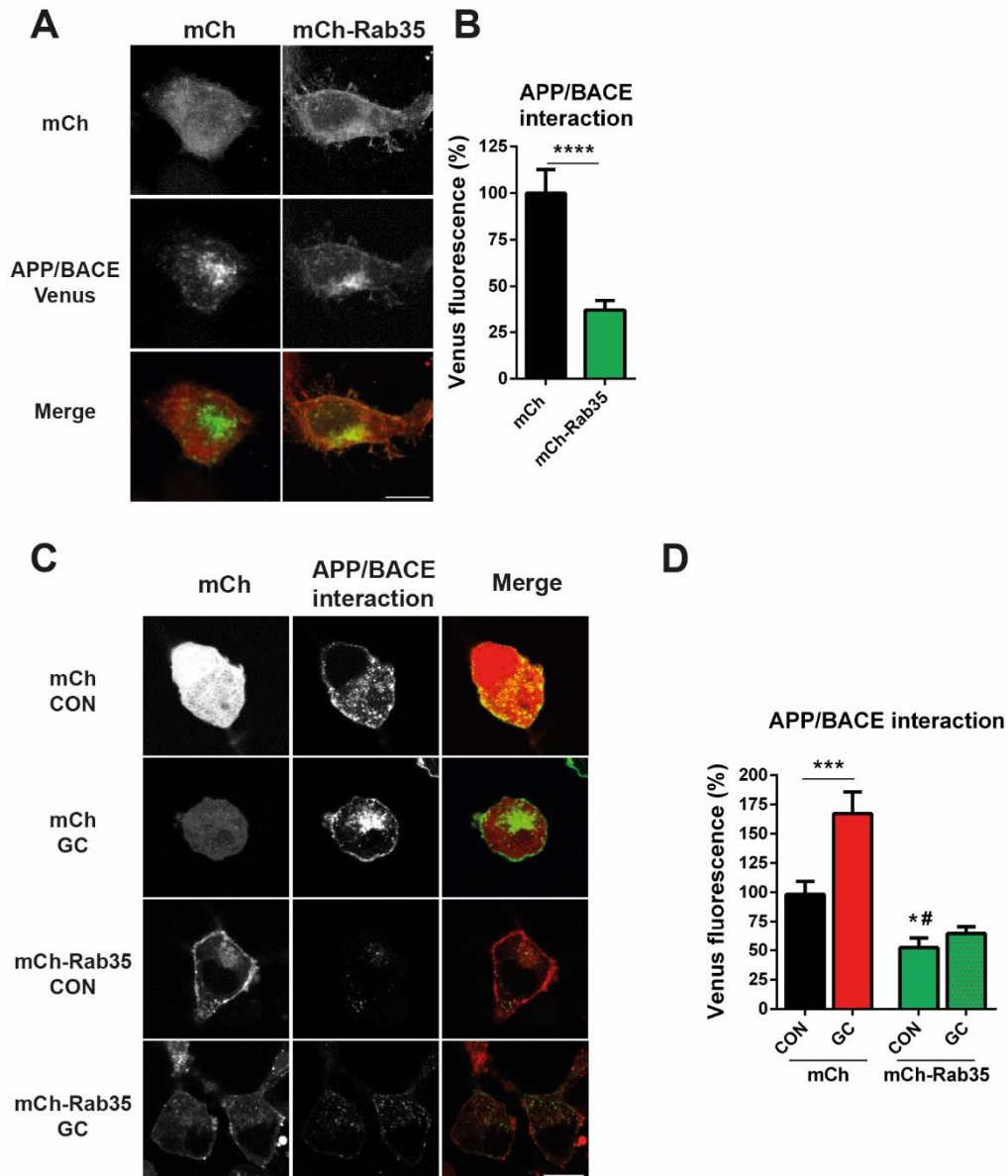
Supplementary Figure 1. GC-induced APP/BACE interaction is blocked by Rab35 overexpression. A, B) Validation of Rab35 as a regulator of APP/BACE interaction by immunofluorescence microscopy of N2a cells expressing mCh or mCh-Rab35, co-transfected with APP:VN or BACE:VC. Rab35 overexpression significantly decreased VFP fluorescence, representing APP/BACE interaction (Scale bar: 10 μm) (n=26-27 cells per condition, Mann–Whitney U-test, ****P<0.0001). C, D) Representative immunofluorescence images of APP/BACE Venus signal in N2a cells expressing mCh or mCh-Rab35 and treated with either GC or vehicle control. GC treatment led to an increase in APP/BACE interaction, quantified by Venus fluorescence intensity,

in mCh-expressing cells, but this effect was blocked and comparable to the control condition in mCh-Rab35 expressing cells, which exhibit an overall decrease in Venus fluorescence (Scale bar: 10 μm) (n=3 experiments, two-way ANOVA, Rab35 x GC interaction F1, 291=5,989 P=0,015, overall Rab35 effect F1, 291= 41,35, P<0,0001, overall GC effect F1, 291= 12,19, p=0,0006, Tukey post hoc analysis *# p<0.05 against mCh control, ***p<0.001).

Rab35 regulates APP and BACE intracellular distribution

Rab35 regulates multiple cellular trafficking events to maintain a normal distribution of plasma membrane and endosomal proteins (Chaineau et al., 2013). To determine whether Rab35 influences the trafficking of APP and/or BACE, we investigated the effects of Rab35 gain- or loss-of-function on APP and BACE colocalization with endosomal markers in hippocampal neurons. We found that Rab35 indeed regulates APP distribution within the endocytic pathway, as its overexpression decreased APP colocalization with both EEA1-positive early endosomes and Rab11-positive recycling endosomes, while its knockdown had the opposite effect (Fig. 4A, B; Suppl. Fig. 2 A, B). We previously demonstrated that Rab35 mediates protein degradation through the recruitment of the Endosomal Sorting Complex Required for Transport (ESCRT) pathway (Sheehan et al., 2016). Since APP has been shown to undergo degradation through the ESCRT pathway (Edgar et al., 2015), we analyzed the effects of Rab35 on APP degradation and colocalization with late endosomes (LEs)/lysosomes. Using a previously described cycloheximide (CHX)-chase assay to measure APP degradation, we found that Rab35 gain or loss-of-function did not significantly alter the degradation kinetics of APP or APP CTFs (Suppl. Fig. 2 E, F). Moreover, Rab35 knockdown led to an increased colocalization of APP with LAMP-1 positive LEs/lysosomes, further indicating that Rab35 activation does not stimulate APP degradation. We also assessed the effects of Rab35 overexpression/knockdown on APP colocalization with trans-Golgi Network (TGN) marker syntaxin-6, but found no significant differences between these conditions and the control (Fig. 4C, D). Our results demonstrate that Rab35 promotes APP sorting out of the endosomal network, without altering APP degradation or localization at the TGN.

We next assessed BACE1 distribution in the endosomal and TGN compartments. As with APP, we found that Rab35 overexpression decreased, and knockdown increased, BACE1 localization to Rab11-positive endosomes (Fig. 5A, B). However, in contrast to APP, Rab35 overexpression led to an increase in BACE1 colocalization with syntaxin-6, indicative of higher levels of BACE1 in the TGN (Fig. 5C, D). Since Aβ production occurs mainly in acidic recycling endosomes where APP and BACE1 converge following endocytosis, our findings suggest that Rab35 activation decreases Aβ generation by decreasing APP and BACE1 residence within this compartment.
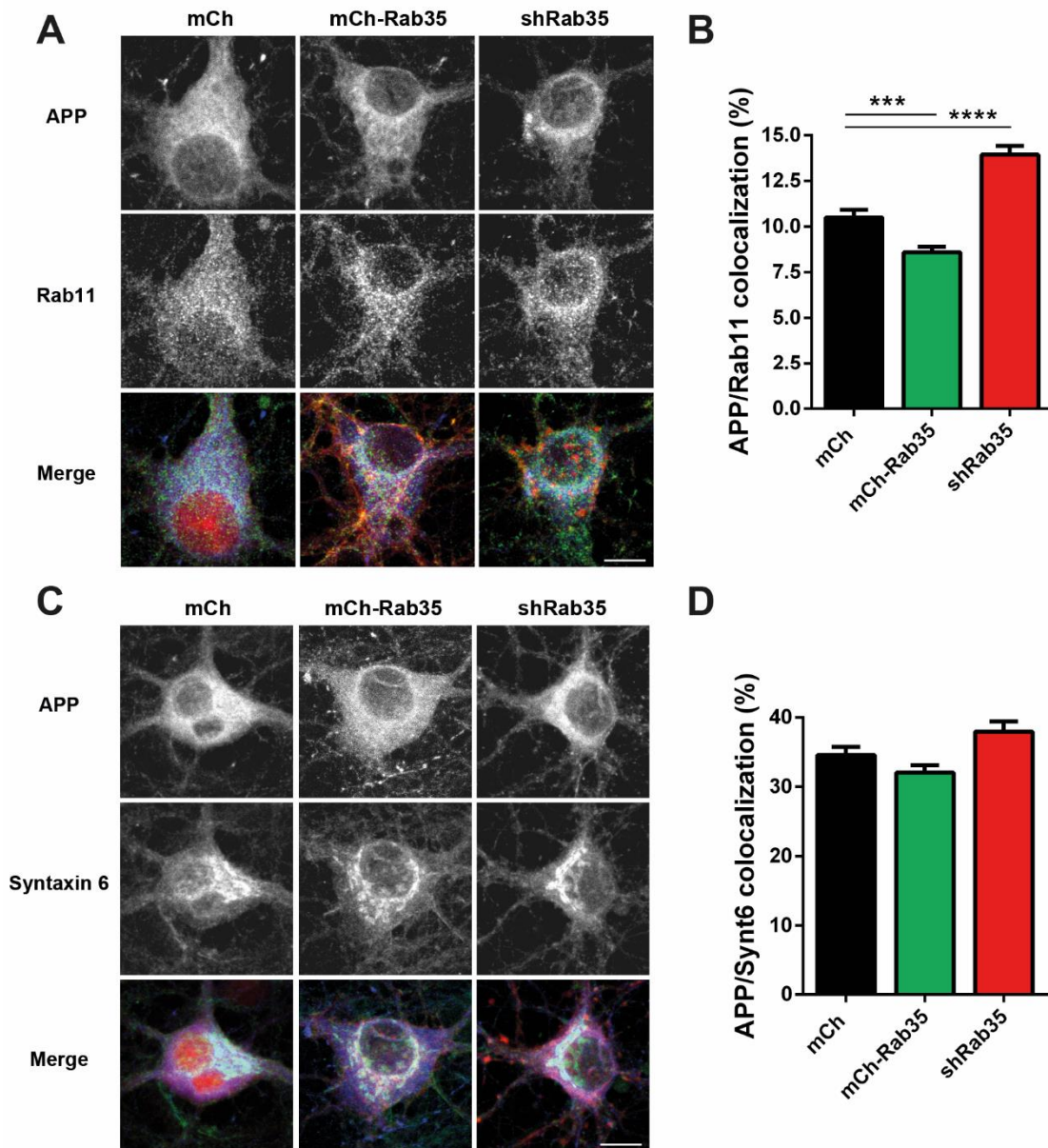
Figure 4. Rab35 decreases APP colocalization with recycling endosomes but not the TGN. A, B) Representative images and quantification of 14 DIV neurons transduced with mCh, mCh-Rab35, or shRab35, and immunostained for APP and Rab11. Rab35 knockdown increased APP colocalization with Rab11-positive recycling endosomes, while Rab35 overexpression had the opposite effect, indicating that Rab35 stimulates sorting of APP out of the endosomal network (Scale bar: 10 μm) (n = 62–78 cells per conditions, one-way ANOVA, Dunnet pos hoc analysis, ***PmCh vs. mCh-Rab35= 0.0010, ****PmCh vs. shRab35 <0.0001). C, D) Representative images and quantification of 14 DIV neurons transduced with mCh, mCh-Rab35, or shRab35, and immunostained for APP and syntaxin-6. No significant changes were observed in APP colocalization with syntaxin-6 by depletion and/or overexpression of Rab35 (Scale bar: 10 μm) (n=64-70 cells per condition).
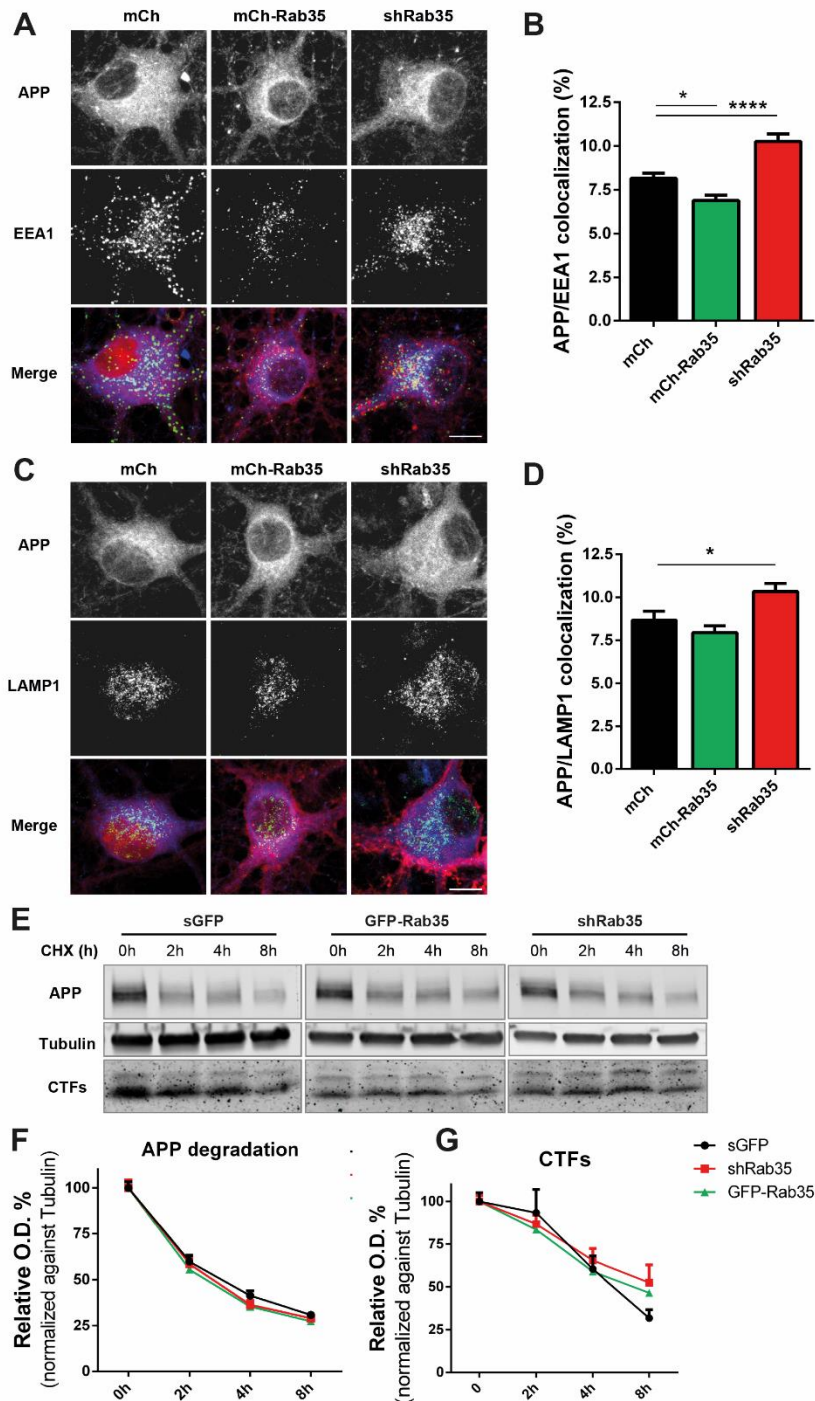
Supplementary Figure 2. APP endosomal distribution, but not degradation, is regulated by Rab35. A-B) Representative images and quantification of 14 DIV neurons transduced with mCh, mCh-Rab35, or shRab35, and immunostained for APP and early endosome marker EEA1. Rab35 knockdown increased, and overexpression decreased, APP colocalization with EEA1 (Scale bar: 10 μm) (n = 51–62 cells per conditions, one-way ANOVA, Dunnet pos hoc analysis, ***PmCh vs. mCh-Rab35= 0.0155, ****PmCh vs. shRab35 <0.0001). C, D) Representative images and quantification of 14 DIV neurons transduced with mCh, mCh-Rab35, or shRab35, and immunostained for APP and late endosome/lysosome marker LAMP1. Rab35 knockdown increased APP colocalization with LAMP1, while Rab35 overexpression did not significantly alter this change (Scale bar: 10 μm) (n = 50–54 cells per conditions, one-way ANOVA, Dunnet pos hoc analysis,

PmCh vs. mCh-Rab35= 0.4369, *PmCh vs. shRab35 =0.0213). E-G) Representative immunoblots (E) and quantification of APP and CTF degradation (F, G) from 14 DIV primary neurons transduced with EGFP, GFP-Rab35 or shRab35, treated with cycloheximide (CHX) for 0, 2, 4 or 8 hours, and probed for APP, CTFs and tubulin. Modulation of Rab35 levels did not alter APP and/or CTF degradation dynamics (n_{APP}=7-8 per condition/timepoint, n_{CTFs}=5-6 per condition/timepoint).
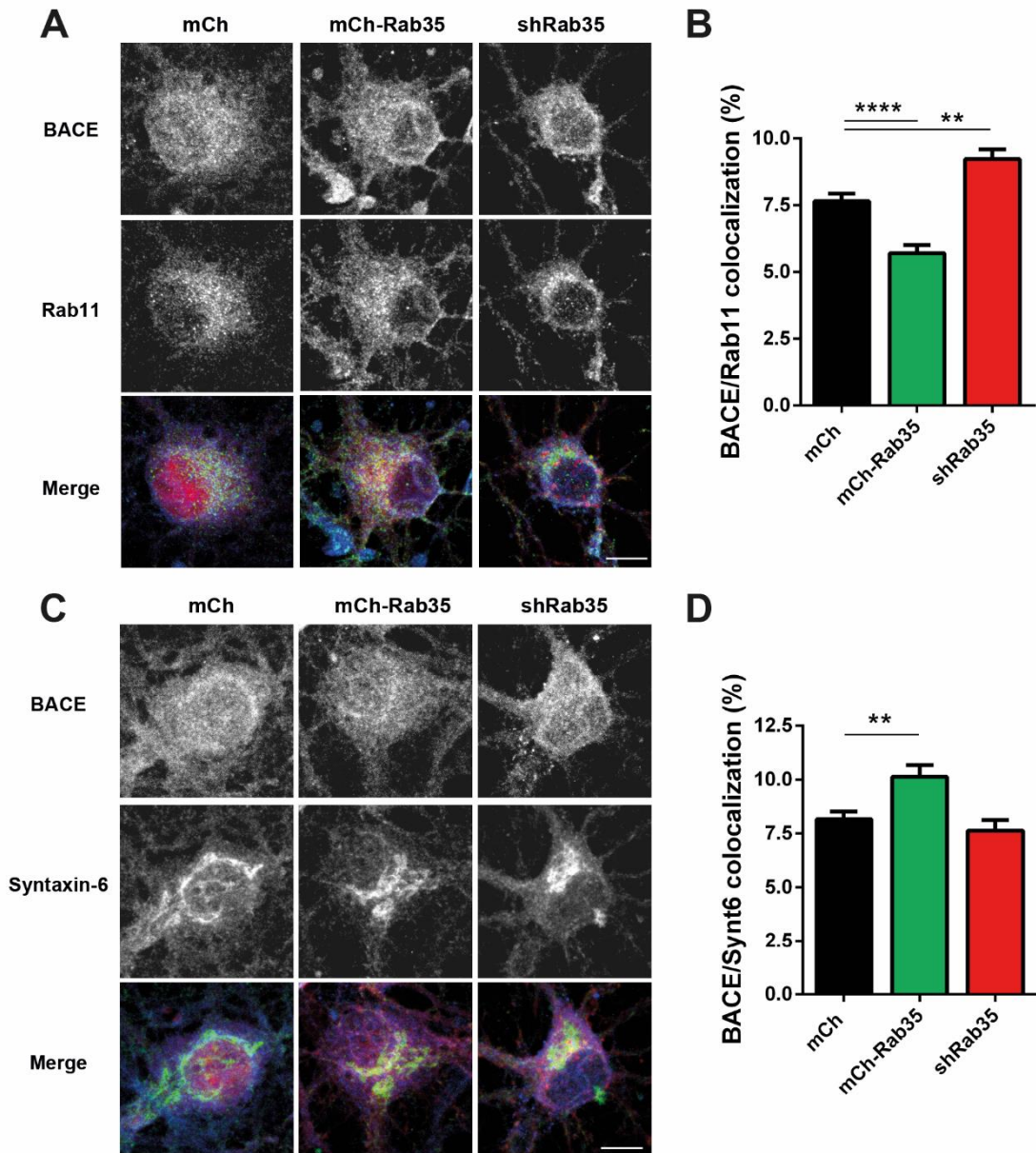
Figure 5. Rab35 decreases BACE1 colocalization with recycling endosomes, and increases colocalization with TGN. A, B) Representative images and quantification of 14 DIV neurons transduced with mCh, mCh-Rab35, or shRab35, and immunostained for BACE1 and Rab11. Rab35 overexpression decreased, and knockdown increased, BACE1 colocalization with Rab11, suggesting that Rab35 regulates BACE1 trafficking to the endosomal network (Scale bar: 10 µm) (n = 58-66 cells per condition, one-way ANOVA, Dunnet pos hoc analysis, ****PmCh vs. mCh-Rab35<0.0001, **PmCh vs. shRab35 = 0.0011). C, D) Representative images and quantification of 14 DIV neurons transduced with mCh, mCh-Rab35, or shRab35, and immunostained for BACE1 and syntaxin-6. Overexpression of Rab35 increased BACE1 colocalization with the TGN; however,

knockdown of Rab35 did not significantly change this colocalization (Scale bar: 10 µm) (n = 68-69 cells per condition, one-way ANOVA, Dunnet pos hoc analysis, **PmCh vs. mCh-Rab35 = 0.0068).

Rab35 stimulates APP recycling into the plasma membrane

Rab35 has been shown to regulate a fast endocytic recycling pathway from early endosomes to the PM that operates in parallel to Rab11 recycling endosomes (Kouranti et al., 2006). Moreover, Rab35 activation stimulates the retrograde trafficking of Mannose-6-Phosphate Receptor to the TGN, suggesting a role in sorting proteins into the retrograde pathway (Cauvin et al., 2016). To determine whether Rab35 mediates APP and/or BACE sorting into either of these pathways, we used antibody feeding assays to monitor APP and BACE internalization and trafficking in N2a cells. We first assessed the retrograde trafficking of APP. Here, cell-surface GFP-APP was labeled with 22C11 antibody, and colocalization of the internalized, antibody-labeled protein with syntaxin-6 was measured at different timepoints (0, 10, 30, 60 minutes post-labeling) in cells expressing control or HA-Rab35 constructs. We found that Rab35 overexpression did not alter the colocalization of internalized APP with the TGN (Fig. 6A, B), suggesting that APP trafficking through the retrograde pathway was not affected by Rab35. However, we did observe significantly increased cell-surface APP levels in N2a cells overexpressing Rab35 versus the control construct (Fig. 6A, C). Since surface APP is mainly cleaved by α-secretase, which prevents Aβ production, this finding is consistent with Rab35's role as a negative regulator of amyloidogenic APP processing. Moreover, these data suggest that Rab35 may promote the fast endocytic recycling of APP to the PM. To test this concept, we measured the recycling of internalized APP back to the PM at several time points, again using 22C11 antibody to label cell-surface GFP-APP, followed by incubation with unlabeled secondary antibody to block the signal from residual non-internalized APP. Recycled APP was then detected at the PM with fluorophore-conjugated secondary antibodies. Here, our results showed that Rab35 overexpression increased both APP internalization and recycling to the PM after a 60 min incubation period (Fig. 6D-F). These data indicate that Rab35 overexpression stimulates APP endocytosis recycling, and time at the PM, thereby decreasing its accumulation in endosomes.
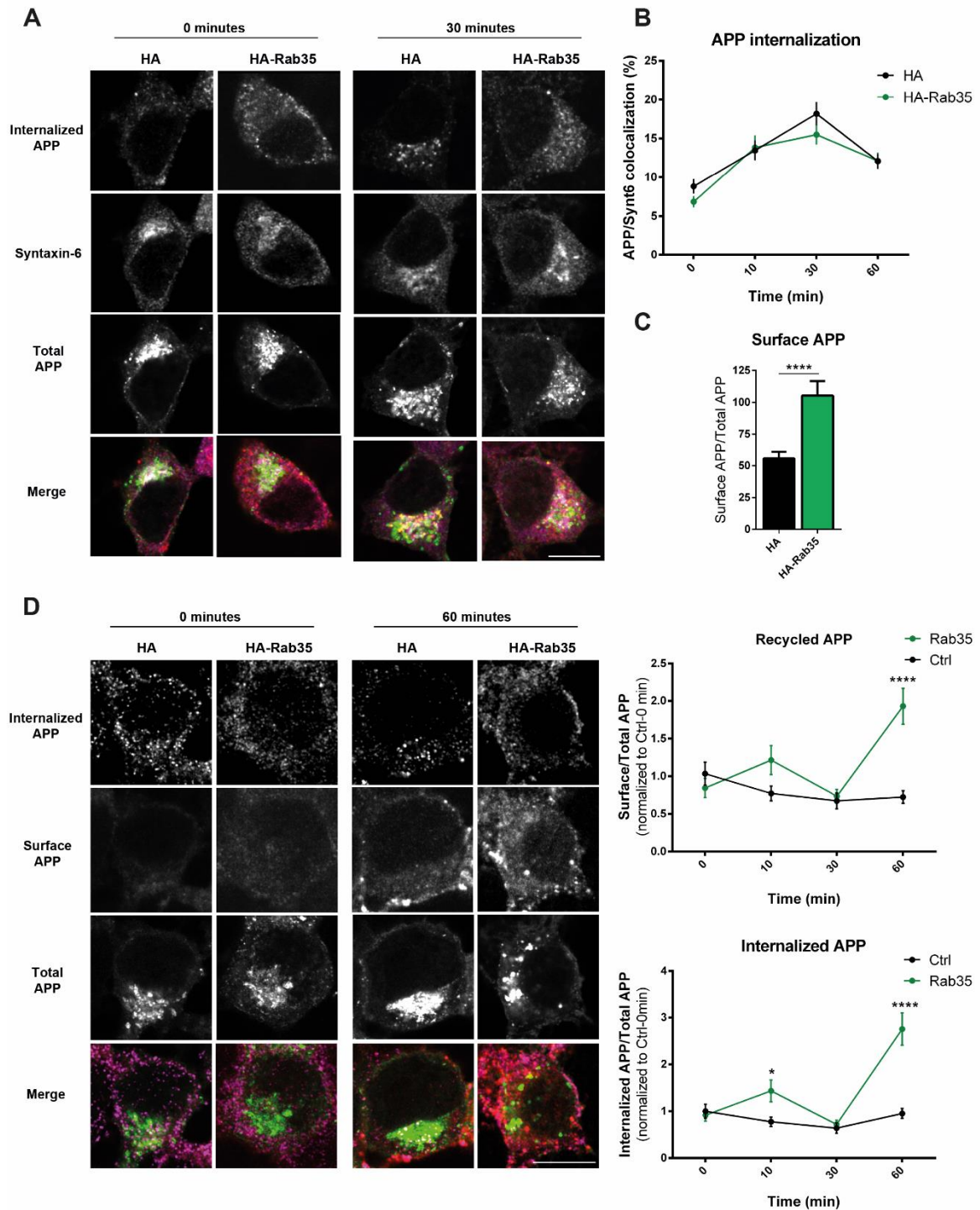
Figure 6. Rab35 stimulates APP recycling to the plasma membrane A-B) Representative images and quantification of N2a cells cotransfected with GFP-APP and HA vector control or HA-Rab35, in which cell-surface APP was labeled with 22C11 antibody, and cells were incubated for 0, 10, 30 or 60 minutes of 'chase' time prior to their fixation and immunostaining with syntaxin-6 to label the TGN. Overexpression of Rab35 did not significantly alter the colocalization of APP with syntaxin-6 at any timepoint, indicating no change in its trafficking to the TGN (n=53-69 cells per condition/timepoint). C) Rab35 overexpression increased the level of cell-surface APP assessed at timepoint 0, indicating that Rab35 boosts APP levels at the PM (n = 62–66 cells per condition, Mann–Whitney U-test, ****P < 0.0001). D-F) Representative images and quantification of N2a cells cotransfected with GFP-APP and either HA or HA-Rab35, in which APP recycling was assessed after labelling

cell-surface APP with 22C11 and analyzing its internalization or reappearance at the PM after 0, 10, 30 and 60 minutes of chase. Rab35 overexpression increased APP internalization and recycling at the 60 minute timepoint, indicating its ability to stimulate fast endocytic recycling of APP (APP recycling, n=39-58 cells per condition/timepoint, 2-way ANOVA, Time × Rab35 interaction $F_{3,377}$ = 8.866 P < 0.0001, overall Rab35 effect $F_{1,377}$ = 14.11 P=0.0002, Sidak post hoc analysis ****P<0.0001) (APP internalization, n=39-58 cells per condition/timepoint, 2-way ANOVA, Time × Rab35 interaction $F_{3,375}$ = 12.34 P < 0.0001, overall Rab35 effect $F_{1,375}$ = 26.57 P < 0.0001, Sidak post hoc analysis *P = 0.0163, ****P<0.0001).

Rab35 promotes BACE1 trafficking through the retrograde pathway

We similarly assessed whether Rab35 stimulates BACE1 trafficking into the retrograde and/or fast endocytic recycling pathways, using an N-terminal FLAG-tagged BACE1 construct together with FLAG antibody. Interestingly, we found that Rab35 overexpression increased the colocalization of internalized BACE1 with syntaxin-6 at the 30- and 60-minute time points (Fig. 7A, B), and increased BACE1 internalization at the 0 min timepoint (Fig. 7D), but decreased BACE1 recycling to the PM after 60 minutes (Fig. 7D, E). Moreover, cell-surface BACE1 levels are decreased in Rab35-overexpressing cells, in contrast to surface APP levels (Fig. 7A, C). Together, these findings demonstrate that Rab35 stimulates BACE1 trafficking through the retrograde pathway, increasing its retrieval from the PM and endosomal compartment to the TGN, and decreasing its localization to recycling endosomes, where it would converge with APP and stimulate Ab production.
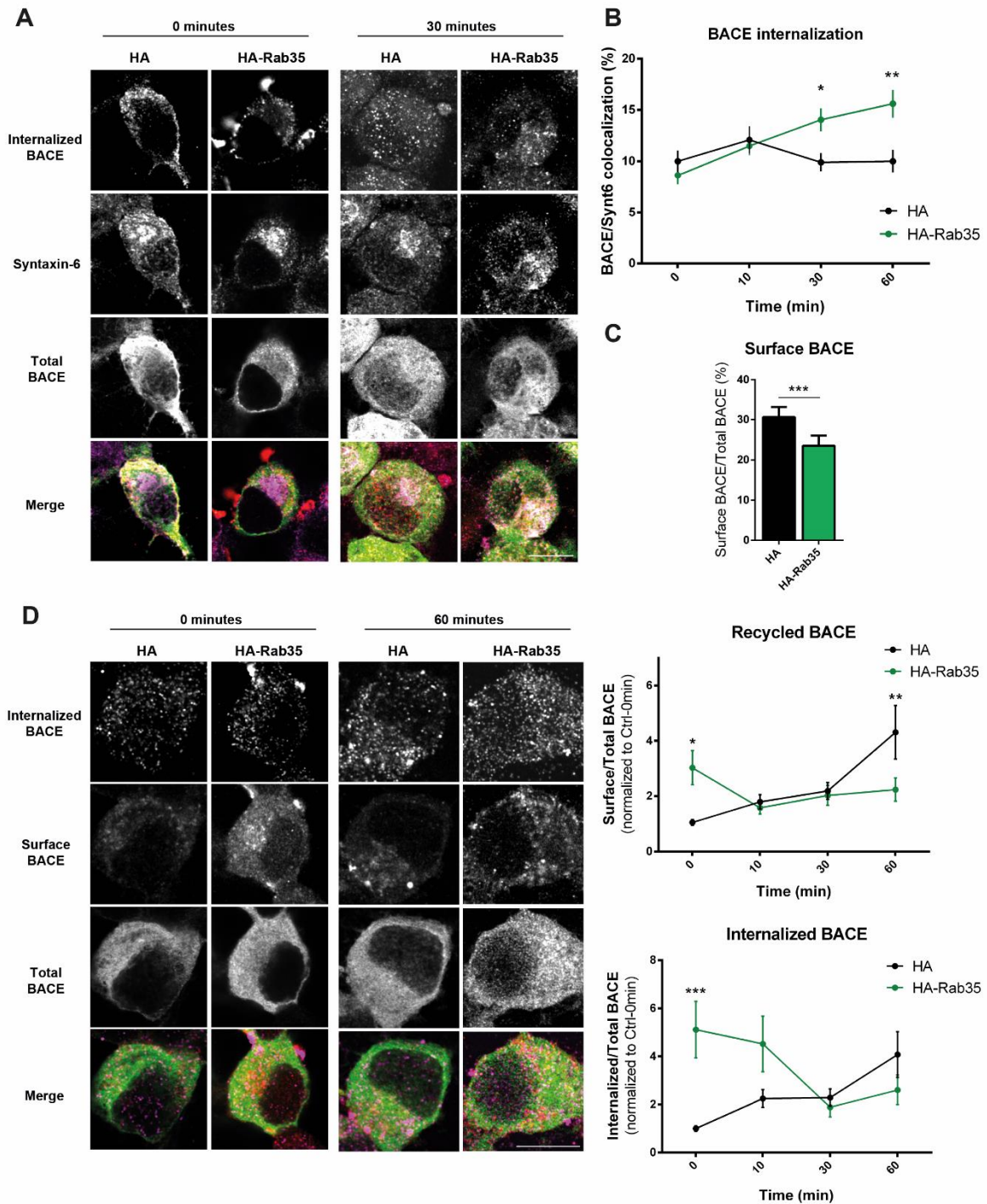
Figure 7. Rab35 stimulates the retrograde trafficking of BACE1. A-C) Representative images and quantification of N2a cells cotransfected with FLAG-BACE1 and either HA or HA-Rab35, in which cell-surface BACE1 was labeled with anti-FLAG antibody, and cells were incubated for 0, 10, 30 and 60 minutes of chase time prior to fixation and immunostaining with syntaxin-6. Overexpression of Rab35 increased trafficking of internalized BACE1 to the TGN at both the 30- and 60-minute timepoints (n=61-72 cells per condition/timepoint, 2-way ANOVA, Time × Rab35 interaction F3,521 = 4.936 P = 0.0022, overall Rab35 effect F1,572 = 6.211 P = 0.0130, Sidak post hoc analysis *P = 0.0323, **P=0.0014). C) Rab35 overexpression increased cell-surface BACE1 levels at timepoint 0 (n=63-70 cells per condition, Mann–Whitney U-test, ***P= 0.0007). D-F) Representative images and quantification of N2a cells cotransfected with FLAG-BACE1 and either HA or HA-

Rab35, in which BACE recycling was assessed after labelling cell-surface BACE with anti-FLAG antibody and analyzed its reappearance at the PM after 0, 10, 30 and 60 minutes incubation. Rab35 overexpression decreased BACE1 recycling to the PM at the 60 minute timepoint (n=41-49 cells per condition/timepoint, 2-way ANOVA, Time × Rab35 interaction $F_{3,337} = 5.951$ $P = 0.0006$, Sidak post hoc analysis *P = 0.0164, **P=0.0088), and increased BACE1 internalization at the 0 minute timepoint (n=40-49 cells per condition/timepoint, 2-way ANOVA, Time × Rab35 interaction $F_{3,331} = 6.049$ $P = 0.0005$, overall Rab35 effect $F_{1,331} = 4.852$ $P = 0.0283$, Sidak post hoc analysis ***P=0.0004).

Discussion

Numerous studies suggest that Aβ production is the triggering event for development of AD, underscoring the need to elucidate the cellular and molecular mechanisms of amyloidogenic APP processing in order to identify therapeutic targets. The current study reveals novel roles for Rab35 in APP and BACE1 trafficking, and implicates this Rab as a potent negative regulator of Aβ generation and thus the earliest event in AD pathogenesis. Moreover, studies indicate that Aβ is not the only toxic component of the amyloidogenic pathway, as β-CTFs are themselves neurotoxic and can promote Tau hyperphosphorylation and accumulation independently of Aβ production (Moore et al., 2015). Thus, instead of focusing exclusively on Aβ production, our study aims to uncover the mechanisms underlying APP/BACE1 interaction, the rate-limiting step for amyloidogenic cleavage of APP. We have identified Rab35 as a negative regulator of APP/BACE interaction both in cell lines and primary neuronal cultures, and shown that its gain-of-function leads to decreased levels of APP CTFs as well as Aβ40/42 peptides.

Interestingly, we find that Rab35 levels are decreased in multiple conditions linked to AD, including ageing, the strongest AD risk factor identified to date (Querfurth and LaFerla, 2010). Indeed, several studies report increased levels of Aβ and APP amyloidogenic processing in aged animals (Cisternas et al., 2018; Kimura et al., 2009, 2016). Although the underlying mechanism is still unknown, our results suggest a possible role for Rab35 in age-induced APP misprocessing. Moreover, Rab35 levels are decreased in animals exposed to chronic stress, another AD risk factor known to trigger Aβ production, leading to synaptic and dendritic atrophy and downstream cognitive and mood deficits (Catania et al., 2009; Lopes et al., 2016; Sotiropoulos et al., 2011). Here, we show that GCs influence APP/BACE interaction and that this effect is blocked by Rab35 overexpression, demonstrating an influence of chronic stress/GCs as well as Rab35 on the intracellular trafficking dynamics of these proteins. Our findings further suggest that upregulation of Rab35 levels or activity is a possible therapeutic intervention for stress-induced AD pathology. In addition, a recent study has demonstrated that aged mice expressing human ApoE4 exhibit decreased levels of Rab35 in their

brains compared to control animals (Alldred et al., 2018). The ApoE4 allele is the strongest genetic risk factor for LOAD, and its carriers exhibit significantly increased Aβ accumulation compared to carriers of other ApoE alleles (Huang et al., 2017). Altogether, these findings indicate that downregulation of Rab35 levels is a shared characteristic of several AD risk factors, highlighting the importance of investigating its relevance for disease etiology.

The earliest cellular features of AD are abnormalities of the endocytic and lysosomal machinery (Nixon, 2005), suggesting that dysfunction of endosomal trafficking is a triggering event for Aβ overproduction/accumulation and AD pathogenesis. Indeed, the endosomal compartment is the major site of Aβ production, and conditions associated with decreased residence of APP in this compartment typically decrease Aβ generation (Small et al., 2017). We recently demonstrated that Rab35 mediates the degradation of synaptic vesicle proteins and microtubule-associated protein Tau through the ESCRT pathway (Sheehan et al., 2016; Vaz-Silva et al., 2018). Thus, it is conceivable that Rab35 promotes the fast removal of APP from endosomes by stimulating its degradation. However, while APP is known to be degraded through the ESCRT pathway, we did not see any effect of Rab35 gain- or loss-of-function on APP or CTF degradation rates, suggesting that Rab35 does not directly mediate the lysosomal degradation of APP. Interestingly, Aβ and β-CTFs are known to impair endosomal protein sorting and induce Tau accumulation, and we observe that infusion of Aβ into the rat hippocampus dramatically decreases Rab35 levels (Moore et al., 2015; Willén et al., 2017). These findings suggest that Aβ could indirectly promote Tau accumulation through inhibition of the Rab35/ESCRT pathway. Future studies are needed to test this concept and clarify the mechanism of Aβ-induced downregulation of Rab35.

Rab35 is also known to regulate a fast recycling pathway from early endosomes to the plasma membrane (Kouranti et al., 2006), and our study demonstrates that Rab35 gain-of-function increases the rate of APP endocytosis and recycling back to the plasma membrane. This function may be responsible for the faster removal of APP from recycling endosomes, thus preventing BACE-mediated cleavage in this compartment. Indeed, we find that Rab35 overexpression also increases levels of APP at the plasma membrane, where APP can be cleaved by α-secretase, preventing its amyloidogenic processing and Aβ production. In addition to its regulation of fast endocytic recycling, Rab35 also regulates protein trafficking through the retrograde pathway, which mediates protein retrieval from the endocytic pathway to the TGN (Cauvin et al., 2016). Interestingly, genes identified as risk factors for LOAD, namely VPS35 and VPS26, encode proteins that regulate the retrograde pathway, and APP trafficking through this pathway is hypothesized to circumvent its processing by BACE1 in endosomes.

Surprisingly, while we did not see any effect of Rab35 on the retrograde trafficking of APP, we found that Rab35 gain-of-function stimulates the retrograde trafficking of BACE1, with a higher percentage of endocytosed BACE1 reaching the TGN after 30 and 60 minutes compared to the control condition. This increase in BACE1 retrograde trafficking is hypothesized to reduce its residence time within the endosomal compartment, thus preventing its interaction with APP and subsequent amyloidogenic processing.

Previous studies report that BACE1 is endocytosed from the plasma membrane into the endosomal network through an Arf6-dependent pathway (Sannerud et al., 2011). Interestingly, Rab35 and Arf6 are known to negatively regulate one another's activation in a variety of cellular processes (i.e. cell migration, vesicle secretion, cytokinesis), suggesting that Rab35 overexpression may reduce BACE endocytosis via Arf6 inhibition, thereby preventing BACE1 interaction with APP in endosomes. Although we have not detected concordant changes in BACE1 internalization dynamics, further studies should be performed to clarify the Arf6/Rab35 signaling relationship in the context of APP and BACE trafficking.

In summary, we identify Rab35 as a crucial regulator of APP and BACE1 trafficking, with important implications for Aβ production and downstream amyloid pathology. Based on emerging evidence implicating endosomal dysfunction in AD etiology, and the role of Rab35-mediated endosomal sorting in both APP processing and Tau degradation, it is clear that additional work is needed to investigate the therapeutic relevance of Rab35 and its trafficking pathways for AD pathology.

Materials and Methods

Primary neurons and cell lines

Primary neuronal cultures were prepared from E18 Sprague Dawley rat embryos and maintained for 14 DIV before use, as described previously (Sheehan et al, 2016). Neuro2a (N2a) neuroblastoma cells (ATCC CCL-131) and HEK293T cells (Sigma) were grown in DMEM-GlutaMAX (Invitrogen) with 10% FBS (Atlanta Biological) and Anti-Anti (ThermoFisher) and kept at 37°C in 5% CO_2. During dexamethasone treatment in N2a cells, FBS content in the growth media was reduced to 3%.

Human iPSC-derived neuronal primary cultures were generated using manual rosette selection and maintained on Matrigel (Corning) (Topol et al., 2015). Concentrated lentiviruses express control-sgRNA or hu-APP-sgRNA were made using Lenti-X concentrator (Clontech). The iPSC-derived neuronal

cultures were transduced with either control-sgRNA or hu-APP-sgRNA after Accutase splitting and were submitted to puromycin selection the subsequent day. Polyclonal lines were expanded and treated with puromycin for 5 more days before banking. Neuronal differentiations were carried out by plating 165,000 cells/12 well-well in N2/B27 media (DMEM/F12 base) supplemented with BDNF (20 ng/ml) and laminin (1 ug/ml).

Pharmacological treatments

Pharmacological agents were used in the following concentrations and time courses: cycloheximide (Calbiochem, 0.2 µg/µl, 2, 4 or 8h), dexamethasone (Invivogen, 10 µM, 48 h)

Lentivirus production, transduction, and DNA transfection

DNA constructs were described previously (Sheehan et al, 2016; Vaz-Silva J et al, 2018). APP:VN and BACE:VC constructs were a gift from Dr. Subhojit Roy. Briefly, Rab GTPases were subcloned into pKH3 vector at the EcoRI site. Lentivirus was produced as previously described (Sheehan et al, 2016). Neurons were transduced with 50–150 µl of lentiviral supernatant per well (12-well plates) or 10–40 µl per coverslip (24-well plates) either at 3 DIV for shRNA transduction or 10 DIV in gain-of-function experiments. Respective controls were transduced on the same day for all experimental conditions. Primary neuronal cultures were collected for immunoblotting or immunocytochemistry at 14 DIV.

N2a cells were transfected using Lipofectamine 3000 after 24h of plating, according to the manufacturer's instructions. For co-transfection in APP/BACE Venus assay, a double transfection was performed 48h after the first, to allow expression of the Rab GTPases constructs. These cells were then collected 18h after the second transfection.

Flow cytometry

N2a cells were detached using TrypLE Express (Life Technologies), for 5 min at 37°C, resuspended in culture medium, and centrifuged (3,000 rpm, 5 minutes, 4˚C). The pellet was washed once with 0.2 mM EDTA and 0.02% BSA in 1x PBS (Flow buffer) and centrifuged again. The cell pellet was resuspended in 100 µl of flow buffer and then fixed with 4% paraformaldehyde solution for 15 min. Cells were washed with 1x PBS and resuspended in 1.5 % FBS and 0.05% saponin in 1x PBS (permeabilization solution) and placed on a shaker for 30 min, before centrifugation. Supernatant was discarded, and the cell pellet resuspended in permeabilization solution with anti-HA-tag Alexa(R)-647 (Cell Signaling technologies) for immunostaining, placed on a shaker for 90 minutes at 4°C. After

washing twice with flow buffer, cells were resuspended in ice-cold Flow Buffer (0,2% FBS, 0.5mM EDTA in PBS) and strained through a 35μm nylon mesh to promote single cell suspensions and kept in ice. Cells and fluorescence were analyzed in a BD Fortessa Cell Analyser and BD FACSDiva software (BD Biosciences). Unstained cells were used as a control for background fluorescence. Far-red (APC) and green (FITC) fluorescence were analyzed, as they marked the HA-tag and Venus fluorescence (APP/BACE interaction), respectively. 50,000 events were recorded for each sample, with two samples for each condition. Flow Cytometry data was analyzed using FCS Express 6 (DeNovo Software). Median fluorescence intensity of the Venus (APP/BACE) signal was calculated for the HA+ cells only, thus in double positive cells. The Venus median fluorescence intensity of each sample was compared to the average Venus median fluorescence of all samples, thus comparing each condition to the average of the whole population. Results were presented as percentage of the average.

Proximity ligation assay

Proximity ligation assay (PLA) was performed in N2a cells according to manufacturer's instructions (Duolink, Sigma). Until the PLA probe incubation step, all manipulations were performed as detailed above for the immunocytochemistry procedure. PLA probes were diluted in blocking solution. The primary antibody pairs used were C1/6.1 (anti-APP, Mouse; Biolegend) and anti-BACE (Rabbit, Cell Signaling Technology). All protocol steps were performed at 37°C in a humidity chamber, except for the washing steps. Coverslips were then mounted using Duolink In situ Mounting Media with DAPI.

Aβ Measurements

Human iPSC-derived neuronal cultures were kept for 3 days post-transduction, after which 50% of the media was changed. Then, conditioned media was collected after 72h, centrifuged at 2,000 rcf for 5 min and stored at –80°C. Aβ42 and Aβ40 levels were measured using V-PLEX Aβ Peptide Panel 1 (4G8) Kit (MesoScaleDiscovery, MSD) following the manufacturer's protocol and their concentration was presented as percentage of control levels.

Animals

Male Wistar rats (Charles River Laboratories, France) were maintained under standard laboratory environmental conditions (lights on from 8a.m to 8p.m, room temperature 22°C, relative humidity 55%, ad libitum access to food and water). 4- and 22/24-month old male Wistar Rats (Charles River Laboratories, Spain), young and age, respectively, were paired under standard laboratory conditions

(8:00 A.M. to 8:00 P.M.; 22 °C) with ad libitum access to food and drink. All experimental procedures were approved by the local ethical committee of University of Minho and national authority for animal experimentation; all experiments were in accordance with the guidelines for the care and handling of laboratory animals, as described in the Directive 2010/63/EU.

Drugs and Treatment

For monitoring the effect of Aβ-driven hippocampal pathology, we used 5 months old animals. Aβ1-40 (Eurogentec) was diluted to 2.5 µg/ul with sterile saline and incubated at 37°C for 1 week, as previously described for the Aβ1-40 aggregates (Prediger et al, 2007). For injection of Aβ1-40, animals were intraperitoneally anesthetized with 75 mg/kg ketamine (Imalgene, Merial) and 1mg/kg medatomidine (Dorbene, Cymedica). Aβ1-40 [2.5µg/µl, 4µl (600ml/min)] was stereotaxically injected bilaterally into the hippocampus (coordinates from Bregma: -3.0mm anteroposterior, +2.2mm mediolateral, -2.8mm dorsoventral according to Paxinos and Watson. The needle was kept in place for 5 minutes before retraction. The animals were removed from the stereotaxic frame, sutured and let to recover one day before starting the drug treatment. Sterile saline was bilaterally injected into the hippocampus of control animals.

Chronic unpredictable stress paradigm lasted for 4 months and consisted of random application of one of the following stressors (one stressor per day): (i) rocking platform, (ii) air dryer, (iii) cold water and (iv) overcrowding.

Western blotting

For western blotting experiments, human iPSC-derived neuronal cultures were collected in Lysis Buffer (50 mm Tris-Base, 150 mm NaCl, 1% Triton X-100, 0.5% deoxycholic acid) with protease inhibitor (Roche) and phosphatase inhibitor cocktails II and III (Sigma) and clarified by centrifugation at high speed (10 min, 20,000 g). Rat dorsal hippocampi were homogenized in lysis buffer (50 mm Tris-Base, 150 mm NaCl, 1% Triton X-100, 0.5% deoxycholic acid) or RIPA buffer with protease inhibitor (Roche) and phosphatase inhibitor cocktails II and III (Sigma) and clarified by centrifugation at high speed (10 min, 20,000 rcf). Protein concentration was determined using the BCA protein assay kit (ThermoFisher Scientific) and the same amount of protein was used for each condition, which was diluted and denatured in 2× SDS sample buffer (Bio-Rad). Samples were subject to SDS–PAGE, transferred to nitrocellulose membranes using wet (Mini Trans-Blot Cell, Bio-Rad), and probed with primary antibody in 5% BSA/PBS + 0.1% Tween-20, followed by DyLight 680 or 800 anti-rabbit, anti-

mouse (Thermo Scientific) or by HRP-conjugated secondaries (Bio-Rad). Membranes were imaged using an Odyssey Infrared Imager (model 9120, LI-COR Biosciences), and protein intensity was measured using the Image Studio Lite software (LI-COR Biosciences).

Immunofluorescence microscopy

Immunofluorescence staining in neurons and N2a cells was performed as previously described (Sheehan et al, 2016). Briefly, cells were fixed with Lorene's Fix (60 mM PIPES, 25 mM HEPES, 10 mM EGTA, 2 mM MgCl2, 0.12 M sucrose, 4% formaldehyde) for 15 min, and primary and secondary antibody incubations were performed in blocking buffer (2% glycine, 2% BSA, 0.2% gelatin, 50 mM NH4Cl in 1× PBS) overnight at 4°C or for 1 h at room temperature, respectively. Images were acquired using a Zeiss LSM 800 confocal microscope equipped with Airyscan module, using either a 63× objective (Plan-Apochromat, NA 1.4), for neurons or N2a cell imaging, or a 40× objective (Neofluar, NA 1.4) for imaging of rat brain sections.

Antibody feeding assay

N2a cells were co-transfected with APP-GFP or FLAG-BACE1 and HA or HA-Rab35 constructs. Approximately 48 hours after plating, cells were starved in serum-free DMEM for 30 minutes. Cells were then incubated for 30 min at 4°C with 22C11 antibody (anti-N-terminus of APP, Millipore) or anti-FLAG (Millipore). Antibodies were diluted in complete medium + 1M HEPES. Following antibody incubation, cells were washed with complete medium + HEPES and fixed with Lorene's fixative for 15 min or incubated at 37°C for 10, 30, or 60 min and then fixed, followed by washing with 1X PBS.

Recycling assay

N2a cells were co-transfected with APP-GFP or FLAG-BACE1 and HA or HA-Rab35 constructs. Approximately 48 hours after plating, cells were starved in serum-free DMEM for 30 minutes. Cells were then incubated for 30 min at 4°C with 22C11 antibody (anti-N-terminus of APP, Millipore) or anti-FLAG (Millipore). Following antibody pulse, coverslips were washed with complete medium + HEPES and incubated with goat-anti-mouse unconjugated antibody for 30 min at 4°C to allow APP or BACE internalization. Antibodies were diluted in complete medium + 1M HEPES. Coverslips were washed with complete medium + HEPES and fixed with Lorene's fixative for 15 min or incubated at 37°C for 10, 30, or 60 min and then fixed, followed by washing with 1X PBS.

Image analysis

Images were analyzed and processed using the Fiji software. PLA puncta were counted using the Multi-point tool, and cell area was measured with Polygon selection tool. Fluorescence intensity was measured after performing a Z-projection using the SUM function.

Colocalization analysis between APP or BACE1 and intracellular compartments was determined using the JACoP plugin, in order to obtain the Mander's coefficient corresponding to the fraction of APP or BACE1 colocalized with each compartment.

For surface protein analysis, a Z-projection using the SUM function was performed for the APP-GFP or BACE1 channels, as well as for N-terminal of APP or BACE1 at the 0min time point. For each image, all cells expressing APP-GFP or BACE1 were outlined. Per cell, the fluorescence intensity N-terminal of APP or FLAG-BACE1 at timepoint 0 min was normalized to fluorescence intensity of total APP-GFP or BACE1.

Antibodies

Antibody	Source	Species	Catalog no.
22C11 (N-Term. APP)	Merck Millipore	Mouse	MAB348
Actin	Abcam	Mouse	ab8226
C1/6.1 (C-Term. APP)	Biolegend	Mouse	802802
EEA1	Cell Signaling Technology	Rabbit	3288S
FLAG	Sigma	Mouse	F1804
HA	Santa Cruz Biotechnology	Rabbit	y-11 sc805
HA	Santa Cruz Biotechnology	Mouse	f-7 sc7392
LAMP1	Abcam	Rabbit	ab24170
mCherry	Biovision	Rabbit	5993
Rab5	Synaptic Systems	Mouse	108011
Rab7	Abcam	Mouse	ab50533
Rab8	Proteintech	Rabbit	55296-1-AP
Rab10	Santa Cruz Biotechnology	Goat	sc6564
Rab11	Cell Signaling Technology	Rabbit	5589
Rab14	Santa Cruz Biotechnology	Rabbit	sc-98610
Rab35	Proteintech	Rabbit	11329-2-AP
Syntaxin-6	abcam	Rabbit	ab140607
Tubulin	Abcam	Rabbit	ab4074
Tubulin	Sigma	Mouse	t9026

Table 1. List of primary antibodies used in this study.

Statistical analysis

Graphing and statistics analysis were performed using Prism (GraphPad). Shapiro–Wilk normality test was used to determine whether data sets were modeled by a normal distribution. Unpaired, two-tailed t-tests, one-way ANOVA, or two-way ANOVAs were used with values of $P < 0.05$ being considered as significantly different.

References

Alldred, M.J., Goulbourne, C.N., Peng, K.Y., Morales-corraliza, J., Saito, M., Saito, M., and Ginsberg, S.D. (2018). Apolipoprotein E4 genotype compromises brain exosome production. Brain 1–13.

Catania, C., Sotiropoulos, I., Silva, R., Onofri, C., Breen, K.C., Sousa, N., and Almeida, O.F.X. (2009). The amyloidogenic potential and behavioral correlates of stress. Mol. Psychiatry 14, 95–105.

Cauvin, C., Rosendale, M., Gupta-Rossi, N., Rocancourt, M., Larraufie, P., Salomon, R., Perrais, D., and Echard, A. (2016). Rab35 GTPase Triggers Switch-like Recruitment of the Lowe Syndrome Lipid Phosphatase OCRL on Newborn Endosomes. Curr. Biol. 26, 120–128.

Chaineau, M., Ioannou, M.S., and McPherson, P.S. (2013). Rab35: GEFs, GAPs and effectors. Traffic 14, 1109–1117.

Cirrito, J.R., Yamada, K. a, Finn, M.B., Sloviter, R.S., Bales, K.R., May, P.C., Schoepp, D.D., Paul, S.M., Mennerick, S., and Holtzman, D.M. (2005). Synaptic activity regulates interstitial fluid amyloid-beta levels in vivo. Neuron 48, 913–922.

Cisternas, P., Zolezzi, J.M., Lindsay, C., Rivera, D.S., and Martinez, A. (2018). New Insights into the Spontaneous Human Alzheimer's Disease-Like Model Octodon degus : Unraveling Amyloid-b Peptide Aggregation and Age-Related Amyloid Pathology. J. Alzheimer's Dis. 66, 1145–1163.

Das, U., Wang, L., Ganguly, A., Saikia, J.M., Wagner, S.L., Koo, E.H., and Roy, S. (2016). Visualizing APP and BACE-1 approximation in neurons yields insight into the amyloidogenic pathway. Nat. Neurosci. 19.

Edgar, J.R., Wille, K., Gouras, G.K., and Futter, C.E. (2015). ESCRTs regulate amyloid precursor protein sorting in multivesicular bodies and intracellular amyloid- β accumulation. J. Cell Sci. 2520–2528.

Ginsberg, S.D., Mufson, E.J., Counts, S.E., Wuu, J., Alldred, M.J., Nixon, R.A., and Che, S. (2010). Regional selectivity of rab5 and rab7 protein upregulation in mild cognitive impairment and Alzheimer's disease. J. Alzheimer's Dis. 22, 631–639.

Ginsberg, S.D., Mufson, E.J., Alldred, M.J., Counts, S.E., Wuu, J., Nixon, R.A., and Che, S. (2012). Upregulation of select rab GTPases in cholinergic basal forebrain neurons in mild cognitive impairment and Alzheimer's disease. J Chem Neuroanat. 42, 102–110.

Green, K.N., Billings, L.M., Roozendaal, B., Mcgaugh, J.L., and Laferla, F.M. (2006). Glucocorticoids Increase Amyloid- ß and Tau Pathology in a Mouse Model of Alzheimer's Disease. J. Neurosci. 26, 9047–9056.

Haass, C., Kaether, C., Thinakaran, G., and Sisodia, S. (2012). Trafficking and Proteolytic Processing of APP. Cold Spring Harb. Perspect. Biol. 1–26.

Huang, Y.A., Zhou, B., Wernig, M., Su, T.C., Huang, Y.A., Zhou, B., Wernig, M., and Su, T.C. (2017). ApoE2, ApoE3, and ApoE4 Differentially Stimulate APP Transcription and Ab Secretion. Cell 427–441.

Jiang, Y., Mullaney, K.A., Peterhoff, C.M., Che, S., Schmidt, S.D., and Boyer-boiteau, A. (2010). Alzheimer 's-related endosome dysfunction in Down syndrome is Aβ -independent but requires APP and is reversed by BACE-1 inhibition. Proc. Natl. Acad. Sci. 107, 1630–1635.

Kimura, N., Makoto, I., Okabayashi, S., Ono, F., and Negishi, T. (2009). Dynein Dysfunction Induces Endocytic Pathology Accompanied by an Increase in Rab GTPases. J. Biol. Chem. 284, 31291–31302.

Kimura, N., Samura, E., Suzuki, K., Okabayashi, S., Shimozawa, N., and Yasutomi, Y. (2016). Dynein Dysfunction Reproduces Age-Dependent Retromer Deficiency: Concomitant Disruption of Retrograde Trafficking Is Required for Alteration in β-Amyloid Precursor Protein Metabolism. Am. J. Pathol. 186, 1952–1966.

Kouranti, I., Sachse, M., Arouche, N., Goud, B., and Echard, A. (2006). Rab35 Regulates an Endocytic Recycling Pathway Essential for the Terminal Steps of Cytokinesis. Curr. Biol. 16, 1719–1725.

Lopes, S., Vaz-Silva, J., Pinto, V., Dalla, C., Kokras, N., Bedenk, B., Mack, N., Czisch, M., Almeida, O.F.X., Sousa, N., et al. (2016). Tau protein is essential for stress-induced brain pathology. Proc. Natl. Acad. Sci. 113, E3755–E3763.

Moore, S., Evans, L.D.B., Andersson, T., Portelius, E., Smith, J., Dias, T.B., Saurat, N., McGlade, A., Kirwan, P., Blennow, K., et al. (2015). APP Metabolism Regulates Tau Proteostasis in Human Cerebral Cortex Neurons. Cell Rep. 11, 689–696.

Mucke, L., and Selkoe, D.J. (2012). Neurotoxicity of amyloid-b protein. Cold Spring Harb. Perspect. Med. 1–18.

Nixon, R.A. (2005). Endosome function and dysfunction in Alzheimer's disease and other neurodegenerative diseases. Neurobiol. Aging 26, 373–382.
Querfurth, H.W., and LaFerla, F.M. (2010). Alzheimer's disease. N. Engl. J. Med. 362, 329–344.

Prediger RDS, Franco JL, Pandolfo P, Medeiros R, Duarte FS, Di Giunta G et al. Differential susceptibility following β-amyloid peptide-(1-40) administration in C57BL/6 and Swiss albino mice: Evidence for a dissociation between cognitive deficits and the glutathione system response. Behav Brain Res 2007; 177: 205–213.

Sannerud, R., Declerck, I., Peric, A., Raemaekers, T., Menendez, G., and Zhou, L. (2011). ADP ribosylation factor 6 (ARF6) controls amyloid precursor protein (APP) processing by mediating the endosomal sorting of BACE1. Pro 6.

Sheehan, P., Zhu, M., Beskow, A., Vollmer, C., and Waites, C.L. (2016). Activity-Dependent Degradation of Synaptic Vesicle Proteins Requires Rab35 and the ESCRT Pathway. J. Neurosci. 36, 8668–8686.

Small, S.A., Simoes-Spassov, S., Mayeux, R., and Petsko, G.A. (2017). Endosomal Traffic Jams Represent a Pathogenic Hub and Therapeutic Target in Alzheimer's Disease. Trends Mol. Med. 40, 592–602.

Sotiropoulos, I., Catania, C., Pinto, L.G., Silva, R., Pollerberg, G.E., Takashima, A., Sousa, N., and Almeida, O.F.X. (2011). Stress acts cumulatively to precipitate Alzheimer's disease-like tau pathology and cognitive deficits. J. Neurosci. 31, 7840–7847.

Stenmark, H. (2009). Rab GTPases as coordinators of vesicle traffic. Nat. Rev. Mol. Cell Biol. 10, 513–525.

Topol, A., Tran, N.N., and Brennand, K.J. (2015). A Guide to Generating and Using hiPSC Derived NPCs for the Study of Neurological Diseases. J. Vis. Exp. 1–9.

Ubelmann, F., Burrinha, T., Salavessa, L., Gomes, R., and Ferreira, C. (2017). Bin1 and CD2AP polarise the endocytic generation of beta-amyloid. EMBO Rep. 18, 102–122.

Udayar, V., Buggia-Prévot, V., Guerreiro, R.L., Siegel, G., Rambabu, N., Soohoo, A.L., Ponnusamy, M., Siegenthaler, B., Bali, J., Simons, M., et al. (2013). A paired RNAi and RabGAP overexpression screen identifies Rab11 as a regulator of β-amyloid production. Cell Rep. 5, 1536–1551.

Vaz-Silva, J., Gomes, P., Jin, Q., Zhu, M., Zhuravleva, V., Meira, T., Silva, J., Dioli, C., Soares-cunha, C., Daskalakis, P., et al. (2018). Endolysosomal degradation of Tau and its role in glucocorticoid-driven hippocampal malfunction. EMBO J. 1–16.

Willén, K., Edgar, J.R., Hasegawa, T., Tanaka, N., Futter, C.E., and Gouras, G.K. (2017). Aβ accumulation causes MVB enlargement and is modelled by dominant negative. 1–18.

Zou, L., Zou, L., Wang, Z., Shen, L., Bao, G. Bin, Wang, T., Kang, J.H., and Pei, G. (2007). Receptor tyrosine kinases positively regulate BACE activity and Amyloid-β production through enhancing BACE internalization. Cell Res. 389–401.

CHAPTER 3

DISCUSSION, CONCLUSIONS AND FUTURE PERSPECTIVES

General Discussion

The endosomal-lysosomal system is essential for cell function and health. Indeed, considerable evidence suggests a close relation between endosomal-lysosomal dysfunction and a surprising number of neurodegenerative disorders. Despite the distinct etiologies and clinical presentations of AD, NPC and Down Syndrome, they all share similar brain pathological features, presenting neurodegeneration together with NFT formation and, importantly, very early development of endosomal-lysosomal abnormalities (Nixon, 2005). However, morphological and functional abnormalities of the endocytic and lysosomal organelles are not only associated with disease, as a recent study demonstrated that ageing leads to impaired endosomal-lysosomal function (Cannizzo et al., 2012). Notably, as age is the main risk factor for developing AD (Mayeux and Stern, 2012; Querfurth and Laferla, 2010), we can hypothesize that disturbances in the normal ageing process are responsible for endosomal disfunction, eventually leading to disease. Furthermore, accumulation of dysfunctional proteins such as Tau appears to drive the pathological processes underlying AD and other neurodegenerative diseases, while relieving the protein burden seems to be protective, suggesting a critical role of proteostasis regulation for disease progression. Therefore, it is of major interest to identify the genetic and environmental factors that regulate the endolysosomal system, which will allow us to decipher the mechanisms of disease and provide new therapeutic targets.

In the current PhD thesis, we demonstrate that the Rab35/ESCRT pathway plays an essential role in the turnover of Tau, and that downregulation of this pathway by GCs leads to dysregulation of Tau proteostasis. Moreover, Rab35 gain-of-function rescues GC-induced Tau accumulation, indicating that upregulation of this pathway could have therapeutic benefit for mitigating stress-related brain pathology. Additionally, we identify Rab35 as a negative regulator of APP amyloidogenic processing in neurons, through the regulation of both APP and BACE membrane trafficking dynamics, decreasing their convergence within the endosomal system. Furthermore, Rab35 is downregulated in several AD-related risk factors, such as ageing and chronic stress, with possible relevance for stress influence on AD-related pathomechanisms.

3.1 The endosomal-lysosomal system and Tau pathology

Classically, the endolysosomal pathway, and ESCRT complex in particular, are thought to mediate membrane-associated receptor degradation. However, recent evidence has shown that

inhibiting the ESCRT complex through knockdown of ESCRT-I or -III components also affects the delivery of soluble cytosolic proteins, i.e. GAPDH and aldolase, to the vesicles of LE/MVBs. These findings suggest that the ESCRT pathway also contributes to the degradation of soluble cytosolic proteins (Sahu et al., 2011). Tau was first described as a cytosolic protein, but it is now known that Tau has both cytosolic and membrane-associated pools, and that it localizes to the plasma membrane (PM), synaptosomal membranes, and synaptic vesicle membranes (Lopes et al., 2016; Pinheiro et al., 2016; Pooler et al., 2012; Zhou et al., 2017).

To examine whether the endolysosomal pathway mediates Tau degradation, we analyzed Tau distribution along the endocytic pathway. We were able to identify Tau in early endosome (EE), (late endosome/multiple vesicular bodies (LE/MVBs), and lysosomes by high resolution light as well as electron microscopy, thus demonstrating that Tau is present throughout the compartments of the endolysosomal pathway. Since the ESCRT pathway is responsible for ubiquitinated protein sorting to MVBs, our finding that Tau interacts with Hrs, the initial ESCRT protein and a major cargo sorter, in a ubiquitination-dependent manner suggests that Tau is a cargo of this pathway. Furthermore, we have shown that modulation of the ESCRT pathway impacts the degradation of Tau in healthy neurons, demonstrating that Tau is indeed a cargo of the ESCRT complex. Recent studies demonstrate that dysfunction of the ESCRT machinery leads to the accumulation of ubiquitylated proteins, impaired endosomal trafficking and cell death in the brain (Oshima et al., 2016; Watson et al., 2015; Zhang et al., 2017); thus, it is likely that some components of the ESCRT have a yet unreported role in neurodegenerative diseases such as AD. Thus far, a mutation in the ESCRT-III component, CHMP2b, has been described in the etiology of a familial form of frontotemporal dementia (FTD) termed 'FTD linked to chromosome 3' (Han et al., 2012).

Our lab has previously shown that the small GTPase Rab35 is a key regulator of the ESCRT pathway, recruiting ESCRT-0 component Hrs to synaptic vesicle (SV) pools in order to facilitate protein degradation (Sheehan et al., 2016). Here, we report that Rab35 also stimulates Tau degradation, promoting ESCRT and Tau interaction, and leading to increased delivery of Tau to lysosomes. Notably, AD patients are thought to manifest synaptic dysfunction early in disease (Morris, 2001; Scheff et al., 2006). Furthermore, Tau was recently shown to associate with SV membranes, and mutated pathological forms of Tau to interfere with presynaptic function and decrease neurotransmission through the reduction of SV cycling/release and mobility (Zhou et al., 2017). Together with our findings, these suggest that Rab35/ESCRT function could facilitate Tau removal and degradation from

the presynaptic protein pool, while impairment to this pathway could result in decreased clearance of SV-associated Tau, resulting in its accumulation and impairment of presynaptic function.

Interestingly, Tau phosphorylation at specific epitopes can regulate its distribution between cytosolic and membrane-associated pools (Pooler et al., 2012). Our findings demonstrate that the phosphorylation signature of Tau determines its ability to undergo degradation via the Rab35/ESCRT pathway. Specifically, Tau phosphorylated at pSer396/404 and pSer262, but not pSer202, can undergo degradation by the Rab35/ESCRT pathway through the endosomal-lysosomal system. Future studies should address the relationship between phosphorylation and Tau's membrane association and ability to undergo sorting and degradation through this pathway.

Besides phosphorylation, other Tau PTMs such as acetylation and ubiquitylation are also known to affect its neuronal fate (Morris et al., 2015). Tau acetylation has been shown to reduce turnover rates by inhibiting ubiquitination, leading to impaired Tau function and promoting its pathological aggregation (Cohen et al., 2011; Min et al., 2010). On the other hand, ubiquitination targets proteins for degradation. The most studied chains for degradative protein sorting are Lys-48 and Lys-63, which sort proteins into the UPS or lysosomal system, respectively (Chesser et al., 2013; Piper et al., 2014). Interestingly, Lys-63 tagged proteins are often found in protein aggregates (Tan et al., 2008), suggesting a relationship between dysfunctional lysosomal degradation and the accumulation of Lys-63 ubiquitinated proteins. In this study, we show that GC exposure leads to a dramatic accumulation of ubiquitinated Tau, most likely related to a failure in degradation rather than an increase in Tau ubiquitination, since total Tau levels similarly increase in these cells. Interestingly, activation of the Rab35/ESCRT pathway prevents this accumulation, restoring Tau to normal levels. Thus, dysregulation of this pathway by GC seems to promote ubiquitylated Tau accumulation and ultimately its aggregation.

3.2 Rab35 and Alzheimer's Disease genetic risk factor

Most animal models of AD express mutations implicated in familial forms of AD, which represent a minority of AD cases, have earlier age of onset, and exhibit faster rates of disease progression. Familial AD usually affects genes encoding APP or presenilin-1 or -2, which increase Aβ production and lead to plaque formation. However, 95% of the reported AD cases are sporadic and late-onset (LOAD) and have multifactorial causes, highlighting the urgent need to identify environmental and genetic risk factors in order to identify possible therapeutic targets and preventive strategies (Small et al., 2017). Genome-wide association studies (GWAS) have identified several

genetic risk factors, many of which are involved in endocytic membrane recycling, retromer transport and lysosomal degradation, such as BIN1, SORL1, CD2AP and PICALM (Small et al., 2017) . So far, the ApoE4 allele is the strongest genetic risk factor for LOAD, whereas the ApoE2 allele is protective (Huang et al., 2017; Schmukler and Michaelson, 2018). In both AD patients and apparently healthy individuals, ApoE4 carriers exhibit brain Aβ accumulation, and *in vitro* it has been demonstrated that ApoE4 increases Aβ production when compared to the other ApoE isoforms (Huang et al., 2017). Additionally, ApoE4 enhances Aβ oligomerization, possibly promoting its toxicity (Schmukler and Michaelson, 2018). Although the effects of ApoE4 on Aβ have been a major focus of study, it was recently shown that ApoE4 also markedly exacerbates Tau pathology in a P301S mouse model of tauopathy (Shi et al., 2017). Indeed, *in vitro* treatment of P301S-Tau-expressing neurons with any ApoE isoform reduces neuritic arborization and increases cell death, with these effects being the most prominent with the ApoE4 isoform. Furthermore, in patients with sporadic primary tauopathies or AD, the presence of the ApoE4 allele worsens neurodegeneration independently of Aβ pathology, and increases the rate of disease progression (Shi et al., 2017). These findings demonstrate that ApoE4 promotes Tau-mediated neurodegeneration and Tau pathology, although the mechanisms behind this effect are not fully understood. Notably, a very recent study has demonstrated that ApoE4 expressing mice exhibit decreased levels of Rab35 with ageing, resulting in an overall decrease of Rab35 protein levels on the brain (Alldred et al., 2018). Furthermore, it is known that inheritance of the ApoE4 allele accentuates endosomal pathology at early stages of AD while accumulating work suggests an etiopathogenic relationship between ApoE4 and APP misprocessing (Nixon, 2005; Schmukler and Michaelson, 2018). In line to this notion, this PhD thesis findings show that Rab35 levels are reduced in different pathological conditions that promote APP misprocessing such as AD Tg and non-Tg rodent models as well as in aged animals and animals under chronic stress. Note that ageing is the strongest risk factor for AD, while chronic stress and elevated GC levels are susceptibility factors for brain pathology and are shown to trigger both APP misprocessing and accumulation of hyperphosphorylated Tau. Together with the above findings, this PhD studies suggest that reduction to Rab35 and the related dysfunction of the endosomal-lysosomal system, may be central for regulating APP amyloidogenic processing and Tau pathology. However, this hypothesis needs to be further tested.

3.3 Rab35 and Exosomal Secretion of Tau

Pathogenic forms of Tau can be secreted from neurons and glia in exosomes, and recent studies indicate that this mechanism may be responsible for the spreading of Tau pathology between brain regions (Asai et al., 2015; Wang et al., 2017; Xiao et al., 2017). Exosomes derive from MVBs and typically require the ESCRT machinery for their biogenesis (Colombo et al., 2013; Hessvik and Llorente, 2017). Inhibition of Rab35 in oligodendrocytes was found to promote intracellular accumulation of endosomal vesicles and impair exosomal secretion from these cells, suggesting a possible role for Rab35 in exosome secretion through a docking or tethering function (Hsu et al., 2010). However, in a more recent study, Rab35 knockdown did not affect the number or size of exosomes released by lung carcinoma cells, although it did lead to cargo accumulation in late endosomes (Novo et al., 2018). Given these data, it is conceivable that activation of the Rab35/ESCRT pathway could stimulate the loss of Tau via exosome secretion rather than degradation. However, we think this possibility highly unlikely, as Rab35 is not implicated in neuronal exosome secretion (Beckett et al., 2013; Blanc and Vidal, 2017; Koles et al., 2012) and additionally, Rab35-mediated exosome secretion does not appear to require the ESCRT machinery (Abrami et al., 2013; Beckett et al., 2013). Furthermore, all published studies on exosomal secretion of Tau use overexpression models, as only a small fraction of endogenous Tau can be detected in exosomes (Wang et al., 2017). Indeed, many questions remain about the roles of exosomes in both the healthy brain and the development of Tau pathology. Future studies will address whether the Rab35/ESCRT pathway mediates the propagation and/or degradation of mutant pathogenic Tau species, and investigate how these functions contribute to Tau pathology in AD and other diseases.

3.4 Chronic stress as a disruptive factor for pathological ageing and Alzheimer's Disease

Prolonged stressful experiences and excessive GC exposure are known to be susceptibility factors for the development of brain pathology, and here we focus on the implications for AD pathology.

Ageing is highly correlated with alterations of the hypothalamus-pituitary-adrenal (HPA) axis function. Reports show that one third of aged rats exhibit basal GC hypersecretion, which inversely correlates with hippocampal volume and memory function (Lupien et al., 2009). The same was shown to be true in humans, since healthy aged individuals exhibit higher mean diurnal levels of GC than younger individuals, while the increase in cortisol levels was shown to negatively correlate with memory scores and hippocampal volume in aged individuals (Kloet et al., 2005; Lupien et al., 1998).

These results suggest a close relation of HPA axis function in aged animals with hippocampal atrophy and memory impairment, two major characteristics of neurodegenerative diseases, including AD. Therefore, clinical studies assessed HPA function in AD patients, and found high cortisol levels in these individuals, as well as a positive correlation between increased cortisol levels and memory impairment (Dong et al., 2006; Rasmuson et al., 2009). Altogether, stress and HPA axis function appear to be central in the process of healthy ageing, while disruption of its regulation and GC hypersecretion seems to be associated with accelerated/pathological ageing processes.

We observed an effect of ageing on the regulation of Rab35 levels, suggesting an imbalance on membrane trafficking dynamics with age. Indeed, previous studies report an age-dependent endocytic pathology via regulation of Rab GTPases, with aged animals presenting altered levels of both Rab5 and Rab11 (Kimura et al., 2009). Interestingly, elevated GC and chronic stress have also decreased Rab35 levels similarly to aged animals, thus supporting the idea that stress could act through ageing-related mechanisms. Additionally, aged animals present increased APP amyloidogenic processing and Aβ production (Cisternas et al., 2018; Kimura et al., 2009, 2016), which was also shown to be triggered by chronic stress and GC (Catania et al., 2009; Green et al., 2006; Sotiropoulos et al., 2008). Previous studies have reported an increase in APP amyloidogenic processing by GC due to a transcriptional up-regulation of APP and BACE expression by GR, since both proteins contain GRE in their promoter region (Green et al., 2006). Here, we show that GC increased APP/BACE interaction in cells expressing exogenous APP:VN and BACE:VC, which are not under the GRE transcriptional regulation. This GC-induced effect is blocked by Rab35 overexpression, which points towards an GC-induced effect on membrane trafficking dynamics.

In our work, we also demonstrate that GC have an effect on protein sorting and degradation via the endo-lysosomal system. However, since chronic stress affects multiple pathways, more thorough studies must be performed to characterize the complete effects of GC exposure on endocytic function in the brain, including its role in endocytosis, recycling, and retromer trafficking or exosome secretion. Unfortunately, it is not simple to dissect the mechanisms of endosomal-lysosomal dysfunction in brains of animal models, since such studies require high magnification imaging of intracellular compartment morphology and dynamics, which present many technical limitations. Moreover, techniques for biochemically isolating the different compartments are challenging, usually leading to some amount of contamination from other organelles, and preventing precise morphology characterization.

Furthermore, since ageing is also known to affect the endosomal-lysosomal system (Kaushik and Cuervo, 2015), it would be interesting to study the correlation between basal GC secretion and endosomal-lysosomal function in the context of healthy ageing. Analyzing the impact of cumulative stress on endosomal-lysosomal function, and the reversibility of any pathological changes, would also help us to identify the molecular point of no-return for pathological processes. Indeed, previous studies have shown that the detrimental effects of chronic stress on brain structure and function exhibit a cumulative profile, with stress-induced impairments starting in the hippocampus and progressing towards the prefrontal cortex (PFC) and other cortical areas. Notably, similar spatiotemporal patterns are described for Tau pathology and its spreading in AD patients.

Tau is essential for chronic stress and GC-induced brain pathology, with studies demonstrating that stress induces abnormal hyperphosphorylation of Tau in the hippocampus and PFC accompanied by neuronal atrophy (Sotiropoulos et al.), while Tau ablation completely prevents the deleterious effects of stress on the brain (Lopes et al., 2016, 2017). Additionally, previous studies have reported that GC promotes Tau missorting into the dendritic compartment, leading to Tau accumulation at the synaptic level in a phosphorylation-dependent manner (Lopes et al., 2016; Pinheiro et al., 2016). Here, we show that GC impairs Tau turnover, promoting accumulation of ubiquitylated Tau protein by downregulating Rab35 expression and thereby suppressing cargo sorting into the ESCRT pathway. Furthermore, we demonstrate that activation of Rab35 *in vivo* prevents Tau accumulation at the synaptic level. Since Tau has been recently shown to undergo local translation in the dendritic compartment (Li and Götz, 2017), we can hypothesize that stress-induced Tau accumulation in dendritic spines could be the result of decreased endo-lysosomal degradation in this compartment, and thus activation of Tau clearance through this system would ease the burden on the stressed synapse and pose a possible therapeutical target.

Since most neurodegenerative diseases result from accumulation of dysfunctional proteins that compromise neuronal function, future studies should look to the influence of this pathway in other proteionopathies such as Parkinson's Disease, where α-synuclein accumulation and aggregation is described as one of the major mechanisms for disease development. Additionally, since the endosomal-lysosomal pathway communicates with other degradative pathways such as macroautophagy and chaperone-mediated autophagy, studies should focus on the importance of this interplay for disease physiopathology. Indeed, a recent study found that chronic stress triggers mTOR-dependent inhibition of autophagy, leading to the accumulation of Tau aggregates and cell death in P301L-Tau expressing mouse models and cell lines (Silva et al., 2018).

Future studies should focus on the impact of this pathway on Tau aggregation, a major hallmark of AD, which occurs in the cytoplasm and can have neurotoxic effects on the cell (Sierra-fonseca and Gosselink, 2018). Since most of our work was performed in healthy neurons expressing physiological levels of Tau, it was difficult to evaluate the impact of the Rab35/ESCRT pathway on Tau aggregation. Studies with transgenic mouse models expressing aggregation-prone mutant Tau will help us understand the relevance of the endosomal-lysosomal pathway for the removal of pathogenic forms of Tau, as well as the impact of pathological Tau on endosomal function, since it could serve as a destabilizing factor.
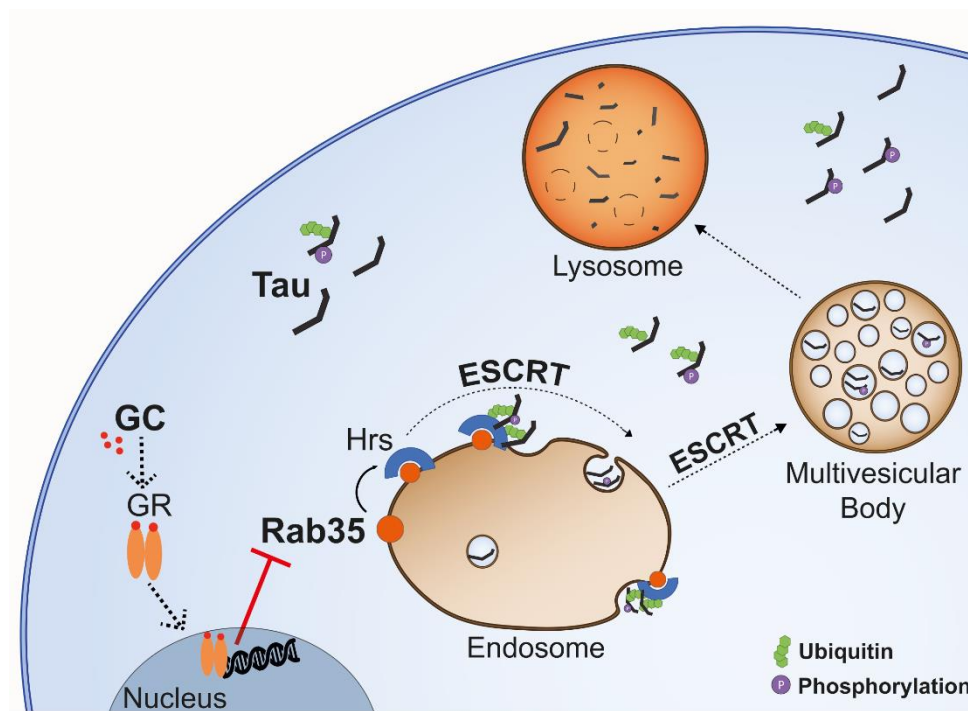

Figure 1. Working model of Tau degradation through the Rab35/ESCRT pathway. Rab35 mediates Tau clearance via the endolysosomal pathway by recruiting initial ESCRT component Hrs, which recognizes and sorts ubiquitylated Tau into early endosomes for packaging into MVBs. GC suppress transcription of Rab35, which in turn decreases Tau sorting into MVBs and its subsequent degradation by lysosomes, leading to Tau accumulation and related neuronal atrophy.

Importantly, we show that sorting of Tau by the Rab35/ESCRT pathway is essential for GC-induced neuronal damage *in vivo*, since Rab35 gain-of-function in the hippocampus of middle-aged rats was able to block dendritic atrophy evoked by increased exposure to GC. Since neuronal atrophy usually underlies stress-induced mood and cognitive deficits, future studies will address the effect of Rab35 on stress-induced behavioral deficits, to determine whether promoting Tau degradative sorting is able to prevent clinical symptoms such as memory impairment. However, since behavior is the

result of neuronal circuitry and synaptic connections between different brain areas, and stress impacts multiple different brain regions, future studies tackling this question should modulate activation of the Rab35/ESCRT pathway throughout the brain, instead of the within the hippocampus as was performed in this PhD thesis.

3.5 Chronic Stress, Rab35 and Aβ production

Experimental studies show that stress and GC trigger the amyloidogenic processing of APP towards Aβ (Catania et al., 2009; Green et al., 2006; Sotiropoulos et al., 2008). Rab35 has a wide array of functions in the regulation of membrane trafficking dynamics, here we demonstrate that GC-induced reduction in Rab35 levels contributes to the amyloidogenic pathology of chronic stress. Recently, Rab35 was suggested as a negative regulator of Aβ production and/or secretion in a screen of Rab GTPases performed in non-neuronal cells (Udayar et al., 2013). Our study shows that Rab35 gain-of-function negatively regulates APP/BACE interaction in neurons, decreasing APP's amyloidogenic processing and thus, reducing CTFs and Aβ levels. Interestingly, β-CTF is also considered to be neurotoxic, independently of Aβ since it impairs endosomal function, leading to endosomal enlargement, and has been shown to alter Tau proteostasis, inducing Tau hyperphosphorylation and accumulation (Jiang et al., 2010; Moore et al., 2015). Thus, Rab35 gain-of-function could prevent deleterious effects of both Aβ and β-CTF. Since Aβ infusion decreases Rab35 levels in the hippocampus, we hypothesize that Aβ could also indirectly impair Tau proteostasis through modulation of the Rab35/ESCRT pathway.

Rab35 regulates APP and BACE1 intraneuronal distribution, decreasing their accumulation in the endocytic pathway, while increasing BACE1 distribution within the TGN. Rab35 is regarded as a master Rab, with multiple roles in the regulation of membrane dynamics, several of which could impact APP or BACE1 interaction. For instance, Rab35 regulates a fast recycling pathway from EEs to the PM (Kouranti et al., 2006), and we've discovered that activation of Rab35 could result in increased removal of APP from endosomes to the PM, thus increasing surface APP levels and preventing BACE-mediated cleavage, which only occurs in the acidic environment of the endosomal pathway. This effect was specific for APP, since BACE1 recycling was decreased by Rab35 gain-of-function. Furthermore, APP undergoes degradation through the ESCRT sorting complex (Edgar et al., 2015), and although activation of this pathway by Rab35 could be responsible for increased sorting of APP to the lysosome for degradation, our results report no concordant change with this hypothesis in APP degradation dynamics or lysosomal distribution in neurons, suggesting that APP undergoes

sorting through the endo-lysosomal pathway on a Rab35-independent manner. Additionally, Rab35 regulates protein trafficking through the retromer pathway, controlling protein recycling from the endocytic pathway to the TGN (Cauvin et al., 2016). APP and/or BACE trafficking through the retrograde pathway has been associated with decreased Aβ production. Indeed, genes identified in GWAS studies as risk factors for AD were implicated in the regulation of this pathway, while ageing itself was shown to impair retrograde trafficking in non-human primate brains with possible implications for Aβ accumulation (Kimura et al., 2016). In our study, Rab35 activation could increase BACE1 trafficking, but not APP, through the retrograde pathway, increasing its transfer to the TGN and thus decreasing its time within the endosomal compartments, where it can cleave APP. Additionally, BACE1 is internalized from the PM into the endocytic pathway through an Arf6-dependent pathway (Sannerud et al., 2011). Rab35 negatively regulates Arf6 activation and vice-versa (Chaineau et al., 2013; Kobayashi and Fukuda, 2012), suggesting that Rab35 inhibition can increase BACE internalization into early endosomes via Arf6 activation, thereby increasing the amount of BACE in the endocytic compartment and promoting APP cleavage. Interestingly, we found that Rab35 gain-of-function decreases both endosomal and surface levels of BACE1, while it presents decreased levels of BACE1 recycling at the 60 minutes timepoint. These findings suggest that the observed effects are likely due to retrograde activation by Rab35, which sequesters BACE1 from the endosome into the TGN, thus blocking its recycling to the PM and decreasing its surface levels. Additionally, we've observed an increased internalization of BACE at timepoint 0, suggesting a faster retrieval of BACE1 from the membrane, thus Rab35 might be affecting BACE1 internalization through an Arf6-independent alternative pathway. Further studies should be performed to understand the role of Rab35 in Aβ production *in vivo*, while also exploring its relevance for the processing of familial mutated forms of APP, since these APP mutations could lead to altered trafficking dynamics and/or affinity for BACE1 interaction (Haass et al., 1995). Overall, due to the multitude of described Rab35 functions that are capable of interfering with APP amyloidogenic processing, we hypothesize that this Rab GTPase is a key protein in the regulation of AD and stress-induced pathomechanims.
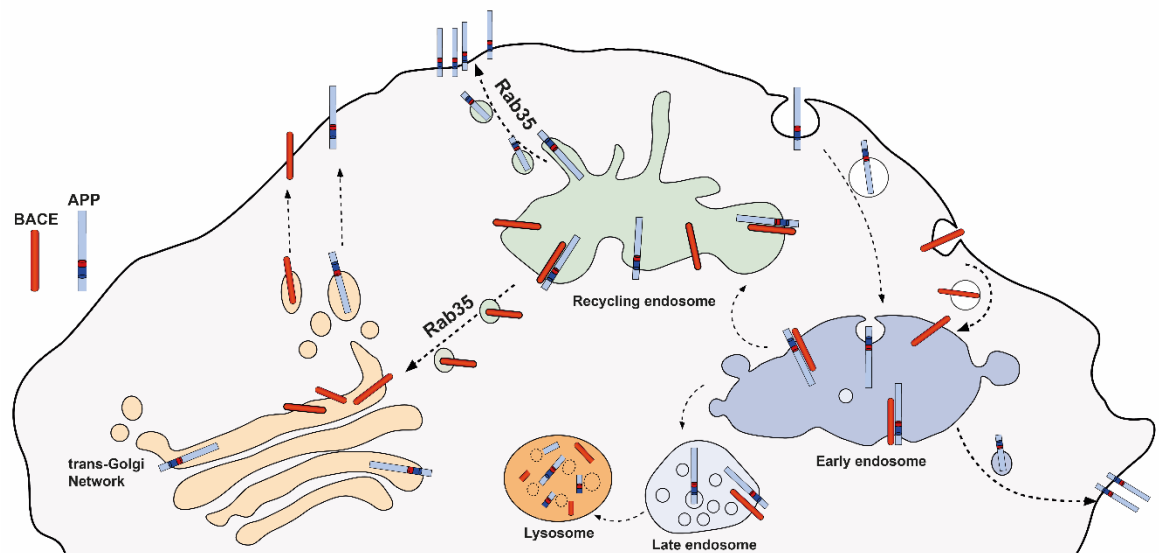
Figure 2. Working model of Rab35 regulation of APP/BACE1 interaction. Rab35 negatively regulates APP/BACE1 interaction, leading to decreased levels of CTF and Aβ production. Rab35 controls APP and BACE1 intracellular trafficking, decreasing their distribution in the endosomal compartment, while increasing BACE1 distribution in the TGN and cell surface levels of APP. Rab35 increases endocytosed BACE1 trafficking to the TGN, also promoting a decreased recycling and cell surface levels of BACE1. On the other hand, Rab35 increases APP recycling to the PM, retrieving APP from the endocytic compartment and increasing APP surface levels at the PM.

In summary, these PhD studies identify the Rab35 as a critical regulator of APP and Tau intraneuronal trafficking and proteostasis in both health and disease conditions. Inhibition of Rab35 expression or activity could evoke APP amyloidogenic processing, as well as ESCRT-driven dysregulation of Tau degradation, facilitating the overproduction of Aβ and Tau accumulation, respectively, in diseased neurons. Further studies should clarify the potential involvement of Rab35 (and/or other Rabs) in different pathological conditions and proteopathies, as well as monitor the therapeutic potential of Rab35 overexpression against Aβ- or Tau-related neuronal malfunction and atrophy in and beyond AD brain pathology.

References

Alldred, M.J., Goulbourne, C.N., Peng, K.Y., Morales-corraliza, J., Saito, M., Saito, M., and Ginsberg, S.D. (2018). Apolipoprotein E4 genotype compromises brain exosome production. Brain 1–13.

Cannizzo, E.S., Clement, C.C., Morozova, K., Valdor, R., Kaushik, S., Almeida, L.N., Follo, C., Sahu, R., Cuervo, A.M., Macian, F., et al. (2012). Age-Related Oxidative Stress Compromises Endosomal Proteostasis. Cell Rep. 2, 136–149.

Catania, C., Sotiropoulos, I., Silva, R., Onofri, C., Breen, K.C., Sousa, N., and Almeida, O.F.X. (2009). The amyloidogenic potential and behavioral correlates of stress. Mol. Psychiatry 14, 95–105.

Cauvin, C., Rosendale, M., Gupta-Rossi, N., Rocancourt, M., Larraufie, P., Salomon, R., Perrais, D., and Echard, A. (2016). Rab35 GTPase Triggers Switch-like Recruitment of the Lowe Syndrome Lipid Phosphatase OCRL on Newborn Endosomes. Curr. Biol. 26, 120–128.

Chaineau, M., Ioannou, M.S., and McPherson, P.S. (2013). Rab35: GEFs, GAPs and effectors. Traffic 14, 1109–1117.

Chesser, A.S., Pritchard, S.M., and Johnson, G.V.W. (2013). Tau clearance mechanisms and their possible role in the pathogenesis of Alzheimer disease. Front. Neurol. 4 SEP, 122.

Cisternas, P., Zolezzi, J.M., Lindsay, C., Rivera, D.S., and Martinez, A. (2018). New Insights into the Spontaneous Human Alzheimer's Disease-Like Model Octodon degus : Unraveling Amyloid-b Peptide Aggregation and Age-Related Amyloid Pathology. J. Alzheimer's Dis. 66, 1145–1163.

Cohen, T.J., Guo, J.L., Hurtado, D.E., Kwong, L.K., Mills, I.P., Trojanowski, J.Q., and Lee, V.M.Y. (2011). The acetylation of tau inhibits its function and promotes pathological tau aggregation. Nat. Commun. 2, 252–259.

Dong, H., Ph, D., Fagan, A.M., Ph, D., Wang, L., Ph, D., Xiong, C., Ph, D., Holtzman, D.M., and Morris, J.C. (2006). Plasma Cortisol and Progression of Dementia in Subjects With Alzheimer-Type Dementia. Am J Psychiatry 2164–2169.

Edgar, J.R., Wille, K., Gouras, G.K., and Futter, C.E. (2015). ESCRTs regulate amyloid precursor protein sorting in multivesicular bodies and intracellular amyloid- β accumulation. J. Cell Sci. 2520–2528.

Green, K.N., Billings, L.M., Roozendaal, B., Mcgaugh, J.L., and Laferla, F.M. (2006). Glucocorticoids Increase Amyloid- ß and Tau Pathology in a Mouse Model of Alzheimer's Disease. J. Neurosci. 26, 9047–9056.

Han, J., Ryu, H., Jun, M., Jang, D., and Lee, J. (2012). The functional analysis of the CHMP2B missense mutation associated with neurodegenerative diseases in the endo-lysosomal pathway. Biochem. Biophys. Res. Commun. 421, 544–549.

Haass C, Lemere CA, Capell A, Citron M, Seubert P, Schenk D, Lannfelt L, Selkoe DJ. (1995) The Swedish mutation causes early-onset Alzheimer's disease by beta-secretase cleavage within the secretory pathway. Nat Med. Dec;1(12):1291-6.

Hsu, C., Morohashi, Y., Yoshimura, S., Manrique-hoyos, N., Jung, S., Lauterbach, M.A., Bakhti, M., Grønborg, M., Möbius, W., Rhee, J., et al. (2010). Regulation of exosome secretion by Rab35 and its GTPase-activating proteins TBC1D10A–C. 189, 223–232.

Huang, Y.A., Zhou, B., Wernig, M., Su, T.C., Huang, Y.A., Zhou, B., Wernig, M., and Su, T.C. (2017). ApoE2, ApoE3, and ApoE4 Differentially Stimulate APP Transcription and Ab Secretion. Cell 427–441.

Jiang, Y., Mullaney, K.A., Peterhoff, C.M., Che, S., Schmidt, S.D., and Boyer-boiteau, A. (2010). Alzheimer 's-related endosome dysfunction in Down syndrome is Aβ -independent but requires APP and is reversed by BACE-1 inhibition. Proc. Natl. Acad. Sci. 107, 1630–1635.

Kaushik, S., and Cuervo, A.M. (2015). Proteostasis and aging. Nat. Med. 21, 1406–1415.

Kimura, N., Makoto, I., Okabayashi, S., Ono, F., and Negishi, T. (2009). Dynein Dysfunction Induces Endocytic Pathology Accompanied by an Increase in Rab GTPases. J. Biol. Chem. 284, 31291–31302.

Kimura, N., Samura, E., Suzuki, K., Okabayashi, S., Shimozawa, N., and Yasutomi, Y. (2016). Dynein Dysfunction Reproduces Age-Dependent Retromer Deficiency: Concomitant Disruption of Retrograde Trafficking Is Required for Alteration in β-Amyloid Precursor Protein Metabolism. Am. J. Pathol. 186, 1952–1966.

Kloet, E.R. De, Joëls, M., and Holsboer, F. (2005). Stress and the brain: from adaption to disease. Nat. Rev. Neurosci. 463–475.

Kobayashi, H., and Fukuda, M. (2012). Rab35 regulates Arf6 activity through centaurin- 2 (ACAP2) during neurite outgrowth. J. Cell Sci. 125, 2235–2243.

Kouranti, I., Sachse, M., Arouche, N., Goud, B., and Echard, A. (2006). Rab35 Regulates an Endocytic Recycling Pathway Essential for the Terminal Steps of Cytokinesis. Curr. Biol. 16, 1719–1725.

Li, C., and Götz, J. (2017). Somatodendritic accumulation of Tau in Alzheimer's disease is promoted by Fyn-mediated local protein translation. 36, 3120–3138.

Lopes, S., Vaz-Silva, J., Pinto, V., Dalla, C., Kokras, N., Bedenk, B., Mack, N., Czisch, M., Almeida, O.F.X., Sousa, N., et al. (2016). Tau protein is essential for stress-induced brain pathology. Proc. Natl. Acad. Sci. 113, E3755–E3763.

Lopes, S., Teplytska, L., Vaz-Silva, J., Dioli, C., Trindade, R., Morais, M., Webhofer, C., MaCcarrone, G., Almeida, O.F.X., Turck, C.W., et al. (2017). Tau deletion prevents stress-induced dendritic atrophy in prefrontal cortex: Role of synaptic mitochondria. Cereb. Cortex 27, 2580–2591.

Lupien, S.J., Leon, M. De, Santi, S. De, Convit, A., Tarshish, C., Thakur, M., Mcewen, B.S., Hauger, R.L., and Meaney, M.J. (1998). Cortisol levels during human aging predict hippocampal atrophy and memory deficits. Nat. Neurosci. 69–73.

Lupien, S.J., Mcewen, B.S., Gunnar, M.R., and Heim, C. (2009). Effects of stress throughout the lifespan on the brain, behaviour and cognition. Nat. Rev. Neurosci. 10.

Mayeux, R., and Stern, Y. (2012). Epidemiology of Alzheimer Disease.

Min, S., Cho, S., Zhou, Y., Schroeder, S., Haroutunian, V., Seeley, W.W., Huang, E.J., Shen, Y., Masliah, E., Mukherjee, C., et al. (2010). Acetylation of Tau Inhibits Its Degradation and Contributes to Tauopathy. Neuron 67, 953–966.

Moore, S., Evans, L.D.B., Andersson, T., Portelius, E., Smith, J., Dias, T.B., Saurat, N., McGlade, A., Kirwan, P., Blennow, K., et al. (2015). APP Metabolism Regulates Tau Proteostasis in Human Cerebral Cortex Neurons. Cell Rep. 11, 689–696.

Morris, J.C. (2001). Altered expression of synaptic proteins occurs early during progression of Alzheimer's disease. Neurology 127–130.

Morris, M., Knudsen, G.M., Maeda, S., Trinidad, J.C., Ioanoviciu, A., Burlingame, A.L., and Mucke, L. (2015). Tau post-translational modifications in wild-type and human amyloid precursor protein transgenic mice. Nat. Neurosci.

Nixon, R.A. (2005). Endosome function and dysfunction in Alzheimer's disease and other neurodegenerative diseases. Neurobiol. Aging 26, 373–382.

Novo, D., Heath, N., Mitchell, L., Caligiuri, G., Macfarlane, A., Reijmer, D., Charlton, L., Knight, J., Calka, M., Mcghee, E., et al. (2018). Mutant p53s generate pro-invasive niches by influencing exosome podocalyxin levels. Nat. Commun. 25–28.

Oshima, R., Hasegawa, T., Tamai, K., Sugeno, N., and Yoshida, S. (2016). ESCRT-0 dysfunction compromises autophagic degradation of protein aggregates and facilitates ER stress-mediated neurodegeneration via apoptotic and necroptotic pathways. Nat. Publ. Gr. 1–15.

Pinheiro, S., Silva, J., Mota, C., Vaz-silva, J., and Veloso, A. (2016). Tau Mislocation in Glucocorticoid-Triggered Hippocampal Pathology. Mol. Neurobiol. 4745–4753.

Piper, R.C., Dikic, I., and Lukacs, G.L. (2014). Ubiquitin-Dependent Sorting in Endocytosis. Cold Spring Harb. Perspect. Med.

Pooler, A.M., Usardi, A., Evans, C.J., Philpott, K.L., Noble, W., and Hanger, D.P. (2012). Dynamic association of tau with neuronal membranes is regulated by phosphorylation. Neurobiol. Aging 33, 431.e27-431.e38.

Querfurth, H.W., and Laferla, F.M. (2010). Alzheimer's Disease. N. Engl. J. Med. 329–344.

Rasmuson, S., Andrew, R., Na, B., Seckl, J.R., Walker, B.R., and Olsson, T. (2009). Increased Glucocorticoid Production and Altered Cortisol Metabolism in Women with Mild to Moderate Alzheimer ' s Disease. Biol. Psychiatry 3223.

Sahu, R., Kaushik, S., Clement, C.C., Cannizzo, E.S., Scharf, B., Follenzi, A., Potolicchio, I., Nieves, E., Cuervo, A.M., and Santambrogio, L. (2011). Short Article Microautophagy of Cytosolic Proteins by Late Endosomes. DEVCEL 20, 131–139.

Sannerud, R., Declerck, I., Peric, A., Raemaekers, T., Menendez, G., and Zhou, L. (2011). ADP ribosylation factor 6 (ARF6) controls amyloid precursor protein (APP) processing by mediating the endosomal sorting of BACE1. Pro 6.

Scheff, S.W., Price, D.A., Schmitt, F.A., and Mufson, E.J. (2006). Hippocampal synaptic loss in early Alzheimer ' s disease and mild cognitive impairment. Neurobiol. Aging 27, 1372–1384.

Schmukler, E., and Michaelson, D.M. (2018). The Interplay Between Apolipoprotein E4 and the Autophagic – Endocytic – Lysosomal Axis. Mol. Neurobiol.

Sheehan, P., Zhu, M., Beskow, A., Vollmer, C., and Waites, C.L. (2016). Activity-Dependent Degradation of Synaptic Vesicle Proteins Requires Rab35 and the ESCRT Pathway. J. Neurosci. 36, 8668–8686.

Shi, Y., Yamada, K., Liddelow, S.A., Smith, S.T., Zhao, L., Luo, W., Tsai, R.M., Spina, S., Grinberg, L.T., Rojas, J.C., et al. (2017). ApoE4 markedly exacerbates tau-mediated neurodegeneration in a mouse model of tauopathy. Nature 549, 523–527.

Sierra-fonseca, J.A., and Gosselink, K.L. (2018). Tauopathy and neurodegeneration : A role for stress. Neurobiol. Stress 9, 105–112.

Silva, J.M., Rodrigues, S., Sampaio-marques, B., Gomes, P., Neves-carvalho, A., Dioli, C., Soares-cunha, C., Mazuik, B.F., Takashima, A., Ludovico, P., et al. (2018). Dysregulation of autophagy and stress granule-related proteins in stress-driven Tau pathology. Cell Death Differ.

Small, S.A., Simoes-Spassov, S., Mayeux, R., and Petsko, G.A. (2017). Endosomal Traffic Jams Represent a Pathogenic Hub and Therapeutic Target in Alzheimer's Disease. Trends Mol. Med. 40, 592–602.

Sotiropoulos, I., Catania, C., Pinto, L.G., Silva, R., Pollerberg, G.E., Takashima, A., Sousa, N., Almeida, O.F.X., Gualtar, C., Neurobiology, D., et al. Stress acts cumulatively to precipitate Alzheimer ' s disease-like Tau pathology and cognitive deficits. J. Neurosci. 1–21.

Sotiropoulos, I., Cerqueira, J.J., Catania, C., Takashima, a., Sousa, N., and Almeida, O.F.X. (2008). Stress and glucocorticoid footprints in the brain-The path from depression to Alzheimer's disease. Neurosci. Biobehav. Rev. 32, 1161–1173.

Tan, J.M.M., Wong, E.S.P., Kirkpatrick, D.S., Pletnikova, O., Seok, H., Tay, S., Ho, M.W.L., Troncoso, J., Gygi, S.P., Lee, M.K., et al. (2008). Lysine 63-linked ubiquitination promotes the formation and autophagic clearance of protein inclusions associated with neurodegenerative diseases. 17, 431–439.

Udayar, V., Buggia-Prévot, V., Guerreiro, R.L., Siegel, G., Rambabu, N., Soohoo, A.L., Ponnusamy, M., Siegenthaler, B., Bali, J., Simons, M., et al. (2013). A paired RNAi and RabGAP overexpression screen identifies Rab11 as a regulator of β-amyloid production. Cell Rep. 5, 1536–1551.

Watson, J.A., Bhattacharyya, B.J., Vaden, J.H., Wilson, J.A., Icyuz, M., Howard, A.D., Phillips, E., Desilva, T.M., Siegal, G.P., Bean, A.J., et al. (2015). Motor and Sensory Deficits in the teetering Mice Result from Mutation of the ESCRT Component HGS. PLoS Genet. 1–29.

Zhang, Y., Schmid, B., Nikolaisen, N.K., Rasmussen, M.A., Aldana, B.I., Agger, M., Calloe, K., Stummann, T.C., Larsen, H.M., Nielsen, T.T., et al. (2017). Stem Cell Reports. Stem Cell Reports 8, 648–658.

Zhou, L., Mcinnes, J., Wierda, K., Holt, M., Herrmann, A.G., Jackson, R.J., Wang, Y., Swerts, J., Beyens, J., Miskiewicz, K., et al. (2017). Tau association with synaptic vesicles causes presynaptic dysfunction. Nat. Commun. 8, 1–13.